e-ISSN:2602-2079

Volume 7
Issue 5
2023

JOURNAL of Surgery and Medicine

International Medical Journal

JOSAM

Editorial Team

Prasenjit Das, Professor, MD, DNB, MNAMS, MNASc
Department of Pathology
All India Institute of Medical Sciences
New Delhi, India
Website

Seyed Vahid Hosseini, Professor
Shiraz University of Medical Sciences, Shiraz, Iran
Website

Vol. 7 No. 5 (2023)

Published: 2023-05-29

Research Article

Review

Case Report

Primary pancreatic lymphoma and metastatic lymphoma cases diagnosed with ultrasonography guided tru-cut needle biopsy; Two case reports

Pancreatic lymphoma, two case reports

Işıl Bağcı, Nazlı Sena Şeker

355-357

Truncus arteriosus with meandering pulmonary arteries

Atypical truncus arteriosus

Emre Oteyaka , Okan Eren Kuguoglu , Gizem Sari , Mehmet Turan Basunlu , Yilmaz Yozgat , Murat Ugurlucan , Halil Turkoglu

358-360

A rare case of bleeding into the Sylvian arachnoid cyst: A case report

The bleeding into the Sylvian arachnoid cyst

İlyas Tadayyon Einaddin Karakoc, Feyzi Birol Sarica

361-363

J Surg Med. 2023;7(5):307-313.
DOI: 10.28982/josam.1084466

Research article

Journal of Surgery and Medicine
e-ISSN: 2602-2079
https://jsurgmed.com/

Investigation of the effects of inflammatory and metabolic factors on fracture union in head trauma and long bone fractures

Abdülkadir Sarı [1], Berna Erdal [2], Aliye Çelikkol [3], Mehmet Ümit Çetin [1]

[1] Tekirdag Namık Kemal University Faculty of Medicine, Department of Orthopedics and Traumatology, Tekirdag, Turkey
[2] Tekirdag Namık Kemal University Faculty of Medicine, Department of Medical Microbiology, Tekirdag, Turkey
[3] Tekirdag Namık Kemal University Faculty of Medicine, Department of Medical Biochemistry, Tekirdag, Turkey

ORCID ID of the author(s)
AS: 0000-0003-3416-5666
BE: 0000-0003-3375-7926
AÇ: 0000-0002-3799-4470
MÜÇ: 0000-0001-9827-8892

Corresponding Author
Abdülkadir Sarı
Tekirdağ Namık Kemal University Faculty of Medicine, Department of Orthopedics and Traumatology, Süleymanpaşa, Tekirdağ, Turkey
E-mail: drortopedist@yahoo.com

Ethics Committee Approval
The work was carried through at the animal experiments laboratory of our institution, with the approval of Namık Kemal University Experimental Animals Local Ethics Commission (date: 20 December 2019, no: T2019-386).

Conflict of Interest
No conflict of interest was declared by the authors.

Financial Disclosure
The study was supported by the Scientific Research Project Commission of Tekirdağ Namık Kemal University (number: NKUBAP.02.GA.20.251.).

Published
2023 May 5

Abstract

Background/Aim: Fractures are the most common form of trauma in current orthopedic practice. Although studies have shed light on the relationship between the factors affecting the healing process after fracture, this process is still not fully understood. In this study, we aimed to investigate the changes in serum biomediator levels and fracture healing in different trauma patterns, such as head trauma (HT), long bone fracture (LBF), a combination of HT + LBF injury (CI), and in different time points of the healing period.

Methods: Forty Wistar rats were included in the study and divided into five groups. Group 1, the donor group, included rats with HT; Group 2 included rats with LBFs who were administered the serum taken from rats in Group 1; Group 3 included the rats with isolated LBFs; and Group 4 the rats with CI. Group 5 comprised the control rats. An experimental closed HT and fracture model was applied to rats. The rats in Groups 2, 3 and 4 were sacrificed on the 10^{th}, 20^{th}, and 30^{th} days. The biomediator levels in the serum taken after sacrification were studied, while closed femoral fracture models were examined radiologically.

Results: Statistically significant differences were found among the groups regarding radiological scores on the 10^{th}, 20^{th}, and 30^{th} days. On Day 10, Group 2a had significantly higher scores than Group 3a (P=0.03), and Group 3a had lower scores than Group 4a (P=0.01). On Day 20, Group 2b had significantly higher scores than Group 3b (P=0.004) but lower than Group 4b (P=0.03). On Day 30, Group 2c had significantly higher scores than Group 3c but lower than Group 4c (P=0.001). The mean Ca, TGF beta 1, beta-catenin, IL-10, IL-17A, TNF alpha, CRP, Wnt-16, ALP, GH, PTH, IL-1 beta, IL-6, and IL-22 levels were significantly different among the groups (P<0.05). No significant difference was observed in the biomediator levels among the groups at different time points of the healing period.

Conclusion: We concluded that inflammatory cytokines (IL-1 beta, IL-6, IL-17A, IL-17F, IL-23, and TNF alpha) were elevated in the early period in individuals with isolated head trauma and that this effect could be transferred to other individuals by serum transfer. On the other hand, the negative relationship between the IL-10 level, which is a negative modulator in fracture union, and callus thickness was significant. Our study contributes by providing a molecular description of the positive union effect transferred between individuals by serum. We believe our findings will play a significant role in developing new therapeutic agents for fracture healing.

Keywords: biomediator, bone metabolism, fracture healing, interleukin, traumatic brain injury

How to cite: Sarı A, Erdal B, Çelikkol A, Çetin MÜ. Investigation of the effects of inflammatory and metabolic factors on fracture union in head trauma and long bone fractures. J Surg Med. 2023;7(5):307-313.

Introduction

Fractures are the most common form of trauma in current orthopedic practice, which continues to be a socioeconomic problem. For optimal clinical management and treatment, it is essential to understand the biology behind fracture unions [1].

Fracture healing is a complex but balanced process. Previous studies have shown that healing occurs in four stages: inflammation, soft union formation, hard union formation, and remodeling [2]. The process requires the coordinated involvement of various cell types, such as osteoblasts, mesenchymal stem cells, and osteoclasts [3]. These processes must be active at the right time and intensity for healthy bone fusion. An excessive or random inflammatory process may lead to non-union of the fracture [4].

Although studies have shed light on the relationship between the factors affecting the healing process after fracture, this process is still not fully understood [5]. Similarly, our current knowledge of the healing process of long bone fractures after traumatic brain injury is limited [6]. Understanding the molecular changes in the healing process will accelerate the healing rate [7].

This study aims to examine the changes in biomediator levels and fracture healing in different trauma patterns, such as head trauma (HT), long bone fracture (LBF), a combination of HT + LBF injury (CI), and at different time points of the healing period.

Materials and methods

The work was carried out at the animal experiments laboratory of Tekirdağ Namık Kemal University Faculty of Medicine, with the approval of the Namık Kemal University Experimental Animals Local Ethics Commission (dated 20 December 2019, no: T2019-386) and in compliance with the Helsinki Declaration. The study used 40 male Wistar rats weighing between 360 and 400 g and 3 to 4 months old. Rats were provided with a standard diet and unlimited access to water (ad libitum). Rats were exposed to a 12-h light and 12-h dark cycle at 22°C room temperature. Rats were randomly distributed and assigned to five groups. The donor group (Group 1) included rats with HT (n=8) and the Group 2 rats with LBFs who were administered the serum taken from rats in Group 1 (n=9), while Group 3 included the rats with isolated LBFs (n=9) and Group 4 the rats with CI (n=9). Group 5 comprised the control rats (n=5) (Table 1).

Table 1: Grouping of the rats included in the study

	Group 1	Group 2	Group 3	Group 4	Group 5
Number of rats	8	9	9	9	5
Euthanasia days	1-7	10-20-30	10-20-30	10-20-30	---
Number of femur specimen	-	3-3-3	3-3-3	3-3-3	---

Group 1: donor group, Group 2: serum-administered rats with femoral fractures, Group 3: rats with isolated femur fractures, Group 4: rats with head trauma and femur fracture, Group 5: control group.

Group 1 was divided into subgroups 1a and 1b. Afterward, the three groups in the treatment group were divided into subgroups similarly (titled a, b and c). The trauma models were created on the same day in Groups 1 and 2, while the head and bone fracture models were created simultaneously in Group 4.

Our aim in the study was to form a model like that of humans who experienced closed HT. For this purpose, using an apparatus that was set according to the Marmarou technique, the experimental closed HT model was created (Figure 1) [8]. The force to be applied to the head was determined not to exceed 0.5 joules so that the animals would survive the head injury and maintain their nourishment functions. For this purpose, we used weight and height upper limits of 50 g and 1 m, respectively [9].

All procedures were carried out under general anesthesia, with the inhalation of isoflurane (Forane; Abbott Laboratories, Abbott Park, IL, USA) at 4% for induction and 2% for maintenance. Dexketoprofen 5 mg/kg/day (Arveles; Menarini Turkey, Istanbul, Turkey) was administered to all rats, while one dose of cefazolin sodium 15 mg/kg (Cefozin; Bilim Pharmaceuticals, Istanbul, Turkey) was administered to the animals that were performed fixation.

With an anterior approach over the knee, the patella was lateralized with a longitudinal incision, and the distal femur was exposed. Later, a fracture was created in the femoral shaft. The femoral canal was reamed with a 1.2 mm K-wire, and a 1 mm K-wire crossing the fracture line was inserted into the femoral medulla. The proximal part was bent to prevent the wire from coming back. After the wire was cut, the subcutaneous tissue was closed with 3/0 Vicryl, and the skin was sutured with 3/0 silk sutures (Figure 2). The experimental fracture model described by Bonnarens and Einhorn was applied unilaterally to the left leg of rats following the principles used in numerous studies of experimental fracture healing [10]. For this, a weight of 150 g was dropped on the thigh from a height of 1 m.

Two rats had to be replaced with new rats due to the segmental fractures they developed, which we noticed during our radiological checks. After the procedure, no movement restriction was applied to the animals, and they were placed in cages with four rats in each cage.

Figure 1: Closed head trauma apparatus.

Figure 2: Intramedullary insertion of the K-wire into the femur.

Figure 3: Cardiac blood withdrawal after thoracotomy.

The rats were sacrificed by exsanguination following thoracotomy 24 h later for Group 1a and on the seventh day for Group 1b (Figure 3). To affect the analysis results in the blood samples taken, the blood was drained with a 45-degree slope after the injector was removed to prevent changes in serum content due to hemolysis. The samples were taken to the

centrifuge device and centrifuged at 1000 rpm for 15 min, and the serum portions were separated. Sera (1.5 ccs) from Group 1a was given to Groups 2a, 2b and 2c, and sera from Group 1b (1.5 ccs) were given to Groups 2a, 2b and 2c intraperitoneally and without waiting. On the 10th day, the rats in Groups 2a, 3a, and 4a were sacrificed. Groups 2b, 3b, and 4b were sacrificed on day 20, and 2c, 3c, and 4c were sacrificed on day 30. The biomediator levels were determined by keeping the sera obtained from all groups and healthy control rats at -80°C.

The serum beta-catenin (catalog no: E1153Ra), CRP (catalog no: E0053Ra), TGF beta 1 (catalog no: E1688Ra), Wnt-16 (catalog no: E2542Ra), ALP (catalog no: E0345Ra), GH (catalog no: E0551Ra), PTH (catalog no: E0333Ra), IL-1 beta (catalog no: E0119Ra), IL-6 (catalog no: E0135Ra), IL-10 (catalog no: E0108Ra), IL-17A (catalog no: E0116Ra), IL-17F (catalog no: E0939Ra), IL-22 (catalog no: E1473Ra), and IL-23 (catalog no: E0125Ra), and TNF alpha (catalog no: E0764Ra) levels were tested using commercially available ELISA kit following the manufacturer's instructions (Shanghai Korain Biotech Co. Ltd., Shanghai, China). In addition, serum calcium and phosphorus levels were measured in the C-502 module of the Roche Cobas 8000 analyzer (Roche Diagnostics, Geneva, Switzerland) using commercial kits. All kits' inter-test coefficient of variation (CV) values were 10%. Among the tests, intra-assay CV was <8%.

Following sacrifice, the femurs were disarticulated from the hip joint, and X-rays of the legs were taken (Figures 4–6). In all groups, the ratios defined by Spencer on the lateral radiographs taken on the 10th, 20th, and 30th days were evaluated by an orthopedist blinded to the group information [11].

Figure 4: Radiological appearance of Group 2 on Day 30.

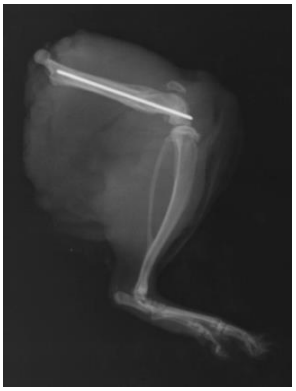

Figure 5: Radiological appearance of Group 3 on Day 30.

Figure 6: Radiological appearance of Group 4 on Day 30.

Statistical analysis

NCSS 2007 software (NCSS, LLC, Kaysville, UT, USA) was used for statistical analysis. The descriptive statistical methods were defined (mean, standard deviation, median, frequency, ratio, minimum, and maximum), and to evaluate the distribution of the data, normality between the groups was evaluated using the Shapiro-Wilk test. While the differences between 3 or more groups were analyzed with the Kruskal-Wallis test, a non-parametric test, the Mann-Whitney U test was used to compare the two groups. We used the Friedman test to compare three or more time points of the recovery period and the Wilcoxon test to compare two time points. Statistical significance was evaluated at $P<0.01$ and $P<0.05$ levels.

Results

Radiological scores increased significantly in all groups from day 10 to day 30 ($P=0.003$), again showing statistically significant differences between groups. When the 10th-day results were compared, Group 3a had significantly lower scores than Group 2a ($P=0.03$), and group 4a scores were higher than group 3a scores ($P=0.01$). When the results of the 20th day were compared, Group 3b had significantly lower scores than Group 2b ($P=0.004$), while the scores of Group 4b were higher than 2b ($P=0.03$). had scores lower than Group 4c (P = 0.001) (Table 2).

Table 2: Comparison of the radiographic measurements in the groups

		n	Mean (SD)	Min-Max (Median)	*P*-value
Day 10	Group 2	6	1.3 (0.1)	1.2-1.4	0.022*
	Group 3	6	1.1 (0.3)	1.1-1.3	
	Group 4	6	1.4 (0.2)	1.3-1.6	
Day 20	Group 2	6	2.2 (0.2)	2-2.4	0.001†
	Group 3	6	1.8 (0.1)	1.7-1.9	
	Group 4	6	2.4 (0.1)	2.3-2.5	
Day 30	Group 2	6	2.6 (0.2)	2.5-2.7	0.006†
	Group 3	6	2.4 (0.2)	2.3-2.5	
	Group 4	6	2.8 (0.1)	2.6-3	

Kruskal-Wallis test. * $P<0.05$, † $P<0.01$

When serum samples were analyzed, the mean Ca levels in all treatment groups were significantly higher in the control group than in the other groups ($P=0.001$). The CA levels of Groups 2 and 3 were significantly higher than the mean Ca levels of Group 1 ($P=0.001$), while the Ca levels of Group 4 were significantly lower than the mean Ca levels of Groups 2 and 3 ($P=0.001$). No significant difference was observed in Ca levels in the within-group evaluations at all follow-up time points of the treatment groups (Table 3). The mean phosphorus levels among the groups did not differ significantly. No significant differences in terms of phosphorus levels were detected in the intragroup evaluations of all groups at all follow-up time points (Table 3).

The mean beta-catenin levels in all treatment groups, except Group 1, were significantly higher than in the control group ($P=0.001$). The mean beta-catenin level in Group 1 was significantly lower than in Groups 2, 3, and 4 ($P=0.001$). No significant differences in beta-catenin levels were observed in intragroup evaluations of the treatment groups at all follow-up time points (Table 3).

The mean CRP level of the control group was significantly lower than the other groups ($P=0.002$). When the CRP levels of Groups 2, 3, and 5 were evaluated, it was seen that it was significantly lower than the Group ($P=0.001$); when the mean CRP level in Group 4 was considered, it was seen that it was significantly higher than the control group ($P=0.001$). No significant difference was observed in CRP levels in the within-group evaluations of the treatment groups at all follow-up time points (Table 3).

Table 3: Comparison of the serum contents in the groups

		n	Mean (SD)	Min-Max (Median)	*P*-value
Ca	Group 1	7	8.26 (0.38)	7.8-8.9 (8.2)	0.001†
	Group 2	8	9.51 (0.26)	9.1-9.8 (9.6)	
	Group 3	6	9.53 (0.18)	9.28-9.8 (9.55)	
	Group 4	9	8.34 (0.27)	7.9-8.7 (8.4)	
	Control group	2	10.1 (0.42)	9.8-10.4 (10.1)	
P	Group 1	7	3.86 (0.41)	3.01-4.28 (3.87)	0.070
	Group 2	8	3.86 (0.23)	3.51-4.18 (3.87)	
	Group 3	6	4.43 (0.16)	4.12-4.58 (4.46)	
	Group 4	9	4.07 (0.55)	3.26-4.72 (3.93)	
	Control group	2	4.23 (0.27)	4.04-4.42 (4.23)	
Beta-catenin	Group 1	7	3.4 (1.01)	2.4-4.91 (2.89)	0.001†
	Group 2	8	7.7 (0.59)	6.83-8.38 (7.77)	
	Group 3	6	7.24 (0.55)	6.44-7.8 (7.31)	
	Group 4	9	7.44 (0.65)	6.77-8.62 (7.55)	
	Control group	2	2.61 (0.3)	2.4-2.82 (2.61)	
CRP	Group 1	7	94.39 (7.02)	84.75-102.1 (97.2)	0.002†
	Group 2	8	56.72 (16.99)	31.01-78.04 (54.22)	
	Group 3	6	38.95 (17)	23.95-70.31 (34.99)	
	Group 4	9	61.31 (32)	26.62-115.73 (63.3)	
	Control group	2	3.47 (1.25)	2.58-4.35 (3.47)	
TGF beta 1	Group 1	7	263.25 (24.78)	223.79-289.6 (273.79)	0.001†
	Group 2	8	319.33 (32.19)	290.06-367.85 (303.21)	
	Group 3	6	314.58 (25.99)	276.89-344.1 (317.39)	
	Group 4	9	347.78 (45.71)	292.91-406.62 (338.6)	
	Control group	2	218.73 (10.31)	211.44-226.02 (218.73)	
Wnt-16	Group 1	7	540.52 (108.41)	412.83-717.35 (499.64)	0.046*
	Group 2	8	477.53 (32.1)	438.94-539.63 (478.44)	
	Group 3	6	445.24 (63)	371.6-551.3 (439.51)	
	Group 4	9	494.38 (48.79)	431.01-601.12 (489.4)	
	Control group	2	383.61 (14.38)	373.44-393.78 (383.61)	
ALP	Group 1	7	483.84 (9.09)	475.79-502.55 (483.38)	0.002†
	Group 2	8	434.53 (29)	401.06-469.72 (425.22)	
	Group 3	6	401.27 (27.22)	371.43-451.76 (395.72)	
	Group 4	9	466.16 (43.38)	411.81-524.48 (483.1)	
	Control group	2	454.67 (36.05)	429.18-480.17 (454.67)	
GH	Group 1	7	17.41 (1.18)	16.08-18.9 (16.7)	0.002†
	Group 2	8	9.46 (3.7)	5.11-14.45 (8.21)	
	Group 3	6	5.81 (2.91)	3.55-11.34 (4.93)	
	Group 4	9	8.37 (5.04)	4.57-17.37 (7.22)	
	Control group	2	9.53 (0.18)	9.4-9.65 (9.53)	
PTH	Group 1	7	14.17 (3.37)	11.03-18.17 (11.85)	0.006†
	Group 2	8	8.6 (3.18)	5.51-12.48 (6.87)	
	Group 3	6	5.79 (2.58)	4.1-10.87 (4.88)	
	Group 4	9	8.37 (2.91)	4.58-11.93 (7.74)	
	Control group	2	10.43 (0.86)	9.82-11.04 (10.43)	
IL-1 beta	Group 1	7	180.3 (5.35)	174.02-186.34 (181.02)	0.001†
	Group 2	8	164.53 (10.31)	148.8-175.62 (163.42)	
	Group 3	6	140.19 (15.11)	122.26-165.32 (139.56)	
	Group 4	9	192.43 (13.92)	178.32-219.08 (190.02)	
	Control group	2	113.63 (10.72)	106.05-121.21 (113.63)	
IL-6	Group 1	7	81.01 (2.3)	76.84-83.07 (82.21)	0.001†
	Group 2	8	68.79 (3.72)	64.44-73.99 (67.82)	
	Group 3	6	63.45 (3.84)	59.11-69.23 (63.29)	
	Group 4	9	84.04 (8.69)	75.16-95.99 (85.93)	
	Control group	2	46.74 (0.23)	46.58-46.9 (46.74)	
IL-10	Group 1	7	25.69 (2.01)	23.47-28.17 (24.64)	0.001†
	Group 2	8	30.17 (2.26)	30.02-35.96 (33.76)	
	Group 3	6	34.87 (1.71)	33.26-37.23 (34.65)	
	Group 4	9	27.18 (3.42)	21.07-30.95 (27.2)	
	Control group	2	5.65 (0.12)	5.57-5.74 (5.65)	
IL-17A	Group 1	7	220.3 (60.73)	161.3-295.68 (179.88)	0.007†
	Group 2	8	151.7 (14.01)	133.97-167.44 (154.97)	
	Group 3	6	146.41 (5.61)	140.85-154.89 (145.08)	
	Group 4	9	160.37 (14.82)	132.89-174.61 (145.11)	
	Control group	2	141.46 (3.97)	138.65-144.27 (141.46)	
IL-17F	Group 1	7	224.64 (69.4)	152.04-309.8 (174.23)	0.173
	Group 2	8	219.77 (18.07)	222.04-275.34 (243.74)	
	Group 3	6	208.62 (24.98)	198.45-254.2 (233.84)	
	Group 4	9	223.36 (26.53)	206.86-276.59 (230.28)	
	Control group	2	159.88 (13.94)	150.03-169.74 (159.88)	
IL-22	Group 1	7	206.61 (23.7)	175.06-241.08 (199.73)	0.938
	Group 2	8	211.75 (29.2)	170.56-250.12 (219.44)	
	Group 3	6	217.18 (38.8)	173.34-264.89 (212.25)	
	Group 4	9	211.81 (11.63)	198.15-236.61 (209.67)	
	Control group	2	222.23 (19.93)	208.14-236.33 (222.23)	
IL-23	Group 1	7	262 (53.69)	213.37-341.21 (230.99)	0.001†
	Group 2	8	162.34 (12.79)	145.72-183.76 (157.49)	
	Group 3	6	150.58 (6.9)	140.52-160.7 (150.58)	
	Group 4	9	173.3 (26.18)	151.15-226.9 (164.52)	
	Control group	2	154.67 (8.34)	148.77-160.57 (154.67)	
TNF alpha	Group 1	7	139.21 (15)	120.1-166.51 (140.15)	0.001†
	Group 2	8	129.86 (11.07)	115.9-145.1 (129.4)	
	Group 3	6	71.28 (8.24)	60.63-84.32 (69.83)	
	Group 4	9	138.14 (7.15)	129.4-150.31 (137.49)	
	Control group	2	60.92 (0.14)	60.82-61.02 (60.92)	

Kruskal-Wallis test. ALP: alkaline phosphatase, Ca: calcium, CRP: C-reactive protein, GH: growth hormone, IL-1 beta: interleukin 1 beta, IL-6: interleukin-6,IL-10: interleukin 10, IL-17A: interleukin 17A, IL-17F: interleukin 17F, IL-22: interleukin 22, IL-23: interleukin-23, P: phosphate, PTH: parathyroid hormone, TGF beta 1: transforming growth factor beta 1, TNF alpha: tumor necrosis factor alpha. **P*<0.05, †*P*<0.01

When the mean TGF beta 1 levels were evaluated, it was seen that there were significant differences between the groups (*P*=0.001). The TGF beta 1 level in Groups 2, 3, and 4 was significantly higher than Group 1 (*P*=0.001), while the mean TGF beta 1 level in Groups 2 and 4 in the control group was significantly lower than the control group (*P*=0.001). No significant difference was observed in terms of TGF beta 1 level in the within-group evaluations of the treatment groups at all follow-up time points (Table 3).

Significant differences were observed when the mean Wnt-16 levels were compared between the groups (*P*=0.046). The control group was significantly lower when compared to the mean Wnt-16 levels in Groups 1, 2, and 4 (*P*=0.001). No significant difference was observed regarding Wnt-16 levels in the within-group evaluations of the treatment groups at all follow-up time points (Table 3).

Mean ALP levels differed significantly between groups (*P*=0.002). The mean ALP levels in Group 3 were significantly lower than in Group 1 (*P*=0.001), while the mean ALP level in Group 4 was significantly lower compared to Group 3 (*P*=0.001). No significant difference was observed in ALP levels in the within-group evaluations of the treatment groups at all follow-up time points (Table 3). The mean GH levels also significantly differed among the groups (*P*=0.002). The mean GH level in Group 1 was significantly higher than in Groups 2, 3, 4, and 5 (P=0.001), while the mean ALP level in Group 2 was significantly higher than in Group 3 (*P*=0.001). No significant differences in ALP levels were observed in intragroup evaluations of the treatment groups at all follow-up time points (Table 3).

When the groups were compared in terms of mean PTH levels, there were similarly significant differences between the groups (*P*=0.006). The PTH level in Groups 3 and 4 was significantly lower than the mean PTH level in Group 1 (*P*=0.001), while the PTH level in Group 3 was significantly lower than the mean PTH level in Groups 2 and 4 (*P*=0.001). No significant difference was observed in PTH levels in the within-group evaluations of the treatment groups at all follow-up time points (Table 3).

The mean IL-1 beta levels in all treatment groups were significantly higher than in the control group (*P*=0.001). The mean IL-1 beta level in Group 1 was significantly higher than in Groups 2 and 3 (P=0.001) but lower than in Group 4 (*P*=0.001). The mean IL-1 beta level in Group 2 was significantly higher than in Group 3 (P=0.001) but lower than in Group 4 (*P*=0.001). In addition, the mean IL-1 beta level in Group 3 was significantly lower than in Group 4 (*P*=0.001). No significant differences in IL-1 beta levels were observed in intragroup evaluations of the treatment groups at all follow-up time points (Table 3).

The mean IL-6 levels in all treatment groups were significantly higher than in the control group (*P*=0.001). The mean IL-6 level in Group 1 was significantly higher than in Groups 2 and 3 (*P*=0.001). The mean IL-6 levels in Groups 2 and 3 were significantly lower than in Group 4 (*P*=0.001). No significant differences in IL-6 levels were observed in intragroup evaluations of the treatment groups at all follow-up time points (Table 3).

The mean IL-10 levels in all treatment groups were significantly higher than in the control group (*P*=0.001). The mean IL-10 level in Group 1 was significantly lower than in Groups 2 and 3 (P=0.001), while the mean IL-10 levels in Groups 2 and 3 were significantly higher than in Group 4 (*P*=0.001). No significant differences in IL-10 levels were

observed in intragroup evaluations of the treatment groups at all follow-up time points (Table 3).

The mean IL-17A levels differed significantly among the groups (P=0.007). The mean IL-17A level in Group 1 was significantly higher than in all other groups (P=0.001). No significant differences in IL-17A levels were observed in intragroup evaluations of the treatment groups at all follow-up time points (Table 3).

The mean IL-17F levels among the groups did not differ significantly. No significant differences in IL-17F levels were observed in intragroup evaluations of the treatment groups at all follow-up time points (Table 3).

The mean IL-22 levels among the groups did not differ significantly. No significant differences in IL-22 levels were observed in intragroup evaluations of the treatment groups at all follow-up time points (Table 3).

The mean IL-23 levels showed significant differences among the groups (P=0.001). The mean IL-23 level in Group 1 was significantly higher than in the other treatment groups and the control group (P=0.001). The mean IL-23 level in Group 3 was significantly lower than in Group 4 (P=0.001). No significant differences in IL-23 levels were observed in intragroup evaluations of the treatment groups at all follow-up time points (Table 3).

The mean TNF alpha levels in all treatment groups, except Group 3, were significantly higher than in the control group (P=0.001). The mean TNF alpha levels in Groups 1 and 2 were significantly higher than that in Group 3 (P=0.001), whereas the mean TNF alpha level in Group 3 was significantly lower than that in Group 4 (P=0.001). No significant differences in TNF alpha levels were observed in intragroup evaluations of the treatment groups at all follow-up time points (Table 3).

Discussion

The most important outcome of our study is that inflammatory cytokines in HT cases increased more compared to cases with isolated LBFs in the early period, that there was a negative relationship between anti-inflammatory cytokine levels and fracture callus thickness, and that it presented a perspective on the molecular level to the transfer of the positive effect between cases.

Fracture healing comprises three phases: inflammatory, proliferative, and remodeling. The inflammatory phase includes hematoma formation, releasing inflammatory and growth factors, activating phagocytic cells, and migrating, proliferation, and differentiation of mesenchymal cells. TNF alpha, IL-1 beta, IL-6, and TGF beta can be counted among the active mediators during this period [12]. In the proliferation phase, the hematoma is organized, followed by soft and hard callus formation. When an immature bone is formed, growth factors are very effective during this period. In the remodeling phase, the mineralized callus tissue transforms into a load-bearing, stable lamellar bone tissue [13]. The active mediators in this period are TNF alpha, IL-6, IL-1, growth hormone, and parathormone [14]. Our study's first and seventh days correspond to the inflammation phase, the 10^{th} day to the early callus phase, the 20^{th} day to the mineralization phase, and the 30^{th} day to the ossification phase before remodeling.

HT changes the healing process of the fracture and provides faster healing with abundant callus formation [15]. However, the mechanisms affecting fracture union in such combined traumas have not been fully understood. In the literature, the alkaline blood pH caused by hyperventilation after HT, a central hormonal response, and inhibition of the sympathetic nervous system are listed as possible mechanisms [16]. In the current study, we took the serum samples from Group 1 rats with HT at the 24^{th} hour and on the seventh day and transferred them to Group 2 rats without HT to detect this hormonal effect and see its effectiveness.

In a study performed by Gautschi et al. [17] on human serum samples, the authors observed that the Ca levels in serum samples in patients with HT, LBF, and CI were significantly lower than that of the controls until the seventh day. In our study, despite the serum transfer, the Ca levels in the serum-transferred group of rats were found to be similar to those of rats with LBFs.

In Gautschi et al.'s study [17], the phosphate levels in patients with HT, LBF, and CI were lower than that of the controls until the third day. In our study, phosphate values were not different in inter and intragroup comparisons. It is known that PTH is an effective regulator of Ca and phosphate balance, in addition to its effect in increasing osteoblastic differentiation [18]. In human serum samples taken from patients with HT and CI, PTH levels peaked in the first 24 h and showed higher values than isolated LBFs in Khallaf et al.'s study [19]. In another study, PTH levels were found to peak in the first 6–24 h after HT in samples taken from human cases, while the PTH levels in serum samples with CI were higher at 24 h than in cases with HT and LBFs [17]. In our study, the PTH values of rats with HT were higher than those of other rats because serums were obtained in the early period. PTH values were higher in rats with CI and were given serum than in rats with LBFs was attributed to the effect of HT.

Although GH levels were reported to decrease below normal values in the third week after isolated LBFs, the GH levels peaked in rats with HT and CI in the same period [19]. This suggests that it has more of a stimulating effect on GH. In our study, the fact that the GH levels were higher in the rats with HT than in the group with CI suggests that isolated HT has a more stimulating effect on GH.

CRP, which is a strong acute phase reactant, has been reported to increase in the early inflammatory period of fracture healing, and this increase is even more pronounced after HT [20]. In a study conducted on human serum samples, CRP levels up to the seventh day were higher than the control group in cases with HT, LBFs, and CI, while the cases with isolated fractures had the lowest values [17]. In our study, the highest CRP values were found in the sera of rats with HT in the early period.

Alkaline phosphatase is an indicator of early osteogenic differentiation [21]. It has been reported that ALP levels, which indicate bone regeneration, gradually decrease during the first 4 weeks after LBFs, remaining below the control values [1]. In our study, although ALP levels decreased after LBFs, ALP levels suggestive of increased osteoblastic activity were observed in both the HT and the serum-transferred groups. This was evaluated to indicate that serum could transfer the osteoblastic effect between individuals.

TGF beta 1, a powerful stimulator of osteoblastic bone formation, has been reported to increase up to the sixth week following LBFs [1]. In a study conducted on rat tibia fracture models, the researchers stated that local applications of TGF beta positively affected fracture union [22]. In our study, high TGF beta 1 levels were noticed in both the HT and the serum-transferred groups, consistent with the increased fracture callus tissue in these groups.

It has been reported that Wnt-16 directly proliferates the development of osteoblasts while indirectly suppressing osteoclast formation and differentiation. It is also known that, due to its effects on both osteoblasts and osteoclasts, Wnt-16 does not increase initially but rather later in patients with LBFs [23]. The Wnt-16-beta-catenin signaling pathway is activated after HT [24]. Bao et al. [25] stated that slight activation of the Wnt-16-beta-catenin signaling pathway might positively affect fracture healing in the late phase, while Huang et al. [26] reported that inhibition of the beta-catenin signaling pathway delayed fracture healing in mice. The activation of the Wnt-beta-catenin signal pathway reduces inflammatory markers TNF alpha, IL-6, and IL-1 beta [27]. In our study, we observed that the Wnt-16-beta-catenin signal pathway was activated, especially after HT, and this effect was observed in rats in whom serum was transferred.

Tumor necrosis factor alpha has a dual effect; it can suppress new bone formation by stimulating bone reabsorption and destruction. At low concentrations, it stimulates osteogenic differentiation, while at high concentrations, it inhibits it. Tumor necrosis factor alpha has a dual effect; it can suppress new bone formation by stimulating bone reabsorption and destruction. It stimulates osteogenic differentiation at low concentrations and inhibits it at high concentrations. TNF alpha has the effect of stimulating ossification at an early stage. In the following process, TNF alpha suppresses the non-tissue-specific ALP activity and reduces the mineralization process, thus preventing bone formation. Besides, it promotes the secretion of vascular endothelial growth factor (VEGF), which is secreted by neutrophils and directly affects the formation of blood vessels. Together with IL-1 beta [2], it can promote the mineralization of the bone matrix. Chan et al. stated that TNF alpha injections could have a positive effect in the early period (first 24 h) of fracture healing [28]. The high rates of the union in the serum-transferred group in our study may be related to the early collection of these sera from rats with HT.

Interleukin-1 is an inflammatory mediator that appears in the early post-fracture period and activates healing [29]. However, this positive effect is limited to low doses. Brenner et al. [30] reported that IL-1 beta at high concentrations inhibited osteoblast migration while increasing osteoclast activity, thus delaying fracture healing. Ozeki et al. [31] reported that IL-1 beta increased the proliferation of osteoblast-like cells through the Wnt signaling pathway. In our study, we observed that the Wnt-16 levels and IL-1 beta levels showed similar correlations in the groups.

Interleukin-6 is one of the inflammatory mediators released abundantly by osteogenic cells in the early post-fracture period [32]. Beeton et al. [33] reported higher IL-6 levels in CI cases than in HT cases. It is believed that IL-6 regulates osteoblast and osteoclast activity, increases soft callus formation, and affects osteoclastogenesis [34]. In the current study, the IL-6 levels were high in the early period, while the mean IL-6 level in Group 4 rats was higher than that of Group 2. It has been reported that Interleukin 6 and Tumor necrosis factor-alpha levels, which are pro-inflammatory factors, increase first in the first and second weeks after LBFs, and then gradually decrease [1].

Interleukin-17 is a family of pro-inflammatory cytokines. IL-17A suppresses osteoclast differentiation at high doses, and its effects on bone formation are contradictory [35]. IL-17F induces osteogenic differentiation and positively affects osteoblast maturation [21]. In addition, IL-17F increases in the early phase of fracture healing [21]. Our study shows that both IL-17A and IL-17F are elevated early after HT.

Interleukin-23 is a pro-inflammatory cytokine responsible for bone non-union caused by inflammation [36]. It has been stated that the IL-23 levels in rats with a HT model were above those of the controls until the 14th day, peaking on the third day [37]. Our study showed the greatest increase in IL-23 values in Group 1 rats due to HT.

Interleukin-10 has a strong anti-inflammatory effect. It negatively affects the production of pro-inflammatory cytokines, such as IL-1 and IL-6, and inhibits their release [38]. In addition, the cytokine has been reported to suppress osteoclastic activity [39]. In evaluating the group averages of IL-10 levels in our study, the values were lower in rats that had HT and were transferred to serum. We believe that low IL-10 levels are associated with increased union rates. Although IL-22, a member of the IL-10 cytokine family, showed a similar outcome pattern to IL-10 in the treatment groups, no significant difference was observed between the groups.

Our study had some limitations. First, the number of our subjects was relatively few; by increasing the number of subjects, an evaluation could be made with the data to be obtained in similar periods in all groups. Second, we only had radiological outcomes and molecular parameters. A biomechanical and or histopathological evaluation was not performed. Finally, conventional radiography was employed instead of micro CT for radiological examinations.

The literature suggests that the sera obtained from HT cases in *in vitro* cell culture media positively affects osteoblastic cell proliferation [17]. Sari et al. [40] stated that fracture union could be induced radiologically and histopathologically by *in vivo* serum transfer. The importance of inflammatory and anti-inflammatory cytokine balance in the bone union process has been shown at the molecular level.

Conclusion

Our study demonstrates that, at the macro level, the callus thickness was higher in the serum-transferred group than in the cases with isolated fractures. The study also enabled us to obtain more information about the early inflammatory molecular changes of fracture healing, especially in cases with HT. Based on our findings, we concluded that inflammatory cytokines (IL-17A, IL-1 beta, IL-17F, IL-6, IL-23, and tumor necrosis factor-alpha) were elevated in the early period in HT groups and that this effect could be transferred to Group 2 rats by serum transfer.

It is noteworthy that the Wnt-16, IL-1 beta, and TNF alpha values, which positively affect union, were higher in the serum transfer group than the isolated fracture group and that IL-10 levels, a negative modulator on the union, were negatively correlated with callus thickness. Our findings will contribute to developing new therapeutic agents for fracture healing.

References

1. Yu MD, Su BH, Zhang XX. Morphologic and molecular alteration during tibia fracture healing in rat. Eur Rev Med Pharmacol Sci. 2018 Mar;22(5):1233-40. doi: 10.26355/eurrev_201803_14463.
2. Zhang T, Yao Y. Effects of inflammatory cytokines on bone/cartilage repair. J Cell Biochem. 2019 May;120(5):6841-6850. doi: 10.1002/jcb.27953.
3. Echeverri LF, Herrero MA, Lopez JM, Oleaga G. Early stages of bone fracture healing: formation of a fibrin-collagen scaffold in the fracture hematoma. Bull Math Biol. 2015 Jan;77(1):156-83. doi: 10.1007/s11538-014-0055-3.
4. Copuroglu C, Calori GM, Giannoudis PV. Fracture non-union: who is at risk? Injury. 2013 Nov;44(11):1379-82. doi: 10.1016/j.injury.2013.08.003.
5. Oryan A, Monazzah S, Bigham-Sadegh A. Bone injury and fracture healing biology. Biomed Environ Sci. 2015 Jan;28(1):57-71. doi: 10.3967/bes2015.006.
6. Morioka K, Marmor Y, Sacramento JA, Lin A, Shao T, Miclau KR, et al. Differential fracture response to traumatic brain injury suggests dominance of neuroinflammatory response in polytrauma. Sci Rep. 2019 Aug 21;9(1):12199. doi: 10.1038/s41598-019-48126-z.
7. Doblare M, Garcia JM, Gomez MJ. Modelling bone tissue fracture and healing: a review. Eng Fract Mech. 2004;71:1809-40.
8. Marmarou A, Foda MA, van den Brink W, Campbell J, Kita H, Demetriadou K. A new model of diffuse brain injury in rats. Part I: Pathophysiology and biomechanics. J Neurosurg. 1994 Feb;80(2):291-300. doi: 10.3171/jns.1994.80.2.0291.
9. Silva Ddos S, Brito JN, Ibiapina JO, Lima MF, Medeiros AR, Queiroz BH, et al. Traumatic brain injury: clinical and pathological parameters in an experimental weightdrop model. Acta Cir Bras. 2011 Apr;26(2):94-100. doi: 10.1590/s0102-86502011000200004.
10. Bonnarens F, Einhorn TA. Production of a standard closed fracture in laboratory animal bone. J Orthop Res. 1984;2(1):97-101. doi: 10.1002/jor.1100020115.
11. Spencer RF. The effect of head injury on fracture healing. A quantitative assessment. J Bone Joint Surg Br. 1987 Aug;69(4):525-8. doi: 10.1302/0301-620X.69B4.3611151.
12. Brandi ML. How innovations are changing our management of osteoporosis. Medicographia. 2010;32:1-6.
13. Schindeler A, McDonald MM, Bokko P, Little DG. Bone remodeling during fracture repair: The cellular picture. Semin Cell Dev Biol. 2008 Oct;19(5):459-66. doi: 10.1016/j.semcdb.2008.07.004.
14. Mountziaris PM, Mikos AG. Modulation of the inflammatory response for enhanced bone tissue regeneration. Tissue Eng Part B Rev. 2008 Jun;14(2):179-86. doi: 10.1089/ten.teb.2008.0038.
15. Smith R. Head injury, fracture healing and callus. J Bone Joint Surg Br. 1987 Aug;69(4):518-20. doi: 10.1302/0301-620X.69B4.3611149.
16. Giannoudis PV, Mushtaq S, Harwood P, Kambhampati S, Dimoutsos M, Stavrou Z, et al. Accelerated bone healing and excessive callus formation in patients with femoral fracture and head injury. Injury. 2006 Sep;37 Suppl 3:S18-24. doi: 10.1016/j.injury.2006.08.020. Erratum in: Injury. 2007 Oct;38(10):1224.
17. Gautschi OP, Cadosch D, Frey SP, Skirving AP, Filgueira L, Zellweger R. Serum-mediated osteogenic effect in traumatic brain-injured patients. ANZ J Surg. 2009 Jun;79(6):449-55. doi: 10.1111/j.1445-2197.2008.04803.x.
18. Wang YH, Liu Y, Rowe DW. Effects of transient PTH on early proliferation, apoptosis, and subsequent differentiation of osteoblast in primary osteoblast cultures. Am J Physiol Endocrinol Metab. 2007 Feb;292(2):E594-603. doi: 10.1152/ajpendo.00216.2006.
19. Khallaf FG, Kehinde EO, Hussein S. Bone Healing and Hormonal Bioassay in Patients with Long-Bone Fractures and Concomitant Head Injury. Med Princ Pract. 2016;25(4):336-42. doi: 10.1159/000445250.
20. Estrores IM, Harrington A, Banovac K. C-reactive protein and erythrocyte sedimentation rate in patients with heterotopic ossification after spinal cord injury. J Spinal Cord Med. 2004;27(5):434-7. doi: 10.1080/10790268.2004.11752233.
21. Nam D, Mau E, Wang Y, Wright D, Silkstone D, Whetstone H, et al. T-lymphocytes enable osteoblast maturation via IL-17F during the early phase of fracture repair. PLoS One. 2012;7(6):e40044. doi: 10.1371/journal.pone.0040044.
22. Wildemann B, Schmidmaier G, Ordel S, Stange R, Haas NP, Raschke M. Cell proliferation and differentiation during fracture healing are influenced by locally applied IGF-I and TGF-beta1: comparison of two proliferation markers, PCNA and BrdU. J Biomed Mater Res B Appl Biomater. 2003 Apr 15;65(1):150-6. doi: 10.1002/jbm.b.10512.
23. Alam I, Alkhouli M, Gerard-O'Riley RL, Wright WB, Acton D, Gray AK, et al. Osteoblast-Specific Overexpression of Human WNT16 Increases Both Cortical and Trabecular Bone Mass and Structure in Mice. Endocrinology. 2016 Feb;157(2):722-36. doi: 10.1210/en.2015-1281.
24. Salehi A, Jullienne A, Baghchechi M, Hamer M, Walsworth M, Donovan V, et al. Up-regulation of Wnt/β-catenin expression is accompanied with vascular repair after traumatic brain injury. J Cereb Blood Flow Metab. 2018 Feb;38(2):274-89. doi: 10.1177/0271678X17744124.
25. Bao Q, Chen S, Qin H, Feng J, Liu H, Liu D, et al. An appropriate Wnt/β-catenin expression level during the remodeling phase is required for improved bone fracture healing in mice. Sci Rep. 2017 Jun 2;7(1):2695. doi: 10.1038/s41598-017-02705-0.
26. Huang Y, Zhang X, Du K, Yang F, Shi Y, Huang J, et al. inhibition of β-catenin signaling in chondrocytes induces delayed fracture healing in mice. J Orthop Res. 2012 Feb;30(2):304-10. doi: 10.1002/jor.21505.
27. Zhao C, Yu T, Dou Q, Guo Y, Yang X, Chen Y. Knockout of TLR4 promotes fracture healing by activating Wnt/β-catenin signaling pathway. Pathol Res Pract. 2020 Feb;216(2):152766. doi: 10.1016/j.prp.2019.152766.
28. Chan JK, Glass GE, Ersek A, Freidin A, Williams GA, Gowers K, et al. Low-dose TNF augments fracture healing in normal and osteoporotic bone by up-regulating the innate immune response. EMBO Mol Med. 2015 May;7(5):547-61. doi: 10.15252/emmm.201404487.
29. Kon T, Cho TJ, Aizawa T, Yamazaki M, Nooh N, Graves D, et al. Expression of osteoprotegerin, receptor activator of NF-kappaB ligand (osteoprotegerin ligand) and related pro-inflammatory cytokines during fracture healing. J Bone Miner Res. 2001 Jun;16(6):1004-14. doi: 10.1359/jbmr.2001.16.6.1004.
30. Hengartner NE, Fiedler J, Ignatius A, Brenner RE. IL-1β inhibits human osteoblast migration. Mol Med. 2013 Apr 30;19(1):36-42. doi: 10.2119/molmed.2012.00058.
31. Ozeki N, Mogi M, Hase N, Hiyama T, Yamaguchi H, Kawai R, et al. Wnt16 Signaling Is Required for IL-1β-Induced Matrix Metalloproteinase-13-Regulated Proliferation of Human Stem Cell-Derived Osteoblastic Cells. Int J Mol Sci. 2016 Feb 6;17(2):221. doi: 10.3390/ijms17020221.
32. Feyen JH, Elford P, Di Padova FE, Trechsel U. Interleukin-6 is produced by bone and modulated by parathyroid hormone. J Bone Miner Res. 1989 Aug;4(4):633-8. doi: 10.1002/jbmr.5650040422.
33. Beeton CA, Chatfield D, Brooks RA, Rushton N. Circulating levels of interleukin-6 and its soluble receptor in patients with head injury and fracture. J Bone Joint Surg Br. 2004 Aug;86(6):912-7. doi: 10.1302/0301-620x.86b6.14176.
34. Thomas MV, Puleo DA. Infection, inflammation, and bone regeneration: a paradoxical relationship. J Dent Res. 2011 Sep;90(9):1052-61. doi: 10.1177/0022034510393967.
35. Kitami S, Tanaka H, Kawato T, Tanabe N, Katono-Tani T, Zhang F, et al. IL-17A suppresses the expression of bone resorption-related proteinases and osteoclast differentiation via IL-17RA or IL-17RC receptors in RAW264.7 cells. Biochimie. 2010 Apr;92(4):398-404. doi: 10.1016/j.biochi.2009.12.011.
36. Xu J, Wang Y, Li J, Zhang X, Geng Y, Huang Y, et al. IL-12p40 impairs mesenchymal stem cell-mediated bone regeneration via CD4+ T cells. Cell Death Differ. 2016 Dec;23(12):1941-51. doi: 10.1038/cdd.2016.72.
37. Li T, Zhang YM, Han D, Hua R, Guo BN, Hu SQ, et al. Involvement of IL-17 in Secondary Brain Injury After a Traumatic Brain Injury in Rats. Neuromolecular Med. 2017 Dec;19(4):541-54. doi: 10.1007/s12017-017-8468-4.
38. Grütz G. New insights into the molecular mechanism of interleukin-10-mediated immunosuppression. J Leukoc Biol. 2005 Jan;77(1):3-15. doi: 10.1189/jlb.0904484.
39. Yang S, Ding W, Feng D, Gong H, Zhu D, Chen B, et al. Loss of B cell regulatory function is associated with delayed healing in patients with tibia fracture. APMIS. 2015 Nov;123(11):975-85. doi: 10.1111/apm.12439.
40. Sarı A, Dinçel YM, Çetin MÜ, İnan S. Can fracture healing be accelerated by serum transfer in head trauma cases? An experimental head trauma model in rats. Jt Dis Relat Surg. 2021;32(2):306-12. doi: 10.52312/jdrs.2021.8.

J Surg Med. 2023;7(5):314-318.
DOI: 10.28982/josam.7674

Research article

Journal of Surgery and Medicine
e-ISSN: 2602-2079
https://jsurgmed.com/

Inflammation-based biomarkers for the prediction of nephritis in systemic lupus erythematosus

Nurdan Orucoglu

Department of Internal Medicine, Division of Rheumatology, Mersin University Faculty of Medicine, Mersin, Turkey

ORCID ID of the author(s)
NO: 0000-0002-8613-5373

Corresponding Author
Nurdan Orucoglu
Department of Internal Medicine, Division of Rheumatology, Mersin University Faculty of Medicine, Mersin, TR-33343, Turkey
E-mail: nurdanorucoglu@yahoo.com

Ethics Committee Approval
The study was approved by the ethics committee of Mersin University Faculty of Medicine, Turkey (2020/591).
All procedures in this study involving human participants were performed in accordance with the 1964 Helsinki Declaration and its later amendments.

Conflict of Interest
No conflict of interest was declared by the authors.

Financial Disclosure
The authors declared that this study has received no financial support.

Published
2023 May 15

Abstract

Background/Aim: Inflammation is a crucial component in the pathophysiology of systemic lupus erythematosus (SLE) nephritis. Immune-based scores, such as the neutrophil-lymphocyte and the platelet-lymphocyte ratios (NLR and PLR, respectively) have been suggested as predictors of inflammation and prognosis in SLE. This study aimed to investigate the value of the systemic immune-inflammation index (SII), inflammatory prognostic index (IPI), and systemic inflammatory response index (SIRI) in SLE and lupus nephritis (LN).

Methods: This case-control study consisted of 108 newly diagnosed SLE patients (separated into two subgroups, which included 34 patients with biopsy-proven LN and 74 without nephritis) and 108 age- and gender-matched healthy controls who presented to our outpatient clinic between October 2015 and June 2020. Patients with malignancy, lymphoproliferative and hematologic disorders, active infection, and autoimmune diseases other than SLE were excluded. Inflammation-based biomarkers were calculated at the first presentation of the disease and before any medication was administered. SII was calculated as Neutrophil/Lymphocyte x Platelet, SIRI as Neutrophil x Monocyte/Lymphocyte, and IPI as CRP x NLR/serum albumin. The Systemic Lupus Erythematosus Disease Activity Index 2000 (SLEDAI-2K) was used to measure disease activity. The capability of SII, SIRI, NLR, PLR, and IPI to distinguish between SLE patients with or without nephritis was assessed using receiver operating characteristic (ROC) curves. Correlations of inflammation-based scores (SII, SIRI, IPI, NLR) with disease activity and laboratory data of SLE patients were analyzed.

Results: SII, SIRI, and IPI were significantly higher in SLE patients than in healthy controls (P=0.003, P=0.019, and P<0.001, respectively) and also significantly higher in patients with nephritis than in those without (P<0.001, P=0.009, and P=0.007, respectively). The area under the curve (AUC) for SII, SIRI, and IPI in terms of differentiating SLE patients with or without nephritis was 0.748, 0.690, and 0.663, respectively. The cut-off value of SII, SIRI, and IPI to predict LN was 552.25 (sensitivity: 64.7%; specificity: 64.9%; P<0.001), 1.08 (sensitivity: 61.8%; specificity: 62.2%; P=0.002), and 4.48 (sensitivity: 61.8%; specificity, 62.2%; P=0.007), respectively.

Conclusion: SII, SIRI, and IPI may be valuable and promising inflammation-based biomarkers in SLE and for the presence of nephritis in SLE patients. SII was found to be the most reliable predictor of SLE among the inflammation-based biomarkers in our study.

Keywords: lupus nephritis, inflammation, systemic lupus erythematosus

How to cite: Orucoglu N. Inflammation-based biomarkers for the prediction of nephritis in systemic lupus erythematosus. J Surg Med. 2023;7(5):314-318.

Introduction

Systemic lupus erythematosus (SLE) is a complex multisystem, autoimmune disease involving almost all organs [1]. The impact of inflammation on disease pathogenesis and prognosis is well-established [2]. Lupus nephritis (LN) is a leading cause of mortality and morbidity. Despite immunosuppressive treatments, approximately 40% of patients develop renal failure [3]. Thus, prompt identification and early treatment of LN are essential. The need for biomarkers to enable a rapid and easy assessment of inflammatory status in renal involvement in SLE patients exists. Many serum markers, such as C-reactive protein (CRP), erythrocyte sedimentation rate (ESR), complements, and anti-double-stranded DNA (anti-dsDNA), are used to assess the inflammatory status, organ damage, and disease activity of SLE [4]. However, these markers can be costly to use during follow-up and can be influenced by some conditions, such as infections and hypergammaglobulinemia [5,6]. Furthermore, clinical and serological variety in addition to diversity may affect the correct interpretation of disease activity and inflammation.

Neutrophil, lymphocyte, monocyte, and platelet counts are routinely performed during clinical evaluations and follow-ups. Numerous studies have shown the role of neutrophil-to-lymphocyte and platelet-to-lymphocyte ratio (NLR and PLR, respectively) in determining inflammation and prognosis in rheumatic diseases and malignancies [7, 8]. Recent studies have identified NLR and PLR as valuable biomarkers in the assessment of inflammation and disease activity in SLE [7].

The systemic immune-inflammation index (SII) is a combination of platelet count and NLR. SII was recently developed by Hu et al. [9] as a novel inflammation marker to evaluate the predictive value in hepatocellular carcinoma (HCC) and has been widely studied in many malignancies [10]. It has been reported that SII could provide better information than NLR and PLR about systemic inflammation in cancer patients [9]. The Systemic Inflammatory Response Index (SIRI) and the Inflammatory Prognostic Index (IPI) are two other inflammatory biomarkers that have been shown to be valuable in predicting the prognosis of various types of malignancy. [11,12]. In addition to NLR, CRP, and albumin are used to calculate IPI and monocyte count for SIRI.

Limited evidence in the literature evaluating the association between inflammation-based biomarkers such as SII, SIRI, and renal involvement in SLE patients is available. Also, the association between IPI and SLE has not been previously reported. Therefore, the goal of the study was to evaluate the value of the SII, SIRI, and IPI for predicting the presence of nephritis in SLE patients.

Materials and methods

Study design

This case-control study included 108 SLE patients (34 with biopsy-proven lupus nephritis and 74 without nephritis) and gender and age-matched 108 healthy control (HC) groups who applied to our outpatient clinic between October 2015 and June 2020. SLE patients had been newly diagnosed in our center and did not yet receive treatment. Inflammation-based biomarkers are calculated at the first presentation of the disease and before any medication. Patients with malignancy, lymphoproliferative and hematological disorders, active infection, and autoimmune diseases other than SLE were excluded. The flow diagram of included SLE patients and controls is shown in Figure 1. The study was approved by the Research Ethics Committee of Mersin University (2020/591). The study was conducted in compliance with the Declaration of Helsinki.

Figure 1: Flow diagram of included Systemic Lupus Erythematosus (SLE) patients and controls

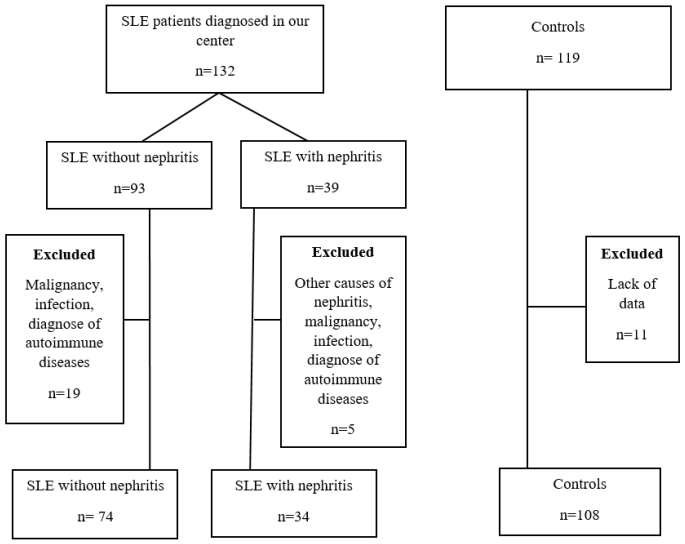

Participant selection

G*power 3.1 was used to calculate the sample size (Franz Faul, University of Kiel, Germany). With a Type I error of 0.05 and an 80% confidence interval, a sample size of at least 29 was required.

All SLE patients' diagnoses were based on the established 2012 Systemic Lupus International Collaborating Clinics Classification (SLICC) criteria [13]. Patients with LN were those who had the diagnosis confirmed by a biopsy.

The healthy control group consisted of healthcare providers who applied to the general internal medicine outpatient clinic for regular periodic checkups and had no known diseases.

Data collection

All subjects' demographic characteristics and clinical and laboratory data were obtained from the medical records. Information was obtained from the patients before treatment, including glucocorticoids: (1) white blood cell count, (2) lymphocyte, neutrophil, and platelet count, (3) ESR, (4) CRP, (5) complement C3 and C4, (6) creatinine, and (7) albumin. Autoantibodies, including anti-dsDNA, anti-nuclear, anti-Smith, and anti-SS-A/anti-SS-B, were recorded.

Disease activity was measured by the Systemic Lupus Erythematosus Disease Activity Index 2000 (SLEDAI-2K) [14].

Calculations of systemic inflammation-related indices

SII was calculated as Neutrophil/Lymphocyte x Platelet, SIRI as Neutrophil x Monocyte/Lymphocyte, NLR as Neutrophil/Lymphocyte, IPI as CRP × NLR/serum Albumin, and PLR as Platelet/Lymphocyte.

Statistical analysis

Statistical analyses were performed using IBM SPSS 18.0 (SPSS Inc., Chicago, USA). The demographic and laboratory data are given as means and standard deviations. The

distribution of the variables was tested with the Kolmogorov–Smirnov test. Student's t-test was used to analyze the difference between the two groups if it's normally distributed. Otherwise, the Mann–Whitney U test was used. The variables' correlation was assessed using Spearman's correlation for non-normal and Pearson's correlation for normal distribution. Receiver operating characteristics (ROC) were used to evaluate the ability of SII, SIRI, NLR, PLR, and IPI to differentiate between SLE patients with nephritis or without nephritis. $P<0.05$ was considered statistically significant.

Results

Demographic data and laboratory findings are shown in Table 1. In both groups, 99 patients were female (91.6%), and nine were male (8.3%). The mean age of SLE patients was 37.33 (12.45) years. No significant differences in gender and age between the groups were found ($P>0.05$). Symptom duration was 8.91 (11.92) months. Biopsy-proven LN was present in 34 (31.5%) patients. All patients were separated into three groups: (1) control, (2) SLE without nephritis, and (3) SLE with nephritis. Neutrophil, lymphocyte, leucocyte, monocyte, platelet counts were lower in SLE patients compared to healthy controls ($P<0.001$ for all). NLR and PLR were higher in SLE patients than in healthy controls ($P<0.001$ for all). SII, IPI, and SIRI were also higher in SLE patients than in healthy controls (685.18 [561.82] versus 512.74 [197.37]; $P=0.003$, 11.04 (20.33) versus 1.30 [1.48]; $P<0.001$, 1.30 [1.19] versus 1.00 [0.48]; $P=0.019$, respectively) as shown in Table 1.

Table 1: Demographic and laboratory parameters of patients and healthy controls.

	Healthy control (n=108) Mean (SD)	SLE (n=108) Mean (SD)	*P*-value
Age (years)	39.59 (12.00)	37.33 (12.45)	0.176
ESR (mm/hour)	12.16 (8.55)	40.94 (28.24)	<0.001
CRP (mg/L)	3.39 (3.52)	13.29 (26.47)	<0.001
Leukocytes ($\times10^3$/mm^3)	7.434 (1.69)	5.491 (2.21)	<0.001
Neutrophils ($\times10^3$/mm^3)	4.357 (1.31)	3.545 (1.69)	<0.001
Lymphocytes ($\times10^3$/mm^3)	2.35 (0.53)	1.379 (0.82)	<0.001
Platelets ($\times10^3$/mm^3)	268.93 (57.61)	222.49 (97.17)	<0.001
Monocyte ($\times10^3$/mm^3)	0.521 (0.151)	0.402 (0.156)	<0.001
NLR	1.90 (0.60)	3.23 (2.51)	<0.001
PLR	119.11 (32.55)	201.59 (135.13)	<0.001
SII	512.74 (197.37)	685.18 (561.82)	0.003
SIRI	1.00 (0.48)	1.30 (1.19)	0.019
IPI	1.30 (1.48)	11.04 (20.33)	<0.001
Creatinine (mg/dL)	0.61 (0.11)	0.75 (0.37)	<0.001
Albumin (g/dL)	43.3 (3.2)	36.11 (8.82)	<0.001
Proteinuria (mg/day)		1240.24 (2339.24)	
SLEDAI-2K		9.70 (8.51)	
C3 (mg/dL)		74.87 (36.32)	
C4 (mg/dL)		14.24 (9.02)	
		n, %	
ANA		104, 96.3%	
Anti-SS-A/Anti-SS-B		34, 31.5%	
Anti-Smith		24, 22.2%	
Anti-dsDNA		51, 47.2%	
Nephritis		34, 31.5%	

ANA: Anti-Nuclear Antibody, CRP: C-Reactive Protein, dsDNA: Anti-Double Stranded Antibodies, ESR: Erythrocyte Sedimentation Rate, IPI: Inflammatory prognostic index, NLR: Neutrophil-to-Lymphocyte Ratio, PLR: Platelet to-Lymphocyte Ratio, SD: Standard Deviation, SII: Systemic Immune-Inflammation Index, SLE: Systemic Lupus Erythematosus, SLEDAI-2K: Systemic Lupus Erythematosus Disease Activity Index 2000, SIRI: Systemic inflammation response index

SII, SIRI, IPI, NLR, and PLR values were significantly higher in SLE patients with nephritis than those without nephritis ($P<0.001$, $P=0.009$, $P=0.007$, $P=0.014$, and $P=0.002$, respectively). ESR, CRP, SLEDAI-2K, and C3 and 4 levels were not statistically different between the SLE patients without nephritis and LN ($P>0.05$ for all) as shown in Table 2.

Table 2: Differences between inflammatory biomarkers and disease activity in patients with lupus nephritis and without nephritis.

	SLE with nephritis (n=34) Mean (SD)	SLE without nephritis (n=74) Mean (SD)	*P*-value
ESR (mm/hour)	39.67 (31.85)	41.52 (26.63)	0.753
CRP (mg/L)	12.50 (17.14)	13.65 (29.90)	0.836
NLR	4.36 (3.55)	2.71 (1.64)	0.014
PLR	258.82 (154.47)	175.29 (117.27)	0.002
SII	1009.0 (730.39)	536.40 (387.58)	<0.001
SIRI	1.74 (1.46)	1.10 (0.98)	0.009
IPI	19.54 (30.58)	7.13 (11.58)	0.007
SLEDAI-2K	10.82 (9.83)	9.18 (7.85)	0.357
C3 (mg/dL)	74.16 (44.03)	75.19 (32.51)	0.891
C4 (mg/dL)	14.93 (10.52)	13.92 (8.30)	0.593

CRP: C-Reactive Protein, ESR: Erythrocyte Sedimentation Rate, IPI: Inflammatory prognostic index, NLR: Neutrophil-to-Lymphocyte Ratio, PLR: Platelet to-Lymphocyte Ratio, SD: Standard Deviation, SII: Systemic Immune-Inflammation Index, SLE: Systemic Lupus Erythematosus, SLEDAI-2K: Systemic Lupus Erythematosus Disease Activity Index 2000, SIRI: Systemic inflammation response index

SII was not correlated with SLEDAI-2K, complement levels, creatinine, proteinuria, ESR, or CRP levels in SLE patients ($P>0.05$ for all). SIRI was correlated with C3, C4 and serum creatinine levels ($r=0.236$; $P=0.014$, $r=0.268$; $P=0.005$, $r=0.195$; and $P=0.043$, respectively). NLR only correlated with serum creatinine ($r=0.215$; $P=0.025$). IPI was positively correlated with SLEDAI-2K, ESR, CRP, serum creatinine, and proteinuria ($r=0.209$; $P=0.030$, $r=0.530$; $P<0.001$, $r=0.625$; $P<0.001$, $r=0.264$; $P=0.006$, and $r=0.345$; $P<0.001$, respectively) as shown in Table 3.

Table 3: Correlations of inflammation-based scores (SII, SIRI, IPI, NLR) with disease activity and laboratory data of SLE patients.

	SII		SIRI		IPI		NLR	
	r	*P*-value	*r*	*P*-value	*r*	*P*-value	*r*	*P*-value
SLEDAI-2K	0.086	0.375	-0.004	0.970	0.209	0.030	0.012	0.906
C3	0.058	0.554	0.236	0.014	0.108	0.264	0.186	0.054
C4	0.041	0.671	0.268	0.005	0.082	0.399	0.175	0.070
ESR	0.139	0.151	-0.072	0.459	0.530	<0.001	0.047	0.631
CRP	-0.088	0.363	-0.149	0.123	0.625	<0.001	-0.118	0.223
Creatinine (mg/L)	0.182	0.059	0.195	0.043	0.264	0.006	0.215	0.025
Proteinuria (mg/day)	0.085	0.384	0.111	0.252	0.345	<0.001	0.094	0.332

CRP: C-Reactive Protein, ESR: Erythrocyte Sedimentation Rate, IPI: Inflammatory prognostic index, NLR: Neutrophil-to-Lymphocyte Ratio, SII: Systemic Immune-Inflammation Index, SLEDAI-2K: Systemic Lupus Erythematosus Disease Activity Index 2000, SIRI: Systemic inflammation response index

The area under the curve (AUC) for SII in terms of differentiating SLE patients with or without nephritis was 0.748. The cutoff SII value was 555.26 sensitivity, 64.7% specificity 64.9%, and 95% confidence interval (CI) 0.651–0.845 ($P<0.001$). However, the AUCs for NLR, PLR, SIRI, and IPI were <0.7. AUC for NLR in terms of differentiating SLE patients with or without nephritis was 0.665 (95% CI: 0.547–0.784; $P=0.006$), and the cutoff NLR value was 2.64 (sensitivity: 64.7%,specificity: 64.9%). AUC for PLR was 0.687 (95% CI: 0.579–0.796; $P=0.002$), and the cutoff PLR value was 182.73 (sensitivity: 64.7%,specificity: 63.5%). AUC for SIRI was 0.690 (95% CI: 0.584–0.797; $P=0.002$), and the cutoff SIRI value was 1.08 (sensitivity: 61.8%, specificity: 62.2%). AUC for IPI was 0.663 (95% CI 0.550–0.776; $P=0.007$), and the cutoff IPI value was 4.48 (sensitivity: 61.8%, specificity: 62.2%) as shown in Figure 2.

Figure 2: Receiver operating characteristics analysis of SII, NLR, and PLR for differentiating SLE patients with nephritis from SLE patients without nephritis.

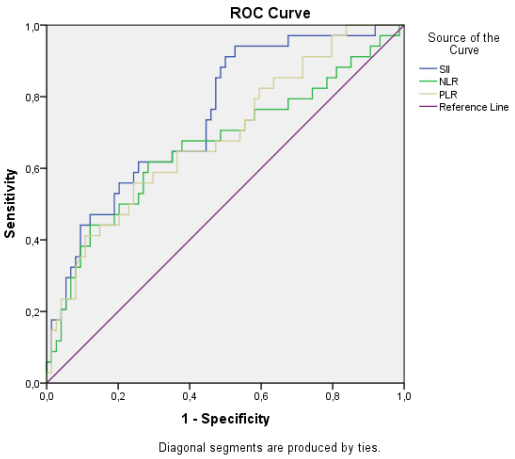

Discussion

The need for biomarkers that can facilitate a fast and easy assessment of ongoing inflammation in SLE is present. NLR and PLR were found to be increased in SLE patients and might be a relevant indicator of inflammation and disease activity [15]. However, the role of SII, SIRI, IPI, which are composite indices, is not entirely clear.

This study was conducted to assess the clinical value of SII, SIRI, and IPI in evaluating SLE and LN. Our results show that SII, SIRI, and IPI were higher in SLE patients than in controls, and they were also higher in SLE with nephritis than without. This finding indicates that SII, SIRI, and IPI may be easy-to-use, widely available, and inexpensive inflammation markers for SLE and LN.

SLE is characterized by enhanced autoantibody generation, leukocyte recruitment, immune complex deposition, and complement activation, all of which result in acute and chronic inflammation and tissue damage [16]. The interactions between neutrophils, dendritic cells, interferon alpha (IFN)-alpha, and autoantibodies are essential events in SLE pathogenesis, which initiates and maintains chronic inflammation [17]. Systemic inflammation can induce neutrophilia and lymphopenia in the peripheral blood and correlates with the severity of inflammation [18]. Neutrophils and platelets play an active role in both systemic and local inflammatory responses [19, 20]. Based on this process, many hematological indices, including the NLR, PLR, and mean platelet value (MPV), have been reported as potential biomarkers of systemic inflammation in various rheumatic disorders in recent years [7, 21].

Qin et al.'s [22] studies show that NLR, MPV, and PLR were higher in SLE patients and correlated with acute phase reactants and disease activity. Wu et al. [15] reported that NLR and PLR were higher in SLE compared to controls and also positively correlated with SLEDAI scores. Additionally, NLR was higher in patients with nephritis. Similarly, Yu et al. [23] reported a positive correlation between NLR and ESR, CRP, and SLEDAI-2K in a study that included 201 healthy controls and 212 SLE patients. However, they emphasized that NLR did not correlate with complement levels, possibly due to different inflammatory markers involved in distinct biological processes. NLR was higher in SLE than in healthy controls according to a meta-analysis of 14 article that included SLE (1,781 patients) and healthy controls (1,330). Furthermore, NLR indicates active disease and renal involvement [24].

SLEDAI-2K is a weighted index developed for evaluating SLE-related disease activity [14]. Although this index includes thrombocytopenia and leukopenia, the index does not include lymphopenia. However, lymphopenia is the most common white blood count abnormality among patients with SLE [10]. Furthermore, SLEDAI-2K assesses the disease manifestations as absent or present rather than according to their severity, so it may not be capable of detecting the degree of disease activity or inflammation with adequate sensitivity [25].

As a consequence of immunological responses, LN is characterized by immune complex deposition, autoantibody generation, and infiltration of inflammatory cells [16]. Aggressive and rapid treatment is essential to achieve remission and prevent renal damage. It has been shown that platelets mediate neutrophil-induced glomerular injury and immune complex nephritis [26]. Li et al. [27] reported that NLR is independently associated with SLE and may reflect renal involvement. Similarly, Ayna et al. [28] reported that NLR and MPV could be predictors of LN. In our study, we found that the SII, SIRI, and IPI indices may reflect renal involvement.

A recent study reported that SII was significantly higher in SLE patients, whereas NLR was performed better as a biomarker than SII [29]. However, in our study, SII was the most reliable index among SIRI, NLR, PLR, and IPI indices. In line with our findings, no association between SLEDAI-2K and SII in that study was described. Our findings revealed only a weak correlation between SLEDAI and IPI, but no correlation between other indices and SLEDAI was found.

Our study showed that SII, IPI, and SIRI might predict LN. SII, SIRI, and IPI (which require only whole blood counts, CRP, and serum albumin) and may be promising inflammation biomarkers for the diagnosis of LN and follow-up due to their low cost and practical use. Furthermore, to our knowledge, this study is the first one to evaluate the usefulness of IPI as a marker for SLE and LN.

Limitations

A small sample size and the study's retrospective design are the main limitations of our study. Biomarkers are only based on a single measurement of whole blood count and biochemistry at the time of disease onset. Another limitation is that the study was conducted in a single center. This study is a retrospective study in which data was extracted and entered manually. The measurement of peripheral blood cells with an automated counter may also have caused the measurement error. Bias in patient selection is another possibility. The fact that our study was conducted at a tertiary care center to which more severely ill patients are referred may have resulted in patient selection bias.

Conclusion

In conclusion, SII, SIRI, and IPI may be valuable inflammation biomarkers in SLE nephritis, and they may serve as indicators of nephritis in SLE patients. SII seems to be the most reliable predictor of LN among the inflammation-based biomarkers (SIRI, IPI, NLR, PLR) in our study. SII, SIRI, and IPI can be used to determine patients' renal involvement or exacerbation of renal disease in conjunction with other

inflammatory markers. They may help clinicians identify subgroups of patients who are at risk of high nephritis relapses of or predict treatment response.

Acknowledgments

I would like to thank Professor Dr. Abdullah Canataroglu, my dear mentor and colleague, for sharing his valuable knowledge and experience with me, as well as for his unconditional support. I will remember him with respect and gratitude

References

1. D'Cruz DP. Systemic lupus erythematosus. BMJ. 2006;332(7546):890-4. doi: 10.1136/bmj.332.7546.890.
2. Gottschalk TA, Tsantikos E, Hibbs ML. Pathogenic Inflammation and Its Therapeutic Targeting in Systemic Lupus Erythematosus. Front Immunol. 2015;6:550. doi: 10.3389/fimmu.2015.00550.
3. Davidson A. What is damaging kidney in lupus nephritis? Nat Rev Rheumatol. 2016;12(3):143-53. doi: 10.1038/nrrheum.2015.159.
4. Liu CC, Ahearn JM. The search for lupus biomarkers. Best Pract Res Clin Rheumatol. 2009;23(4):507–23. doi: 10.1016/j.berh.2009.01.008.
5. Littlejohn E, Marder W, Lewis E, Francis S, Jackish J, McCune WJ, et al. The ratio of erythrocyte sedimentation rate to C-reactive protein is useful in distinguishing infection from flare in systemic lupus erythematosus patients presenting with fever. Lupus. 2018;27(7):1123–9. doi: 10.1177/0961203318763732.
6. Lo MS, Zurakowski D, Son MB, Sundel RP. Hypergammaglobulinemia in the pediatric population as a marker for underlying autoimmune disease: a retrospective cohort study. Pediatr Rheumatol. 2013;11:42. doi: 10.1186/1546-0096-11-42.
7. Hao X, Li D, Wu D, Zhang N. The Relationship between Hematological Indices and Autoimmune Rheumatic Diseases (ARDs), a Meta-Analysis. Sci Rep. 2017;7:10833. doi: 10.1038/s41598-017-11398-4.
8. Zhang Y, Lu JJ, Du YP, Feng CX, Wang LQ, Chen MB. Prognostic value of neutrophil-to-lymphocyte ratio and platelet-to-lymphocyte ratio in gastric cancer. Medicine (Baltimore). 2018;97(12): e0144. doi: 10.1097/MD.0000000000010144.
9. Hu B, Yang XR, Xu Y, Sun YF, Sun C, Guo W, et al. Systemic Immune-Inflammation Index Predicts Prognosis of Patients after Curative Resection for Hepatocellular Carcinoma. Clin Cancer Res. 2014;20(23):6212-22. doi: 10.1158/1078-0432.CCR-14-0442.
10. Zhong JH, Huang, DH, Chen ZY. Prognostic role of systemic immune-inflammation index in solid tumors: a systematic review and meta-analysis. Oncotarget. 2017;8(43):75381–8. doi: 10.18632/oncotarget.18856.
11. Dirican N, Dirican A, Anar C, Atalay S, Ozturk O, Bircan A, et al. A New Inflammatory Prognostic Index, Based on C-reactive Protein, the Neutrophil to Lymphocyte Ratio and Serum Albumin is Useful for Predicting Prognosis in Non-Small Cell Lung Cancer Cases. Asian Pac J Cancer Prev 2016;17(12):5101–5106. doi: 10.22034/APJCP.2016.17.12.5101
12. Gu L, Ma X, Wang L, Li H, Chen L, Li X, et al. Prognostic value of a systemic inflammatory response index in metastatic renal cell carcinoma and construction of a predictive model. 2016;8(32):52094-103. doi: 10.18632/oncotarget.10626
13. Petri M, Orbai AM, Alarcón GS, Gordon C, Merrill JT, Fortin PR, et al. Derivation and validation of the Systemic Lupus International Collaborating Clinics classification criteria for systemic lupus erythematosus. Arthritis Rheum. 2012;64(8):2677-86. doi:10.1002/art.34473.
14. Gladman DD, Ibañez D, Urowitz MB. Systemic lupus erythematosus disease activity index 2000. J Rheumatol. 2002;29(2):288–91.
15. Wu Y, Chen Y, Yang X, Chen L, Yang Y. Neutrophil-to-lymphocyte ratio (NLR) and platelet-to-lymphocyte ratio (PLR) were associated with disease activity in patients with systemic lupus erythematosus. Int Immunopharmacol. 2016;36:94–9. doi: 10.1016/j.intimp.2016.04.006.
16. Lema GP, Maier H, Nieto E, Vielhauer V, Luckow B, Mampaso F, et al. Chemokine expression precedes inflammatory cell infiltration and chemokine receptor and cytokine expression during the initiation of murine lupus nephritis. JASN. 2001;12(7):1369–82. doi: 10.1681/ASN.V1271369.
17. Elkon KB, Stone VV. Type I interferon and systemic lupus erythematosus. J Interferon Cytokine Res. 2001;31(11):803–12. doi: 10.1089/jir.2011.0045.
18. Zahorec R. Ratio of neutrophil to lymphocyte counts rapid and simple parameter of systemic inflammation and stress in critically ill. Bratisl Lek Listy. 2001;102(1): 5-14.
19. Semple JW, Italiano JE Jr, Freedman J. Platelets and the immune continuum. Nat Rev Immunol. 2011;11(4):264–74. doi: 10.1038/nri2956.
20. Linge P, Fortin PR, Lood C, et al. The non-haemostatic role of platelets in systemic lupus erythematosus. Nat Rev Rheumatol. 2018;14(4):195–213.
21. Uslu AU, Küçük A, Şahin A, Ugan Y, Yılmaz R, Güngör T, et al. Two new inflammatory markers associated with Disease Activity Score-28 in patients with rheumatoid arthritis: neutrophil-lymphocyte ratio and platelet-lymphocyte ratio. Int J Rheum Dis. 2015;18(7):731–5. doi: 10.1111/1756-185X.12582.
22. Qin B, Ma N, Tang Q, Wei T, Yang M, Fu H, et al. Neutrophil to lymphocyte ratio (NLR) and platelet to lymphocyte ratio (PLR) were useful markers in assessment of inflammatory response and disease activity in SLE patients. Mod Rheumatol. 2016;26(3):372-6. doi: 10.3109/14397595.2015.1091136.
23. Yu H, Jiang L, Yao L, Gan C, Han X, Liu R, et al. Predictive value of the neutrophil-to-lymphocyte ratio and hemoglobin in systemic lupus erythematosus. Exp Ther Med. 2018;16(2):1547–53. doi: 10.3892/etm.2018.6309.
24. Wang L, Wang C, Jia X, Yang M, Yu J. Relationship between Neutrophil-to-Lymphocyte Ratio and Systemic Lupus Erythematosus: A Meta-analysis. Clinics. 2020;75:e1450. doi: 10.6061/clinics/2020/e1450.
25. Castrejón I, Tani C, Jolly M, Huang A, Mosca M. Indices to assess patients with systemic lupus erythematosus in clinical trials, long-term observational studies, and clinical care. Clin Exp Rheumatol. 2014;32(5):85-95.
26. Johnson RJ, Alpers CE, Pritzl P, Schulze M, Baker P, Pruchno C, et al. Platelets mediate neutrophil-dependent immune complex nephritis in the rat. J Clin Invest. 1988;82(4):1225–35. doi: 10.1172/JCI113720.
27. Li L, Xia Y, Chen C, Cheng P, Peng C. Neutrophil-lymphocyte ratio in systemic lupus erythematosus disease: a retrospective study. Int J Clin Exp Med. 2015;8(7):11026-31.
28. Ayna AB, Ermurat S, Coşkun BN, Harman H, Pehlivan Y. Neutrophil to Lymphocyte Ratio and Mean Platelet Volume as Inflammatory Indicators in Systemic Lupus Erythematosus Nephritis. Arch Rheumatol. 2016;32(1):21-5. doi: 10.5606/ArchRheumatol.2017.5886.
29. Ozdemir A, Baran E, Kutu M, Celik S, Yılmaz M. Could systemic immune inflammation index be a new parameter for diagnosis and disease activity assessment in systemic lupus erythematosus? Int Urol Nephrol. 2023;55(1):211-6. doi: 10.1007/s11255-022-03320-3.

J Surg Med. 2023;7(5):319-323.
DOI: 10.28982/josam.7715

Research article

Journal of Surgery and Medicine
e-ISSN: 2602-2079
https://jsurgmed.com/

The efficiency of volumetric apparent diffusion coefficient histogram analysis in breast papillary neoplasms

Mustafa Orhan Nalbant, Aysegul Akdogan Gemici, Mehmet Karadag, Ercan Inci

Department of Radiology, University of Health Sciences, Bakirkoy Dr. Sadi Konuk Training and Research Hospital, Turkey

ORCID ID of the author(s)
MON: 0000-0002-5277-9111
AAG: 0000-0002-7707-1849
MK: 0000-0002-7646-7200
EI: 0000-0002-3791-2471

Corresponding Author
Mustafa Orhan Nalbant
University of Health Sciences, Bakirkoy Dr. Sadi Konuk Research and Training Hospital, Radiology Department, Tevfik Saglam Cad. No:11 Zuhuratbaba 34147 Bakırkoy, Istanbul, Turkey
E-mail: musnalbant88@hotmail.com

Ethics Committee Approval
This study was performed at the University of Health Sciences, Bakirkoy Dr. Sadi Konuk Training and Research Hospital. The study protocol (approval number: 2023/35) was approved by the Institutional Review Board on 23.01.2023. Informed written consent was obtained from all patients.
All procedures in this study involving human participants were performed in accordance with the 1964 Helsinki Declaration and its later amendments.

Conflict of Interest
No conflict of interest was declared by the authors.

Financial Disclosure
The authors declared that this study has received no financial support.

Published
2023 May 15

Abstract

Background/Aim: Papillary neoplasia encompasses both malignant and benign lesions, and core needle biopsy (CNB) is crucial in their diagnosis. Histological findings determine their management. Here we compare volumetric apparent diffusion coefficient (ADC) histogram analysis of carcinomas and benign pathologies identified by histopathology from excisional biopsies.

Methods: This retrospective study included 524 patients who underwent breast magnetic resonance imaging (MRI) for a suspicious breast mass from January 2018 to October 2022. Patients with benign lesions, incompatible ultrasound-guided CNB results with papillary neoplasia, and those with MRI exams insufficient for diagnosis due to motion artifacts were excluded. After applying the exclusion criteria, the study included 48 patients (average aged 61.5 (14.8) years; range, 31 to 72 years). After excisional biopsies, 30 benign lesions and 18 carcinomas were identified. MRI was acquired at 1.5 T (Verio; Siemens Medical Solutions, Erlangen, Germany), and the b-values for diffusion-weighted imaging were calculated at 1000 s/mm^2. Histogram parameters were computed. Receiver operating characteristic (ROC) curve analysis was performed to investigate diagnostic accuracy, evaluate histogram analysis performance, and determine threshold values.

Results: The ADCmin, ADCmean, ADCmax, and all ADC value percentiles were significantly lower in the carcinoma group than in the benign group (P<0.001). The variance, skewness, and kurtosis were higher in the carcinoma group. ADCmax had the highest area under the curve (AUC: 0.985; cut-off 1.247 × 10^{-3} mm^2/s; sensitivity 86%, and specificity 92%), followed by ADCmean (AUC: 0.950; cut-off 0.903 × 10^{-3} mm^2/s; sensitivity 94%, and specificity 96%).

Conclusion: Volumetric ADC histogram analysis of papillary neoplasia at higher b-values can be an imaging marker to detect carcinoma and quantitatively reveal the lesions' diffusion characteristics.

Keywords: apparent diffusion coefficient, magnetic resonance imaging, papillary neoplasia, volumetric histogram analysis

How to cite: Nalbant MO, Gemici AA, Karadag M, Inci E. The efficiency of volumetric apparent diffusion coefficient histogram analysis in breast papillary neoplasms. J Surg Med. 2023;7(5):319-323.

Introduction

Lesions with unknown malignant potential, or B3 lesions, include papillary neoplasia of the breast and other tumors such as flat epithelial atypia, radial scars, lobular intraepithelial neoplasia, and phyllodes tumors [1,2]. These lesions are found in 3 to 17% of cases, and their detection rate increases with sensitive imaging modalities such as MRI. Ultrasound-guided core needle biopsy is essential for identifying these lesions, but an association with the acquired images is crucial for determining the generalizability of the sample [3-6].

Dynamic contrast-enhanced (DCE) MRI is useful for identifying B3 lesions with less characteristic morphodynamic presentations, reducing the incidence of misdiagnosis and unnecessary procedures. However, some B3 lesions may not be detected by imaging, especially those that are incidental or limited to the periphery of higher-grade lesions [6,7].

Diffusion-weighted imaging (DWI) is a non-contrast MRI method that evaluates the tissue's capability to diffuse fluids. The apparent diffusion coefficient (ADC) can differentiate benign from malignant breast tumors, with malignant lesions showing much lower ADC values due to increased cellularity. Volumetric ADC histogram analysis is used to examine the entire range of ADC parameters, eliminating ROI selection bias and ensuring computation accuracy and repeatability [8-12].

This study compares volumetric ADC histogram analysis between patients with excisional biopsy-confirmed carcinoma and those with benign lesions in papillary neoplasia. To our knowledge, no study has been conducted on volumetric ADC histogram analysis in cases with papillary neoplasia.

Materials and methods

This retrospective case-control study was conducted at the Bakirkoy Dr. Sadi Konuk Training and Research Hospital of the University of Health Sciences. The study protocol (approval number: 2023/35) was approved by the Institutional Review Board on January 23, 2023. Written informed consent was obtained from all participants, and the study was conducted following the Helsinki Declaration guidelines.

This retrospective case-control study included patients who had undergone breast MRI exams within a month before surgery between January 2018 and October 2022 and were diagnosed with either carcinomas or benign lesions through excisional biopsy. The study's inclusion criteria were: (a) patients diagnosed with papillary neoplasia with biopsy; (b) patients who underwent preoperative breast MRIs (including DWI and ADC sequences); (c) patients with histologically confirmed carcinoma or benign lesion with excisional biopsies.

The search yielded 524 patients who underwent breast MRI for a suspicious breast mass. We excluded 253 patients with benign lesions, 211 patients whose ultrasound-guided CNB was incompatible with papillary neoplasia, and 12 patients with poor image quality due to artifacts. Ultimately, our study included 18 patients with histologically confirmed carcinoma and 30 patients with histologically confirmed benign lesions (17 patients with intraductal papilloma, six patients with intraductal papillomatosis, four patients with lobular intraepithelial neoplasia, and three patients with sclerosing adenosis with apocrine metaplasia. Every result was reported with a 95% confidence interval (CI).

A 1.5-T MR system (Verio; Siemens Medical Solutions, Erlangen, Germany) equipped with a 32-channel phased array surface coil for signal reception was used to perform MRI. The diffusion-weighted sequence was administered at b-values of 1000 s/mm². The conventional sequence, matrix 256 × 144, the field of vision (FOV) 250 × 250 mm, the layer thickness 4 mm, the layer spacing 4 mm; the axial turbo inversion recovery magnitude (TIRM), the repeat time (TR) 3500 ms, the echo time (TE) 70 ms; the axial T1-weighted image (T1WI), TR 6 ms, TE 2,5 ms; the axial dispersion weighted image (DWI) sequence, TR 6000 ms, TE 74 ms, B value 1000 s/mm^2, matrix 160 × 160, FOV 250 × 200 mm, layer thickness 4 mm, layer spacing 4 mm.

Image analysis

The DWI raw data were transferred from the picture archiving and communication system (PACS) to a personal computer and processed using the open-source LIFEx 7.2.0 voxel program (https://lifesoft.org). A radiologist with 14 years of experience in breast MRI separately reviewed all MR images and drew each ROI manually to include the lesions. Each ROI was then merged into a volumetric ROI containing voxel data for the entire region, and a volumetric ADC map was generated. The ADCmin, ADCmean, ADCmax, skewness, kurtosis, variance, and percentiles of ADC values were determined. The nth percentile on the histogram represented where n percent of the voxel values were detected on the left. A positive skewness indicated that the right tail was flatter or longer than the left tail, while high kurtosis was characterized by a prominent peak near the mean, a sharp decrease, and long tails. The radiologist was blinded to the clinical data and independently assessed each scan.

Statistical analysis

Statistical analysis was performed using IBM SPSS 23.0 (Chicago, IL, United States). The ADC values of each patient were merged to generate a dataset, and histograms were generated for each group. Histograms revealed variation in the distribution of all measures. Descriptive statistics, such as mean, minimum, maximum, standard deviation, skewness, kurtosis, and percentiles, were calculated for each patient group using individual data, and changes in these descriptive statistics were visually represented. The t-test for independent samples was used to investigate whether these individual statistics differed between groups. ROC curves were created based on individual data, and a threshold value was computed for the acquired statistics. Sensitivity and specificity values for threshold values were then calculated. *P*-values <0.05 were considered statistically significant.

Results

Demographic Data

The study included 48 patients, with a mean age (SD) of 61.5 (14.8) years, ranging from 31 to 72 years. The carcinoma group included 18 cases (Figure 1), while the benign group included 30 cases (Figures 2 and 3). There was no significant difference in age between the two groups (*P*=0.61).

Figure 1: A 72-year-old patient with pathology on surgical excision confirmed papillary carcinoma. The T1W image (a) reveals an irregularly circumscribed hypointense lesion. Turbo inversion recovery magnitude (TIRM) (b) and diffusion-weighted (c) sequences show high signal intensity (c). Manually drawn ROI on the ADC map for assessing the volumetric histogram analysis can be seen (d).

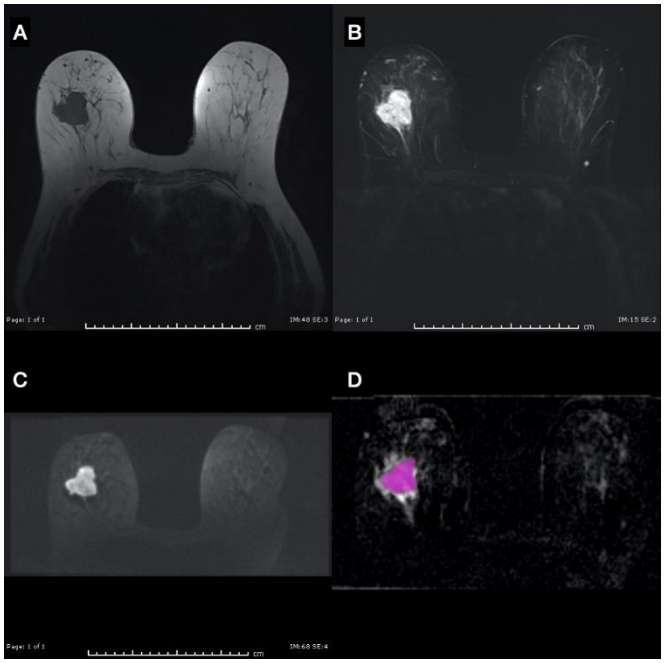

Figure 2: A 44-year-old patient with pathology on surgical excision confirmed intraductal papillomatosis. The T1W image (a) depicts a hypointense lesion with regular margins. Turbo inversion recovery magnitude (TIRM) (b) and diffusion-weighted (c) sequences reveal iso to high signal intensity. A manually drawn ROI is displayed on the ADC map for evaluating the volumetric histogram analysis (d).

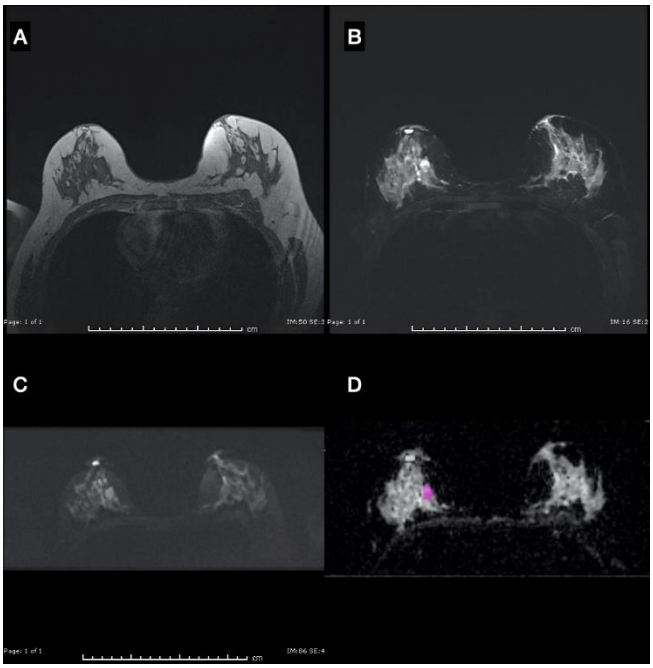

Figure 3: A 42-year-old patient with pathology on surgical excision confirmed sclerosing adenosis with apocrine metaplasia. The T1W image (a) displays a lesion with uniform margins that is hypointense. Turbo inversion recovery magnitude (TIRM) (b) and diffusion-weighted (c) sequences indicate hyperintense lesion. On the ADC map, a manually drawn ROI is shown for assessing the volumetric histogram analysis (d).

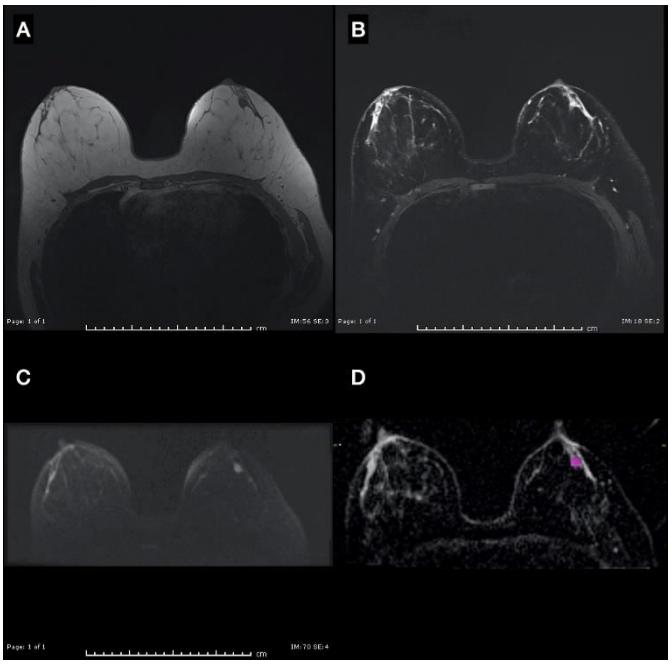

Results of ADC histogram parameters in carcinoma and benign group

The 5th, 10th, 25th, 50th, 75th, 90th, and 95th percentiles of ADC values, as well as the ADCmin, ADCmean, and ADCmax of the carcinoma group, were all significantly lower (P<0.001) than those of the benign group in the volumetric histogram analysis (Figure 4) (Table 1). In contrast, kurtosis and variance were larger in the carcinoma group than in the benign group (P<0.001), with the difference being statistically significant. Skewness was also larger in the carcinoma group but did not reach statistical significance (P=0.06).

Figure 4: Results of the volumetric ADC histogram analysis of papillary neoplasia. The ADCmean, ADCmin, ADCmax, and 5th–95th percentiles of ADC values of the carcinoma group were all lower than those of the benign group (P<0.001). The variance of the carcinoma group was larger (P<0.05). Apparent diffusion coefficient (ADC) values are expressed as $\times 10^{-3}$ mm²/s.

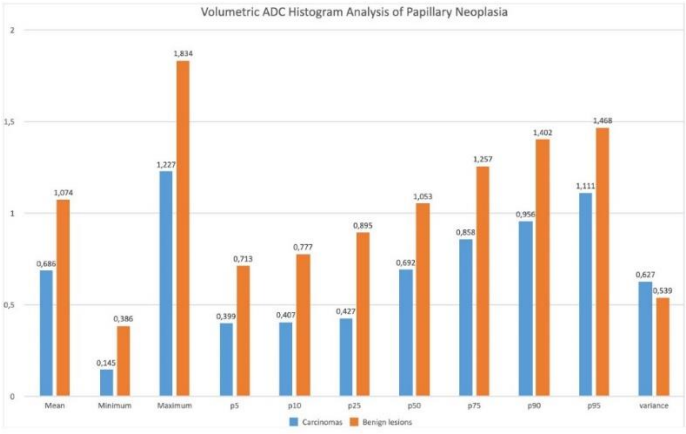

Table 1: Comparisons of ADC histogram parameters between carcinoma group and benign group.

ADC (10^{-3} mm²/s)	Carcinoma group	Benign group	P-value	Significance level
Mean	0.686	1.074	<0.001	99%
Std. Deviation	0.627	0.539	<0.001	99%
Minimum	0.145	0.386	<0.001	99%
Maximum	1.227	1.834	<0.001	99%
Skewness	0.11	0.16	0.06	95%
Kurtosis	0.76	0.21	<0.001	99%
5th	0.399	0.713	<0.001	99%
10th	0.407	0.777	<0.001	99%
25th	0.427	0.895	<0.001	99%
50th	0.692	1.053	<0.001	99%
75th	0.858	1.257	<0.001	99%
90th	0.956	1.402	<0.001	99%
95th	1.111	1.468	<0.001	99%

ADC: apparent diffusion coefficient

Diagnostic performance

The ADCmax had the highest area under the curve (AUC) of 0.985, followed by the ADCmean with an AUC of 0.950, indicating their superior diagnostic effectiveness. Using a cut-off value of 1.247 × 10^{-3} mm^2/s, the ADCmax had a sensitivity of 86% and specificity of 92%. The ADCmean had a threshold of 0.903 × 10^{-3} mm^2/s, with a sensitivity of 94% and specificity of 96%. In contrast, the ADCmin had a lower AUC of 0.716, and a threshold of 0.645 × 10^{-3} mm^2/s yielded a sensitivity of 84% and specificity of 71% (Figure 5).

Figure 5: The ROC (receiver operating characteristic) curve represents the ADCmax, ADCmean, and ADCmin values of the volumetric ADC histogram analysis of papillary neoplasia. The AUC (area under the curve) was 0.985, 0.950, and 0.716, respectively.

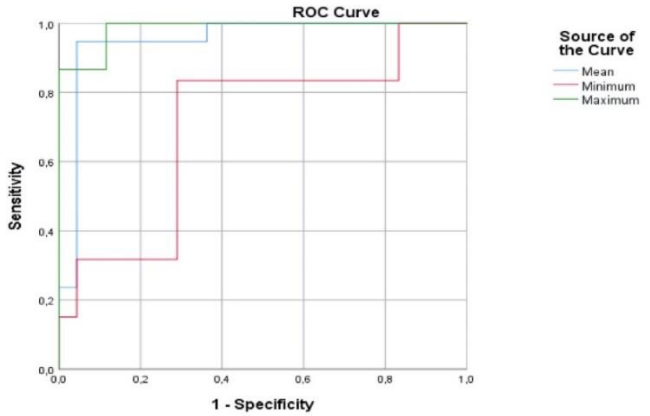

Discussion

Here we compared the volumetric ADC histogram analysis of papillary neoplasia between carcinoma and benign groups based on histopathological results from excisional biopsies.

ADC parameters reflect the tumor microenvironment, including membrane stability, extracellular matrix, and cellular proliferation, and are related to the Brownian motion of fluids [13–15]. The signal attenuation due to diffusion is linear when b values range between 200 and 1000 s/mm^2, as predicted by Gaussian diffusion. However, when b-values are above 1000 s/mm^2, non-Gaussian diffusion occurs, leading to a proportional decline in the ADC value [16].

ADC histogram analysis can be used to assess the signal intensity range of voxels based on clinically acquired ADC. Histogram features describing statistical interrelationships between adjacent voxels can highlight the diversity of lesions, providing significant benefits for tumor grading or prognosis evaluation [17–21]. This method is also employed in treating a wide range of illnesses unrelated to cancer [22,23].

In some published studies, volumetric ADC histogram analysis has been used to evaluate breast lesions. Researchers have examined the consistency and repeatability of ADC histogram parameters using ADC histogram analysis, concluding that the repeatability of lower histogram percentiles is comparable to that of mean ADC, while the repeatability of ADC-thresholded volumetric measures is currently poor but could improve with the development of ROI techniques [24].

Guo et al. [25] used volumetric ADC histogram analysis to investigate the relationship between histogram characteristics and Ki-67 expression in breast cancers. They found that the most effective were the median (AUC: 0.943) and mean (AUC: 0.930) ADC histogram parameters. ROC analysis showed that skewness and entropy could be used to determine the Ki-67 status.

Tagliati et al. [26] assessed papillary lesions and found a significant difference in the ADC mean values between individuals without atypia or malignant foci and those with atypia or malignant foci. They suggested that an ADCmean value ≤ 1.418 × 10^{-3} mm^2/s could predict the presence of malignant foci within a papillary lesion with 84% sensitivity and 76% specificity.

Another study on the distinction between malignant and benign papillary breast tumors using ADC values found that the mean ADC values of borderline and malignant lesions were significantly lower than those of benign lesions (P<0.05). They proposed a suitable ADC value threshold of 1.00 × 10^{-3} mm^2/s [27].

Several studies have compared ADC values for differentiating benign and malignant breast tumors [28–30], and similar to our findings, the ADC parameters of malignant tumors were lower than those of benign lesions in these studies. However, our study measured ADC values volumetrically to ensure reproducibility and analyzed more parameters, including percentile values.

Limitations

Our study has several limitations and strengths. One of the strengths is that we performed volumetric histogram analysis in papillary neoplasia of the breast, which to our knowledge, has not been done in other studies in the literature. However, one limitation is that we only evaluated the ADC values derived from higher b values. Additionally, our study utilized a retrospective analysis methodology, which could lead to possible bias in patient sampling. Some lesions contained more cystic components than others, potentially leading to sampling bias. Further studies are needed to validate our findings.

Conclusion

Our study demonstrates that volumetric ADC histogram analysis of papillary neoplasia of the breast at higher b values is a promising imaging marker for differentiating between benign and carcinoma lesions. This method can provide objective and quantitative information about the lesions' diffusion parameters and eliminate bias through volumetric measurement. Furthermore, it is a suitable method for preoperative lesion diagnosis without the need for excisional biopsies. Our findings suggest that this technique could be a valuable addition to the diagnostic toolset for breast cancer.

References

1. Tan PH, Ellis I, Allison K, Brogi E, Fox SB, Lakhani S, et al. Cree IA; WHO Classification of Tumours Editorial Board. The 2019 World Health Organization classification of tumors of the breast. Histopathology. 2020;77(2):181-5. doi: 10.1111/his.14091.
2. Rakha EA, Ellis IO. Diagnostic challenges in papillary lesions of the breast. Pathology. 2018;50(1):100-10. doi: 10.1016/j.pathol.2017.10.005.
3. Rageth CJ, O'Flynn EAM, Pinker K, Kubik-Huch RA, Mundinger A, Decker T, et al. Second International Consensus Conference on lesions of uncertain malignant potential in the breast (B3 lesions). Breast Cancer Res Treat. 2019;174(2):279-96. doi: 10.1007/s10549-018-05071-1.
4. Richter-Ehrenstein C, Maak K, Röger S, Ehrenstein T. Lesions of "uncertain malignant potential" in the breast (B3) identified with mammography screening. BMC Cancer. 2018;18(1):829. doi: 10.1186/s12885-018-4742-6.
5. Nakhlis F. How Do We Approach Benign Proliferative Lesions? Curr Oncol Rep. 2018;20(4):34. doi: 10.1007/s11912-018-0682-1.
6. Heywang-Köbrunner SH, Nährig J, Hacker A, Sedlacek S, Höfler H. B3 Lesions: Radiological Assessment and Multi-Disciplinary Aspects. Breast Care (Basel). 2010;5(4):209-17. doi: 10.1159/000319326.
7. Linda A, Zuiani C, Bazzocchi M, Furlan A, Londero V. Borderline breast lesions diagnosed at core needle biopsy: can magnetic resonance mammography rule out associated malignancy? Preliminary results based on 79 surgically excised lesions. Breast. 2008;17(2):125-31. doi: 10.1016/j.breast.2007.11.002.

8. Pediconi F, Padula S, Dominelli V, Luciani M, Telesca M, Casali V, et al. Role of breast MR imaging for predicting malignancy of histologically borderline lesions diagnosed at core needle biopsy: prospective evaluation. Radiology. 2010;257(3):653-61. doi: 10.1148/radiol.10100732.
9. Ei Khouli RH, Jacobs MA, Mezban SD, Huang P, Kamel IR, Macura KJ, et al. Diffusion-weighted imaging improves the diagnostic accuracy of conventional 3.0-T breast MR imaging. Radiology. 2010;256(1):64-73. doi: 10.1148/radiol.10091367.
10. Guo Y, Cai YQ, Cai ZL, Gao YG, An NY, Ma L, et al. Differentiation of clinically benign and malignant breast lesions using diffusion-weighted imaging. J Magn Reson Imaging. 2002;16(2):172-8. doi: 10.1002/jmri.10140.
11. Marini C, Iacconi C, Giannelli M, Cilotti A, Moretti M, Bartolozzi C. Quantitative diffusion-weighted MR imaging in the differential diagnosis of breast lesion. Eur Radiol. 2007;17(10):2646-55. doi: 10.1007/s00330-007-0621-2.
12. Partridge SC, Demartini WB, Kurland BF, Eby PR, White SW, Lehman CD. Differential diagnosis of mammographically and clinically occult breast lesions on diffusion-weighted MRI. J Magn Reson Imaging. 2010;31(3):562-70. doi: 10.1002/jmri.22078.
13. Koh DM, Collins DJ. Diffusion-weighted MRI in the body: applications and challenges in oncology. AJR Am J Roentgenol. 2007;188(6):1622-35. doi: 10.2214/AJR.06.1403.
14. Surov A, Meyer HJ, Wienke A. Correlation between apparent diffusion coefficient (ADC) and cellularity is different in several tumors: a meta-analysis. Oncotarget. 2017;8(35):59492-9. doi: 10.18632/oncotarget.17752.
15. Meyer HJ, Leifels L, Hamerla G, Höhn AK, Surov A. ADC-histogram analysis in head and neck squamous cell carcinoma. Associations with different histopathological features including expression of EGFR, VEGF, HIF-1α, Her 2 and p53. A preliminary study. Magn Reson Imaging. 2018;54:214-7. doi: 10.1016/j.mri.2018.07.013.
16. Iima M, Le Bihan D. Clinical Intravoxel Incoherent Motion and Diffusion MR Imaging: Past, Present, and Future. Radiology. 2016;278(1):13-32. doi:10.1148/radiol.2015150244.
17. Choi MH, Oh SN, Rha SE, Choi JI, Lee SH, Jang HS, et al. Diffusion-weighted imaging: Apparent diffusion coefficient histogram analysis for detecting pathologic complete response to chemoradiotherapy in locally advanced rectal cancer. J Magn Reson Imaging. 2016;44(1):212-20. doi: 10.1002/jmri.25117.
18. Surov A, Ginat DT, Lim T, Cabada T, Baskan O, Schob S, et al. Histogram Analysis Parameters Apparent Diffusion Coefficient for Distinguishing High and Low-Grade Meningiomas: A Multicenter Study. Transl Oncol. 2018;11(5):1074-9. doi: 10.1016/j.tranon.2018.06.010.
19. Thust SC, Maynard JA, Benenati M, Wastling SJ, Mancini L, Jaunmuktane Z, et al. Regional and Volumetric Parameters for Diffusion-Weighted WHO Grade II and III Glioma Genotyping: A Method Comparison. AJNR Am J Neuroradiol. 2021;42(3):441-7. doi: 10.3174/ajnr.A6965.
20. Ma X, Shen M, He Y, Ma F, Liu J, Zhang G, et al. The role of volumetric ADC histogram analysis in preoperatively evaluating the tumour subtype and grade of endometrial cancer. Eur J Radiol. 2021;140:109745. doi: 10.1016/j.ejrad.2021.109745.
21. Li S, Liang P, Wang Y, Feng C, Shen Y, Hu X, et al. Combining volumetric apparent diffusion coefficient histogram analysis with vesical imaging reporting and data system to predict the muscle invasion of bladder cancer. Abdom Radiol (NY). 2021;46(9):4301-10. doi: 10.1007/s00261-021-03091-y.
22. Muehlematter UJ, Mannil M, Becker AS, Vokinger KN, Finkenstaedt T, Osterhoff G, et al. Vertebral body insufficiency fractures: detection of vertebrae at risk on standard CT images using texture analysis and machine learning. Eur Radiol. 2019;29(5):2207-17. doi: 10.1007/s00330-018-5846-8.
23. Tsili AC, Astrakas LG, Goussia AC, Sofikitis N, Argyropoulou MI. Volumetric apparent diffusion coefficient histogram analysis of the testes in nonobstructive azoospermia: a noninvasive fingerprint of impaired spermatogenesis? Eur Radiol. 2022;32(11):7522-31. doi: 10.1007/s00330-022-08817-0.
24. Newitt DC, Amouzandeh G, Partridge SC, Marques HS, Herman BA, Ross BD, et al. Repeatability and Reproducibility of ADC Histogram Metrics from the ACRIN 6698 Breast Cancer Therapy Response Trial. Tomography. 2020;6(2):177-85. doi: 10.18383/j.tom.2020.00008.
25. Guo Y, Kong QC, Li LQ, Tang WJ, Zhang WL, Ning GY, et al. Whole Volume Apparent Diffusion Coefficient (ADC) Histogram as a Quantitative Imaging Biomarker to Differentiate Breast Lesions: Correlation with the Ki-67 Proliferation Index. Biomed Res Int. 2021;2021:4970265. doi: 10.1155/2021/4970265.
26. Tagliati C, Ercolani P, Marconi E, Simonetti BF, Giuseppetti GM, Giovagnoni A. Apparent diffusion coefficient value in breast papillary lesions without atypia at core needle biopsy. Clin Imaging. 2020;59(2):148-53. doi: 10.1016/j.clinimag.2019.10.010. Epub 2019 November 20. PMID: 31821971.
27. Lv W, Zheng D, Guan W, Wu P. Contribution of Diffusion-Weighted Imaging and ADC Values to Papillary Breast Lesions. Front Oncol. 2022;12:911790. doi: 10.3389/fonc.2022.911790.
28. Nadrljanski MM, Milosevic ZC. Relative apparent diffusion coefficient (rADC) in breast lesions of uncertain malignant potential (B3 lesions) and pathologically proven breast carcinoma (B5 lesions) following breast biopsy. Eur J Radiol. 2020;124:108854. doi: 10.1016/j.ejrad.2020.108854.
29. Cheeney S, Rahbar H, Dontchos BN, Javid SH, Rendi MH, Partridge SC. Apparent diffusion coefficient values may help predict which MRI-detected high-risk breast lesions will upgrade at surgical excision. J Magn Reson Imaging. 2017;46(4):1028-36. doi: 10.1002/jmri.25656.
30. Tang W, Chen L, Jin Z, Liang Y, Zuo W, Wei X, et al. The diagnostic dilemma with the plateau pattern of the time-intensity curve: can the relative apparent diffusion coefficient (rADC) optimise the ADC parameter for differentiating breast lesions? Clin Radiol. 2021;76(9):688-95. doi: 10.1016/j.crad.2021.04.015.

J Surg Med. 2023;7(5):324-328.
DOI: 10.28982/josam.7710

Research article

Journal of Surgery and Medicine
e-ISSN: 2602-2079
https://jsurgmed.com/

A retrospective study of the effects of anesthesia methods on post-operative delirium in geriatric patients having orthopedic surgery: Anesthesia methods on post-operative delirium

Leman Acun Delen [1], Zeliha Korkmaz Disli [2]

[1] Department of Anesthesiology and Reanimation, Malatya Training and Research Hospital, Malatya, Turkey
[2] Department of Anesthesiology and Reanimation, Inonu University Medical School, Malatya, Turkey

ORCID ID of the author(s)

LAD: 0000-0001-9441-6979
ZKD: 0000-0002-4527-2427

Corresponding Author
Leman Acun Delen
Department of Anesthesiology and Reanimation, Malatya Training and Research Hospital, Malatya, Turkey
E-mail: lmndelen@hotmail.com

Ethics Committee Approval
This study was performed by the ethical permission obtained from Malatya Turgut Özal University, Faculty of Medicine Ethics Committee (Permission No: 2022/177). All procedures in this study involving human participants were performed in accordance with the 1964 Helsinki Declaration and its later amendments.

Conflict of Interest
No conflict of interest was declared by the authors.

Financial Disclosure
The authors declared that this study has received no financial support.

Published
2023 May 18

Abstract

Background/Aim: Post-operative delirium, which usually develops in geriatric patients, also causes an increase in mortality and morbidity for various reasons, such as difficulty in compliance with treatment. Estimating the effects of the anesthesia method on delirium contributes to the prevention of possible complications. In this study, effects due to use of different anesthesia methods on the post-operative delirium development in geriatric patients who underwent orthopedic surgery were investigated.

Methods: In our retrospective cohort study, scanning of the patient files was performed for 276 patients who were older than 65 years and who had undergone surgery for lower extremity fractures in Malatya education and research hospital, orthopedics department between May 1, 2022 and October 15, 2022. Demographic data, comorbid conditions, anesthesia type, lengths of surgery, and level of delirium development were recorded for each scanned patient.

Results: In our study, 201 patients were included. The mean age of the patients was 74.1 (7.3) (min–max: 65–98); 133 (66.2%) were female, and 68 (33.8%) were male. It was noticed that patients who had undergone regional anesthesia developed a significantly smaller rate of delirium development (8.1%) compared to those who had received general anesthesia (20.6%; P=0.012). Ages (P<0.001), lengths of surgery (P<0.001), and lengths of hospitalization stays (P<0.001) were significantly higher in patients with delirium compared to those without.

Conclusion: Based on the data obtained in this study, it was concluded that to reduce the risk of delirium development after orthopedic surgery, regional rather than general anesthesia should be selected, and the time of hospitalization stay should be minimized.

Keywords: post-operation, geriatric, spinal anesthesia, general anesthesia, delirium

How to cite: Delen LA, Disli ZK. A retrospective study of the effects of anesthesia methods on post-operative delirium in geriatric patients having orthopedic surgery: Anesthesia methods on post-operative delirium. J Surg Med. 2023;7(5):324-328.

Introduction

The rate of living longer in the older population is increasing due to developments in health sciences, improvements in life standards and hygiene, and vaccination and sanitation programs in developed and developing countries; however, in parallel with that increase is a corresponding increase in the rate of developing chronic health problems. The number of people older than 65 years worldwide has increased three times in recent years [1], and the rate in Turkey is reported to be 8.8% [2]. As the geriatric population increases, the number of patients needing healthcare is also increasing. One important occurrence within the geriatric population is the higher risk of fall-related injuries with a corresponding increase in the risk of lower extremity fractures. The risk of falls in geriatric patients also increases with changes in lifestyle in that these people more likely to stay alone rather than in care centers since the nuclear family style is much more preferred at present. In such cases, the geriatric patients may face increased risk of serious surgery-related complications, including prolonged recoveries and various chronic conditions.

Hip fractures are among the most feared orthopedic conditions in geriatric patients. Low-energy hip fractures in people over 60 are seen more often than other types of fractures; thus, the related morbidity and mortality risk is also higher. This issue also creates social and emotional problems for the elderly population. It was reported that after application of post-fracture interventions in elderly patients who also present a very fragile emotional status, the possibility of increasing delirium symptoms in 60% of the patients is present [3]. Delirium can be defined as an acute onset and fluctuating course of this clinical syndrome with mental disorders characterized by deteriorations in consciousness, memory, orientation, thought, perception, and behavior [4]. Delirium can most often be seen in elderly patients and may cause fluid–electrolyte disorders, cognitive dysfunction, and an increase in the risk of infections and medication-related side effects. The American Society of Anesthesiologists (ASA) scoring system is used to assess pre-operative physical condition and reduce the risk of delirium development and surgery-related complications [5]. This score is based on a six-degree scoring system and is a useful scale, especially for the choice of anesthesia and monitoring methods for such patients.

In this study, we aimed to investigate the development of delirium in geriatric patients who undergo orthopedic surgery in addition to the risk factors involved in this process.

Materials and methods

This study was performed after ethical permission was obtained from Malatya Turgut Özal University, Faculty of Medicine Ethics Committee (Permission No: 2022/177). The files of 276 patients who were over 65 years and had undergone surgery due to lower extremity fractures in Malatya Education and Research Hospital between May 1, 2022 and October 15, 2022 were scanned. The study was started in accordance with the Strengthening the Reporting of Observational Studies in Epidemiology (STROBE) and Helsinki Declaration. The minimum sample size of the study was calculated as 200 patients with an alpha error of 0.05 and a beta error of 0.8 (with reference to similar studies). Considering possible reasons for exclusion, the study was initiated with 276 patients. However, 75 patients were excluded from the study due to reasons, such as the transition from regional anesthesia to general anesthesia and others, and 201 patients were finally included in the study. Pre-anesthesia anamnesis and mini-mental test were administered to all patients, and it was confirmed that they did not present signs of delirium. Patients with psychiatric and neurological diseases, such as Alzheimer's disease, psychosis, cognitive and conscious state alterations, cerebrovascular diseases, and pre-existing cognitive diseases in addition to kidney and liver diseases, decompensated heart failure, addiction to alcohol and drugs, post-operative hospitalization in the intensive care unit, ASA scores of 4 and higher, and narcotic analgesics received during the post-operative period, all of which may have affected the study results were excluded; hence, a total of 201 patients were included in the study.

During the post-operative period, cognitive changes that did not exist prior to surgery, attention, perception, and orientation disorders, and disturbances in sleep balance were defined as delirium. Mini-mental tests was applied to the patients at 24 and 72 h.

Patients were divided into two groups: (1) patients who had received general anesthesia (GA group) and (2) regional anesthesia (spinal, spinal and epidural combined, epidural, and neuromuscular neural blockage) constituted the RA group.

Information regarding sex, age, comorbidities, ASA scores, whether delirium developed 24 and/or 72 h after surgery, and any administration of pre-operative drugs for patients included in the study were recorded. Total lengths of operation, pre-operative sedation use, hospitalization times, mortality rates, and parameters, such as urea, creatinine, aspartate aminotransferase (AST), and alanine aminotransferase (ALT) values at 24 and 72 h were also noted. Patients who had delirium diagnosis based on consultation with the Neurology and Psychiatry Departments at post-operative day 7 were recorded.

Statistical analysis

Statistical analyses of the data were performed using the SPSS (Statistical Package for Social Sciences; SPSS Inc., Chicago, IL) package program version 22.0 for Windows. While categorical variables were shown as percentages and n values, numerical data were given as the mean standard deviation (SD). The chi-squared test was used for nonparametric variables (Pearson chi-squared). Normal distribution of data was tested using the Kolmogorov–Smirnov test. Mann–Whitney U-test was used for comparison of the groups. *P*-value <0.05 was considered statistically significant.

Results

A total of 201 patients with a mean age of 74.1 (7.3) (min–max: 65–98) with 133 (66.2%) females and 68 (33.8%) males were included in the study. Of these patients, 27.5% had hypertension (HT), 54.2% had diabetes mellitus (DM), 47.8% had congestive heart failure (CHF), 31.8% had ischemic heart disease (IHD), and 16.4% had cancer. ASA scores of the patients were 10.9% ASA 1, 34.8% ASA 2, and 54.2% ASA 3. It was recorded that 13.4% of the patients did not use any prescribed medication, 19.9% used only one medicine, 7% used two medicines, and 59.7% used more than two medications per day

regularly. During the surgeries that these patients underwent, 49.3% received regional anesthesia, while 50.7% underwent general anesthesia. Sedation was administered to 44.3% of the patients. Delirium was noted in 29 out of the total 201(14.4%) patients. Mortality was seen in 6% (Table 1). The rate of patients receiving sedation was significantly higher in patients who had regional anesthesia (66.7%) compared to that of had general anesthesia (22.5%; $P<0.001$). Contrary to that finding, the rate of delirium development was significantly lower in patients who had regional anesthesia (8.1%) compared to general anesthesia (20.6%; $P=0.012$) as shown in Table 2. In patients who received regional anesthesia, creatinine levels both at 24 h ($P=0.006$) and 72 h ($P=0.11$) in addition to hospitalization time ($P=0.037$) were significantly lower than in those who received general anesthesia. ALT levels were significantly higher in patients who received regional anesthesia compared to those who received general anesthesia ($P=0.042$) as shown in Table 3.

Table 1: Demographic information of the patients (n=201) in the study.

		mean	SD
Age		74.1	7.3
		n	**%**
Sex	Woman	133	66.2
Comorbidity*	Hypertension	55	27.5
	DM	109	54.2
	CHF	96	47.8
	IHD	64	31.8
	Cancer	33	16.4
ASA score	1	22	10.9
	2	70	34.8
	3	109	54.2
Medication use	None	27	13.4
	1 per day	40	19.9
	2 per day	14	7.0
	> 2 per day	120	59.7
Anesthesia type	Regional anesthesia	99	49.3
	General anesthesia	102	50.7
Sedation		89	44.3
Delirium		29	14.4
Mortality		12	6.0

*There were cases with more than one comorbidity. SD: standard deviation, DM: diabetes mellitus, CHF: Congestive heart failure, IHD: Ischemic heart disease, ASA: American Society of Anesthesiologists

Table 2: Comparison of categorical parameters according to anesthesia type

		Regional anesthesia		General anesthesia		*P-value
		n	%	n	%	
Sex	Woman	63	63.6	70	68.6	0.455
Hypertension		32	32.7	23	22.5	0.110
DM		53	53.5	56	54.9	0.846
CHF		43	43.4	53	52.0	0.226
IHD		35	35.4	29	28.4	0.292
Cancer		20	20.2	13	12.7	0.154
ASA score	1	12	12.1	10	9.8	0.833
	2	35	35.4	35	34.3	
	3	52	52.5	57	55.9	
Medication use	none	15	15.2	12	11.8	0.057
	1 per day	12	12.1	28	27.5	
	2 per day	7	7.1	7	6.9	
	>2 per day	65	65.7	55	53.9	
Sedation		66	66.7	23	22.5	<0.001
Delirium		8	8.1	21	20.6	0.012
Mortality		5	5.1	7	6.9	0.588

*A chi-squared analysis was performed. DM: diabetes mellitus, CHF: Congestive heart failure, IHD: Ischemic heart disease, ASA: American Society for Anesthesiologists

Table 3: Comparison of the numerical parameters according to anesthesia type

		Regional anesthesia Mean (SD)	General anesthesia Mean (SD)	*P-value
Age (years)		73.4 (7.2)	74.7 (7.4)	0.148
Length of surgery (minutes)		114.8 (42.0)	106.7 (41.7)	0.095
Glucose mg/dl	at 24 h	152.1 (79.3)	151.9 (65.3)	0.565
Urea mg/dl		54.1 (39.6)	57.0 (69.9)	0.761
Creatinine mg/dl		1.2 (1.2)	1.6 (5.2)	0.006
AST u/l		50.5 (30.1)	56.0 (44.8)	0.294
ALT u/l		46.2 (41.4)	41.3 (31.4)	0.564
Glucose mg/dl	at 72 h	159.7 (90.4)	150.0 (79.1)	0.361
Urea mg/dl		57.6 (38.8)	56.8 (35.8)	0.715
Creatinine mg/dl		0.9 (0.3)	1.0 (0.5)	0.011
AST u/l		72.2 (96.2)	48.7 (28.5)	0.145
ALT u/l		59.1(82.4)	42.0 (35.2)	0.042
Hospitalization stay (days)		9.4 (4.0)	10.7 (4.6)	0.037

*A Mann–Whitney U analysis was performed. SD: standard deviation, AST: aspartate aminotransferase, ALT: alanine aminotransferase

The rate of delirium development in IHD patients (21.9%) was significantly higher than that of non-HD patients (10.0%; $P=0.04$). Delirium development was observed in all ASA score groups (I–III) in this study. Delirium occurred in 4.5% in ASA 1, 8.6% in ASA 2, and 20.2% in ASA 3 groups; the latter was significantly higher than in the other score groups ($P=0.037$). The rate of delirium development in patients who had received sedation (4.5%) was significantly lower than who did not receive sedation (22.3%; $P<0.001$). The mortality rate in patients with delirium (17.2%) was significantly higher than those who did not develop delirium (4.1%; $P=0.017$) as shown in Table 4. Ages ($P<0.001$), lengths of surgery ($P<0.001$), and lengths of hospitalization stays ($P<0.001$) in patients who had delirium were significantly higher than those who did not develop delirium. AST levels at 72 h in patients who had delirium were significantly lower than that of who did not have delirium ($P=0.007$) as shown in Table 5.

Table 4: Comparison of categorical parameters according to the presence of delirium.

		Delirium		Non-delirium		*P-value
		n	%	n	%	
Sex	Woman	19	14.3	114	85.7	0.939
Hypertension		7	12.7	48	87.3	0.661
DM		17	15.6	92	84.4	0.608
CHF		15	15.6	81	84.4	0.644
IHD		14	21.9	50	78.1	0.04
Cancer		6	18.2	27	81.8	0.587
ASA score	1	1	4.5	21	95.5	0.037
	2	6	8.6	64	91.4	
	3	22	20.2	87	79.8	
Medication use	None	2	7.4	25	92.6	0.547
	1 per day	7	17.5	33	82.5	
	2 per day	3	21.4	11	78.6	
	> 2 per day	17	14.2	103	85.8	
Sedation		4	4.5	85	95.5	< 0.001
Mortality		5	17.2	7	4.1	0.017

*A chi-squared analysis was performed. DM: diabetes mellitus, CHF: Congestive heart failure, IHD: Ischemic heart disease

Table 5: Comparison of the numeric parameters according to the presence or absence of delirium.

		Delirium Mean (SD)	Non-delirium Mean (SD)	*P-value
Age (years)		82.1 (6.1)	72.7 (6.6)	<0.001
Length of operation (minutes)		170.2 (43.9)	100.7 (32.2)	<0.001
Glucose mg/dl	at 24 hours	136.1 (35.6)	154.7 (76.6)	0.665
Urea mg/dl		51.1 (27.4)	56.3 (60.5)	0.796
Creatinine mg/dl		1.1(0.4)	1.5 (4.1)	0.194
AST u/l		70.9 (74.8)	50.3 (27.2)	0.408
ALT u/l		58.3 (51.9)	41.2 (33.0)	0.068
Glucose mg/dl	at 72 hours	165.0 (63.1)	153.1 (88.0)	0.070
Urea mg/dl		62.2 (40.4)	56.3 (36.7)	0.364
Creatinine mg/dl		1.1(0.4)	1.0 (0.4)	0.158
AST u/l		39.7 (24.8)	63.8 (75.9)	0.007
ALT u/l		32.4 (18.4)	53.5 (67.8)	0.070
Hospitalization time (days)		19.1 (2.8)	8.5 (2.1)	<0.001

*A Mann–Whitney U analysis was performed. SD: standard deviation, AST: aspartate aminotransferase, ALT: alanine aminotransferase

Discussion

As people age, the risks of orthopedic diseases and conditions increase making it difficult for people to maintain coordination; hence fall-related injuries and fractures significantly increase. It has been estimated that almost half of the people over 65 will need surgical intervention at some point during the rest of their lives [6]. It has been assumed that the life quality after surgical intervention decreases significantly with the development of post-operative complications, including delirium, in addition to complications related to the primary reason for surgery.

It has been reported that presence of comorbidities leads to an increase in the risk of complications during the post-operative period [7]. In our study, HT in 27.5%, DM in 54.2%, CHF in 47.8%, IHD in 31.8%, and cancer in 16.4% of the

patients were recorded. It was noted that in patients with IHD, the risk of delirium development was significantly higher than in those without. It has been suggested that ASA scoring may be helpful in facilitating a decrease in the rate of mortality after surgery. It is evident that patients with high ASA scores such as III/IV show high mortality rates [8]. In addition, studies reporting that the type of anesthesia also affects the rates of morbidity and mortality are available as regional anesthesia causes less mortality compared to general anesthesia [9]. Similarly, Gunturk et al. [10] reported a 3.4% mortality rate in patients with regional anesthesia compared to 8.8% in those receiving general anesthesia. In another study in which in-hospital mortality rates were compared between patients who underwent regional anesthesia, general anesthesia, and intra-surgery change from general to regional anesthesia (Cv), it was reported that the mortality rate between general and regional anesthesia was 1.38, while it was 2.23 between Cv and regional anesthesia [11]. However, studies reporting no significant differences between the effects of general and regional anesthesia on mortality in addition to cardiovascular complications are available in which the unadjusted rates were compared in patients who underwent hip fracture surgery in adults [12]. In our study, although the mortality rate in patients with regional anesthesia (5.1%) was lower than that of with general anesthesia (6.9%), the difference between the two groups was not significant. However, the mortality rate was found to be closely related to the presence of delirium complications. Mortality rate was 17.2% in patients with delirium complications, while it was 4.1% in without delirium, and this difference was statistically significant. ASA scores were also found to be effective in the presence of delirium complications since patients with ASA3 score were found to have higher rates of delirium complications compared to ASA1 and ASA2 patients.

Lengths of surgery in addition to lengths of hospitalization stays were determined to be related to the presence of delirium in this study. Delirium was suggested to be associated with increased days of mechanical ventilation, intensive care unit lengths of stay, and increased lengths of hospital stay [13]. In addition, delirium may also result to a longer stay in hospital [14]. Delirium was also reported to be related to the patients' functional decline [15]. Increased lengths of hospital stay, especially in geriatric patients, may cause an increase in the risk of new complications, including development of infections; hence, lengthy stays are not preferred. The results clearly indicate that shorter hospital stays should be implemented to reduce the risk of post-operative delirium complications. Delirium is more commonly seen in patients who have pre-cognitive dysfunctional conditions, comorbidities, and intensive care unit care [16]. Since such conditions may significantly affect the results of a study, they were excluded in the present study.

Hip fracture is quite common, especially among elderly women [17,18]. In our retrospective study, a high incidence of hip fracture was similarly noted in women (66.2%) compared to men (33.8%). Increased rate of osteoporosis especially after menopause in women makes this group of patients more vulnerable for hip fractures [19]. In a study, 40% delirium was reported to develop in patients after hip fracture surgery [20]. A 14.4% rate of delirium development was observed in our study, which seems quite low compared to the previous study. Considering the multifactorial reasons for the development of delirium, it is quite difficult to make comparisons between the two studies.

In this study, delirium was detected in 8.1% of the patients who had received regional anesthesia, while the rate was 20.6% for general anesthesia. Similarly, higher delirium rates were reported by others for patients receiving general anesthesia [21]. Multiple drug use and presence of chronic diseases were suggested to be some factors in post-operative development of delirium [22]. However, Atay et al. [17] reported no relationship between multi drug use and post-operative delirium development. Similarly, we did not observe any association between the presence of chronic diseases and multi drug use with post-operative delirium development. It may be more appropriate to scan larger patient groups to allow a clear conclusion to be drawn on the effects of drug use and presence of chronic diseases for development of post-operative delirium.

Sedation use was detected in 66.7% of the patients who had regional anesthesia, while it was only 22.5% in patients receiving general anesthesia. In addition, delirium development in patients who had received regional anesthesia was significantly lower than that of general anesthesia; hence, a reverse association between sedation use and delirium development was noted. It could be suggested that to reduce the risk of delirium development, regional anesthesia should be chosen, especially in geriatric patients.

Limitations

Our study was a single-center study and included only geriatric patients who underwent surgery for the lower extremities. The absence of upper extremity surgery, pediatric patients, and young patient groups caused the number of study patients to be low; therefore, our study data and results from data analyses are more limited.

Conclusions

In conclusion, as a result, when we evaluated the data in our study, delirium appears to develop more frequently in geriatric patients who receive general anesthesia. We concluded that regional anesthesia may be more beneficial than general anesthesia in terms of producing a reduction in the development of delirium.

References

1. Motz Bettelli G. Preoperative evaluation in geriatric surgery: comorbidity, functional status and pharmacological history. Minerva Anestesiol. 2011 Jun;77(6):637-46.
2. Ulukan U. Demographic Change in Turkey and Older Workers. Fiscaoeconomia 2020;4:94-110
3. Robertson BD, Robertson TJ. Postoperative delirium after hip fracture. J Bone Joint Surg Am. 2006;88:2060-8.
4. Cole MG. Delirium in elderly patients. Am J Geriatr Psychiatry. 2004 Jan-Feb;12(1):7-21
5. Abouleish AE, Leib ML, Cohen NH. ASA Provides Examples to Each ASA Physical Status Class. ASA Newsletter. 2015;79:38-49.
6. Dodds C,Murray D. Pre-operative assessment of the elderly. Continuing Education in Anaesthesia, Critical Care & Pain. 2001;1:181-4.
7. Chow WB, Rosenthal RA, Merkow RP, Ko CY, Esnaola NF; American College of Surgeons National Surgical Quality Improvement Program, et al. Optimal preoperative assessment of the geriatric surgical patient: a best practices guideline from the American College of Surgeons National Surgical Quality Improvement Program and the American Geriatrics Society. J Am Coll Surg. 2012;215:453-66.
8. Liu JL, Wang XL, Gong MW, Mai HX, Pei SJ, Yuan WX, et al. Comparative outcomes of peripheral nerve blocks versus general anesthesia for hip fractures in geriatric Chinese patients. Patient Prefer Adherence. 2014 May 7;8:651-9.
9. Luger TJ, Kammerlander C, Gosch M, Luger MF, Kammerlander-Knauer U, Roth T, et al. Neuroaxial versus general anaesthesia in geriatric patients for hip fracture surgery: does it matter? Osteoporos Int. 2010;21(4):555-72.

10. Güntürk S, Aydın G, Alaygut E, Karaman Y, Bozkurt P. Effect of the Anesthesia Method on Mortality and Postoperative Complications in ASA III-IV Graded Geriatric Patients. The Journal of Tepecik Education and Research Hospital. 2019;29:223-8.
11. Qiu C, Chan PH, Zohman GL, Prentice HA, Hunt JJ, LaPlace DC, et al. Impact of Anesthesia on Hospital Mortality and Morbidities in Geriatric Patients Following Emergency Hip Fracture Surgery. J Orthop Trauma. 2018;32:116-23.
12. Neuman MD , Silber JH , Elkassabany NM , Ludwig JM, Fleisher LA. Comparative effectiveness of regional versus general anesthesia for hip fracture surgery in adults. Anesthesiology. 2012;117:72-92.
13. Whitlock EL, Vannucci, A, Avidan, MS. Postoperative delirium. Minerva Anestesiol. 2011;77:448-56.
14. Packard RC. Delirium. Neurologist. 2001;7:327-40.
15. Rudolph JL, Inouye SK, Jones RN, Yang FM, Fong TG, Levkoff SE, Marcantonio ER, et al. Delirium: an independent predictor of functional decline after cardiac surgery. J Am Geriatr Soc. 2010;58(4):643-9
16. Grover S, Shah R. Delirium-related distress in caregivers: a study from a tertiary care centre in India. Perspect Psychiatr Care. 2013;49:21-9.
17. Atay I, Aslan A, Atay T, Burc H. Prevalence of delirium, risk factors and cognitive functions in elderly hip fracture patients with general and spinal anesthesia. Turkish Journal of Geriatrics. 2012;15:273-8.
18. Atay T, Yaman E, Baykal YB, Kirdemir V, Baydar ML, Aslan,A. Postoperative Clinical And Radiological Length Differences In Elderly Patients Who Underwent Partial Endoprosthesis Surgery. Turkish Journal of Geriatrics. 2010;13:238-43.
19. Alpantaki K , Papadaki C , Raptis K , Dretakis K , Samonis, G, Koutserimpas C. Gender and Age Differences in Hip Fracture Types among Elderly: a Retrospective Cohort Study. Maedica (Bucur). 2020;15:185-90.
20. Marcantonio E, Ta T, Duthie E, Resnick NM. Delirium severity and psychomotor types: their relationship with outcomes after hip fracture repair. J Am Geriatr Soc. 2002;50:850-7.
21. Parker MJ, Handoll HH, Griffiths R. Anaesthesia for hip fracture surgery in adults. Cochrane Database Syst Rev. 2004;CD000521.
22. Bjorkelund KB, Hommel A, Thorngren KG, Lundberg D, Larsson S. Factors at admission associated with 4 months outcome in elderly patients with hip fracture. AANA J. 2009;77:49-58.

J Surg Med. 2023;7(5):329-333.
DOI: 10.28982/josam.1127788

Research article

Journal of Surgery and Medicine
e-ISSN: 2602-2079
https://jsurgmed.com/

The effect of a single dose of intravenous tranexamic acid on visual clarity in knee arthroscopic meniscectomy without a tourniquet

Aziz Çataltape, Kadir Öznam

Department of Orthopedic Surgery and Traumatology, Medipol University, Istanbul, Turkey

ORCID ID of the author(s)

AÇ: 0000-0001-9785-9062
KÖ: 0000-0001-7392-7729

Corresponding Author
Aziz Çataltape
Department of Orthopedic Surgery and Traumatology, Medipol University, 34214, Istanbul, Turkey
E-mail: aziz.cataltepe@medipol.edu.tr

Ethics Committee Approval
The study was approved by the institutional ethics committee of Medipol University (08/02/2021, E-10840098-772.02-4395).
All procedures in this study involving human participants were performed in accordance with the 1964 Helsinki Declaration and its later amendments.

Conflict of Interest
No conflict of interest was declared by the authors.

Financial Disclosure
The authors declared that this study has received no financial support.

Published
2023 May 18

Abstract

Background/Aim: Tranexamic acid (TXA) is known to reduce intra-articular bleeding during arthroscopic procedures, which can improve visibility and reduce postoperative pain and knee joint swelling from hemarthrosis. However, insufficient data supports the routine use of TXA in arthroscopic meniscectomy. This study aimed to evaluate the effect of a single dose of intravenous (IV) TXA on visual clarity in arthroscopic meniscectomy without a tourniquet.
Methods: A randomized, double-blind, controlled trial was conducted to assess the use of TXA for visibility in routine arthroscopic meniscectomy without a tourniquet. Between January 2021 and February 2022, 53 patients undergoing arthroscopic meniscectomy were randomly assigned to either the TXA group (n=27), who received 1 g IV-TXA, or the control group (n=26), who received 100 ml of normal saline. Visual clarity was evaluated using a Numeric Rating Scale (NRS). Patients were also assessed for the need for a tourniquet, tourniquet time, total operative time, volume of irrigation fluid, postoperative pain, hemarthrosis, and knee function on postoperative day 3 and weeks 1, 2, and 4, using the Lysholm knee scoring scale.
Results: There was no significant difference in intra-operative arthroscopic visibility between the TXA and control groups (P=0.394). Tourniquet was required in three cases in the TXA group and four cases in the control group (P=0.646). There was no significant difference between the two groups regarding postoperative pain, grade of postoperative hemarthrosis, knee motion, or the Lysholm Knee Score after the operation.
Conclusion: The administration of IV-TXA in arthroscopic meniscectomy without a tourniquet did not provide any benefits such as enhanced surgical visualization, reduction in the need to inflate the tourniquet due to obstructed visibility, or decrease in hemarthrosis, VAS pain score, or improved range of motion of the knee in the postoperative period when compared to the control group.

Keywords: arthroscopic meniscectomy, tranexamic acid, visual clarity, pneumatic tourniquet, cold intra-articular irrigation

How to cite: Çataltape A, Öznam K. The effect of a single dose of intravenous tranexamic acid on visual clarity in knee arthroscopic meniscectomy without a tourniquet. J Surg Med. 2023;7(5):329-333.

Introduction

Despite its advantages, knee arthroscopy can be associated with preventable and unpreventable complications [1,2]. Pneumatic tourniquets are frequently used in arthroscopic knee surgery to facilitate the procedure, improve visualization, reduce operative time, and achieve optimal outcomes. However, tourniquet use has been linked to various complications, including nerve palsy, venous thromboembolism, arterial embolization, skin ulceration, swelling, quadriceps or hamstring weakness, and joint stiffness [3-5].

In knee arthroscopy, the absence of a tourniquet can lead to uncontrolled bleeding, a major factor affecting visual clarity [6-8]. Adequate visual clarity is essential for accurate diagnosis and optimal treatment during arthroscopic procedures [8,9]. Several methods have been developed to improve visualization during arthroscopy, including controlled hypotension, thermal coagulation, pump irrigation systems, and adding epinephrine to the irrigation fluid [6,10]. Additionally, hemarthrosis and pain can negatively impact the functional outcome of knee arthroscopy [11]. Tranexamic acid (TXA) has become popular in orthopedic practice due to its ability to reduce intra-articular bleeding during arthroscopic procedures, improve visibility, and decrease postoperative pain and knee joint swelling from hemarthrosis [12-16]. However, insufficient data supports the routine use of TXA in arthroscopic meniscectomy.

The current study hypothesized that administering TXA without a tourniquet would improve visual clarity in routine arthroscopic meniscectomy. The primary objective was to evaluate the effect of a single dose of intravenous (IV) TXA on visual clarity, while the secondary objective was to determine whether administering 1 g IV-TXA prior to arthroscopic meniscectomy reduces hemarthrosis and postoperative pain and allows for earlier restoration of active range of motion.

Materials and methods

A randomized, double-blind controlled trial was conducted at the Department of Orthopedic Surgery, Istanbul Medipol University, between February 2021 and January 2022, after obtaining approval from the ethics committee [17]. Patients with chondral defects requiring a cartilage restoration procedure, meniscal suturing at the time of surgery, uncontrolled hypertension (systolic pressure >140), or coagulation or bleeding disorders were excluded from the study. Patients over 18 years old with a meniscal tear, with or without cartilage degeneration, underwent partial meniscectomy. All patients provided additional informed consent to participate in the study. Patient randomization was performed using a computer-generated code, printed, and sealed in unmarked envelopes. A total of 53 patients who underwent arthroscopic meniscectomy were assigned to either the TXA group (n=27), who received 1 g IV-TXA in 100 ml of normal saline, or the control group (n=26), who received 100 ml of normal saline without TXA administered 15 min before surgery at the same rate and by the same route. The study flowchart is presented in Figure 1. Although the surgeon, observer, and patients were blinded, the anesthetist administering the TXA or placebo was not blinded.

Figure 1: Flowchart of patient inclusion. (TXA: tranexamic acid)

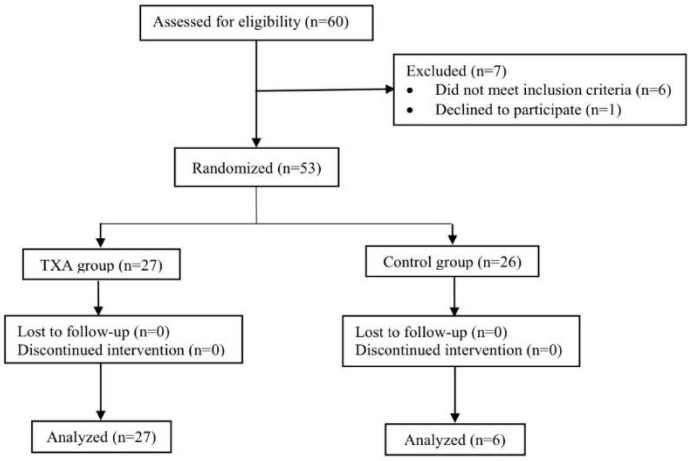

All patients were positioned in the supine position and administered general or spinal anesthesia. In all cases, a tourniquet was applied but not previously inflated. If the surgeon encountered impaired vision intraoperatively due to bleeding reducing visibility into the knee joint, the tourniquet pressure was maintained at 300 mm Hg. The decision to inflate the tourniquet was made by the surgeon responsible for the procedure. No pressure pump or intra-articular cautery was used in any case. All patients underwent standard 2-portal knee arthroscopy with the gravity technique to administer a continuous flow of cold (4°C) saline irrigation solution from a three-liter saline bag elevated to 2.5 meters above the floor. Intraoperative visual clarity was evaluated using a Numeric Rating Scale (NRS), with a score of 1 indicating a complete lack of visibility and a score of 10 indicating the highest level of clear vision at the end of the operation, as previously described by van Montfoort et al. [8] and Avery et al. [17] (Figure 2). All patients were discharged home on the day of the surgery.

Figure 2: A demonstration of clarity of view scored using the NRS through the anterolateral portal (NRS: Numeric Rating Scale). (A) The view scored 10 indicates; the highest clear vision. (B) The view scored 5 indicates; bleeding mixed with the irrigation fluid, which can impede the visibility to perform surgery, but it can be acceptable for knee arthroscopy. (C) The view scored 1 indicates; complete lack of visibility.

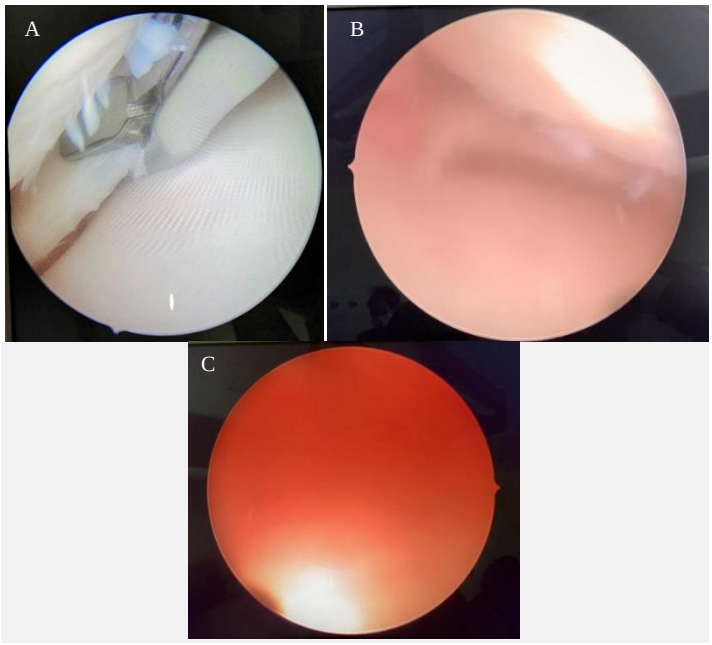

All patients were assessed for the need for a tourniquet, duration of tourniquet time, total operative time, the volume of intraoperative irrigation fluid used, systolic blood pressure, intraoperative complications, postoperative pain, hemarthrosis,

and knee function at postoperative day 3 and postoperative weeks 1, 2, and 4. Knee hemarthrosis was clinically graded according to the classification of Coupens and Yates (CY), subjectively graded from 0 to 4 (Table 1) [18]. Knee aspiration was considered in cases of severe pain and persistent and severe hemarthrosis (CY grade 3–4). Pain score was recorded using a visual analog scale (VAS) ranging from 0 to 10, and the Lysholm Knee Score [19] was used to record knee function. The knees' active range of motion (ROM) was measured using an orthopedic goniometer. Patients were clinically examined for leg swelling or calf pain, and those with clinical suspicion of deep venous thrombosis underwent Doppler ultrasonography.

Table 1: Clinical grading of hemarthrosis according to the classification of Coupens and Yates (CY).

Grade	
0	No detectable fluid
1	Fluid present, no fluid wave
2	Palpable fluid wave
3	Ballotable patella
4	Tense hemarthrosis

Statistical analysis

Data were described using mean (standard deviation [SD]) and analyzed using NCSS (Number Cruncher Statistical System) 2007 Statistical Software (Utah, USA). Normality was tested using the Shapiro-Wilk test. The independent t-test was used to compare normally distributed continuous variables between groups, while the Chi-square test was used to analyze qualitative comparative parameters. The nonparametric Mann-Whitney U test was used to analyze non-normally distributed data. Statistical significance was considered when the *P*-value was below 0.05.

Results

Fifty-three patients undergoing arthroscopic meniscectomy were evaluated, with 27 patients in the TXA group and 26 in the control group. The mean age was 46.3 (10.79) years in the TXA group and 47.54 (12.9) years in the control group (Table 2).

Table 2: Patients' demographics data.

Variables	TXA group (n=27)	Control group (n=26)	*P*-value
Age (year)	46.3 (10.79)	47.54 (12.9)	0.705*
Sex			
Male	13 (48.15%)	11 (42.31%)	0.669+
Female	14 (51.85%)	15 (57.69%)	
BMI (kg/m²)	28.97 (4,26)	29.04 (5.32)	0.964*
Side			
Right	11 (40.74%)	10 (38.46%)	0.865+
Left	16 (59.26%)	16 (61.54%)	
Anesthesia type			
General	5 (18.52%)	4 (15.38%)	0.761+
Spinal	22 (81.48%)	22 (84.52%)	
Mean arterial pressure (mm Hg)	10.25 (1.2)	9.86 (1.08)	0.218*
Operative time (minute)	32.7 (6.93)	33.35 (6.43)	0.728*
Change of serum Hb concentration (g/dL)	1.04 (0.56)	1.11 (0.4)	0.640*
Amount of fluid used (L)	3.55 (1.14)	3.8 (1.31)	0.459*
The need for a tourniquet (n)	3 (11.11%)	4 (15.38%)	0.646*
Tourniquet time, minute	12.67 (2.08)	15.25 (1.71)	0.130*

Values presented as mean (standard deviation) and *P* calculated by using *unpaired t test and + chi square test. BMI: Body mass index.

There was no significant difference in intraoperative arthroscopic visibility between the TXA group and the control group (P=0.394), with visibility rated at 7.41 (1.91) in the TXA group and 6.92 (2.19) in the control group (Table 3). Visibility was enhanced in seven cases after tourniquet inflation. The tourniquet was required in three cases in the TXA group and four cases in the control group. No statistically significant difference was observed between the groups regarding the need for delayed tourniquet inflation (P=0.646). The mean tourniquet time in the TXA group was 12.67 (2.08) min and 15.25 (1.71) min in the control group, although this result did not reach statistical significance (P=0.130).

Table 3: The quality of intra-operative visibility of the TXA group and the control group.

Variable	TXA group (n=27)	Control group (n=26)	*P*-value
Overall score	7.41 (1.91)	6.92 (2.19)	0.394*

Values presented as mean (standard deviation) and *P* calculated by using *unpaired t-test.

There was no significant difference in the mean operative time between the two groups (P=0.728). The mean operative time was 32.7 (6.93) min in the TXA group and 33.35 (6.43) min in the control group. Moreover, the amount of irrigation fluid used during the surgery was not statistically significant between the two groups (P=0.459). The mean amount of irrigation fluid in the TXA group was 3.55 (1.14) L, and 3.8 (1.31) L in the control group.

No statistically significant difference was observed between the TXA and control groups regarding the degree of VAS pain at each time point after the operation. Similarly, there was no significant difference between the two groups regarding the grade of postoperative hemarthrosis, ROM, and the Lysholm Knee Score at each time point after the operation (Table 4). One knee in the TXA group required postoperative knee aspiration, although this result did not reach statistical significance between the two groups (P=0.509). All patients regained their knee ROM within four weeks after surgery, and no evidence of infection or deep venous thrombosis was reported in either group.

Table 4: Comparison of secondary study results of the TXA group and the control group.

Variable	TXA group (n=27)	Control group (n=26)	*P*-value*
Lysholm score			
Preoperative	53.48 (9.42)	51.38 (8.92)	0.410*
POW 1	68.11 (10.52)	66.73 (8.3)	0.599*
POW 2	81.15 (7.74)	79.92 (6.08)	0.526*
POW 3	91.26 (4.76)	90.38 (4.05)	0.475*
VAS score			
Preoperative	7.15 (0.66)	7.27 (0.72)	0.477‡
POD 3	5.3 (0.91)	5.5 (1.33)	0.506‡
POW 1	4.41 (0.84)	4.46 (0.76)	0.744‡
POW 2	3.52 (0.75)	3.58 (0.64)	0.738‡
POW 3	2.37 (0.79)	2.42 (0.86)	0.855‡
ROM			
Preoperative	124.81 (12.88)	122.65 (11.26)	0.519*
POD 3	93.07 (4.87)	91.19 (6.51)	0.238*
POW 1	106.85 (5.87)	105.62 (5.89)	0.448*
POW 2	117.41 (5.79)	116.69 (6.25)	0.667*
POW 3	131.67 (6.79)	131.92 (5.87)	0.884*
CY value			
POD 3	1.67 (0.68)	1.69 (0.68)	0.854‡
POW 1	1.44 (0.75)	1.46 (0.71)	0.843‡
POW 2	0.7 (0.54)	0.77 (0.65)	0.775‡
POW 3	0.22 (0.42)	0.23 (0.43)	0.941‡
PO aspiration	1 (37%)	0 (0%)	0.509+

Values presented as mean (standard deviation) and p calculated by using *unpaired t test, ‡Mann Whitney U test, and +chi Square. POD: Postoperative day, POW: Postoperative week, VAS: Visual analog scale. ROM: Range of motion, CY: Coupens and Yates. PO: Postoperative.

Discussion

The most significant finding of this study is that the administration of IV-TXA (1 g) in arthroscopic meniscectomies without a tourniquet did not enhance surgical visualization or reduce the need to inflate the tourniquet due to obstructed visibility when compared to the control group.

A bloodless field is crucial for optimal visibility during arthroscopic surgery [15,20]. TXA has been used to promote adequate visualization in intra-operative arthroscopy [15,20,21]. However, there is a lack of sufficient data on using TXA in

arthroscopic procedures and whether it enhances visibility during surgery. A recent randomized controlled trial found that administering IV-TXA improved surgical clarity during arthroscopic rotator cuff repair without increasing the risk of side effects [15]. Similarly, Ersin et al. [21] demonstrated that IV-TXA led to improved visual clarity during shoulder arthroscopy. However, the effect of IV-TXA on visual clarity during arthroscopic knee surgery is not well known. To our knowledge, no study has investigated the impact of IV-TXA on surgical clarity during knee arthroscopic meniscectomy without a tourniquet. In this study, we hypothesized that administering TXA would provide better visibility during arthroscopic meniscectomy without a tourniquet. However, at the end of the study, compared to the control group, the administration of IV-TXA did not provide enhanced surgical visualization.

The use of a tourniquet in knee arthroscopy is still debated despite its ability to provide clarity of surgical visibility [7,24-26]. Hoogeslag et al. [7] reported improved visibility with the use of a tourniquet in routine knee arthroscopy procedures, but 10.2% of patients required inflation of the tourniquet due to fair or poor intra-operative arthroscopic visibility. Olszewski et al. [6] found that dilute epinephrine in normal saline irrigation fluid reduced the need for tourniquet utilization during routine arthroscopic knee surgery, with only 24.6% of patients requiring tourniquet inflation. Similarly, Johnson et al. [23] reported no significant difference in operative views between groups with and without inflated tourniquets during knee arthroscopy.

In this study, using a tourniquet during routine knee arthroscopic meniscectomy was unnecessary. The need for tourniquet inflation was 11.1% in the TXA group and 15.38% in the control group, comparable to the literature. The mean tourniquet time for patients in whom the tourniquet was used was considerably shorter in both groups than in the literature. This could help reduce tourniquet-related complications due to prolonged use. The duration of surgery was also not significantly different between the TXA and control groups. These findings suggest that arthroscopic knee surgery can be performed safely and effectively without the routine use of a tourniquet. However, the administration of IV-TXA did not provide any additional benefit in reducing the need for a tourniquet or improving surgical visualization.

In previous studies, a pressure-controlled pump in arthroscopic knee surgery has been suggested to improve visualization [24,25]. However, using an infusion pump system can result in pain and quadriceps inhibition, potentially leading to muscle weakness and joint distension [26,27]. In some rare cases, using an infusion pump has resulted in complications such as complete femoral nerve palsy [28]. In this study, a pressure pump was not used, and instead, the gravity technique was applied to administer a continuous flow of the saline irrigation solution with cold (4°C), which may constrict the blood vessels around the surgical field. Although the administration of IV-TXA was found to be ineffective in promoting visual clarity when compared to the control group, based on our findings, arthroscopic meniscectomy with the irrigation solution with cold (4°C) can be performed without a tourniquet, which is an alternative way to enhance surgical visualization and reduce the need to inflate the tourniquet due to obstructed visibility during arthroscopic meniscectomy. However, further evaluation is needed to determine whether the irrigation solution with cold (4°C) can enhance surgical visualization and reduce the need for a tourniquet.

TXA has been investigated for its potential to decrease hemarthrosis and pain and increase knee function in patients undergoing anterior cruciate ligament reconstruction (ACLR) [14,29]. Karaaslan et al. [14] demonstrated that administering TXA intravenously before tourniquet inflation and continuing for 3 h after surgery reduced hemarthrosis, decreased pain, and improved knee function in the early postoperative period. However, a more recent study by Fried et al. [29] investigating the use of IV-TXA in patients undergoing ACLR suggested that IV-TXA did not result in a reduction of postoperative pain, range of motion, or hemarthrosis. This conclusion was also reached by Nugent et al. [30], who found no significant improvement in pain scores, range of motion, or hemarthrosis at any of the evaluated time points in their study. In the present study, administering 1 g of IV-TXA with a tourniquet in arthroscopic meniscectomy improved Tegner activity scores at 3 days postoperatively. However, consistent with the literature, the outcomes of the present study demonstrated that TXA did not reduce hemarthrosis, alleviate subjective pain, or improve the range of motion in the postoperative period.

In this study, several limitations should be considered. First, the visual clarity was only recorded at the end of the surgery, which may not reflect the bleeding dynamic during the entire surgery. Second, the dose of TXA was not based on the patient's body weight, which may have resulted in some patients not receiving enough effective drug concentrations. Third, using a pressure-controlled pump may have improved visualization but was not used in this study to reflect the common use of gravity flow in routine knee arthroscopy. Fourth, it is unclear how long the surgeon waited to regain visibility to intraoperatively inflate the tourniquet to perform the procedure due to impeded vision. Lastly, the surgeon rated the visual field's intraoperative clarity subjectively using an NRS, which may have introduced bias.

Conclusion

In conclusion, administering IV-TXA in arthroscopic meniscectomy without a tourniquet did not benefit enhanced surgical visualization or reduce the need to inflate the tourniquet. However, using irrigation solution with cold (4°C) may be an alternative way to enhance surgical visualization and reduce the need for a tourniquet. Furthermore, TXA did not decrease hemarthrosis or VAS pain scores or improve knee range of motion in the postoperative period.

Acknowledgment

Special thanks to Renza Konyalioglu for statistical support.

References

1. Reigstad O, Grimsgaard C. Complications in knee arthroscopy. Knee Surg Sports Traumatol Arthrosc. 2006;14(5):473-7.
2. Salzler MJ, Lin A, Miller CD, Herold S, Irrgang JJ, Harner CD. Complications after arthroscopic knee surgery. Am J Sports Med. 2014;42(2):292-6.
3. Dobner JJ, Nitz AJ. Postmeniscectomy tourniquet palsy and functional sequelae. Am J Sports Med. 1982;10(4):211-4.
4. Kornbluth ID, Freedman MK, Sher L, Frederick RW. Femoral, saphenous nerve palsy after tourniquet use: a case report. Arch Phys Med Rehabil. 2003;84(6):909-11.
5. Huang HF, Tian JL, Sun L, Yang XT, Shen YK, Li SS, et al. The effect of anticoagulants on venous thrombosis prevention after knee arthroscopy: a systematic review. Int Orthop. 2019;43(10):2303-8.
6. Olszewski AD, Jones R, Farrell R, Kaylor K. The effects of dilute epinephrine saline irrigation on the need for tourniquet use in routine arthroscopic knee surgery. Am J Sports Med. 1999;27(3):354-6.

7. Hoogeslag RA, Brouwer RW, van Raay JJ. The value of tourniquet use for visibility during arthroscopy of the knee: a double-blind, randomized controlled trial. Arthroscopy. 2010;26(9 Suppl):S67-72.
8. van Montfoort DO, van Kampen PM, Huijsmans PE. Epinephrine Diluted Saline-Irrigation Fluid in Arthroscopic Shoulder Surgery: A Significant Improvement of Clarity of Visual Field and Shortening of Total Operation Time. A Randomized Controlled Trial. Arthroscopy. 2016;32(3):436-44.
9. Kuo LT, Chen CL, Yu PA, Hsu WH, Chi CC, Yoo JC. Epinephrine in irrigation fluid for visual clarity in arthroscopic shoulder surgery: a systematic review and meta-analysis. Int Orthop. 2018;42(12):2881-2889.
10. Hsiao MS, Kusnezov N, Sieg RN, Owens BD, Herzog JP. Use of an Irrigation Pump System in Arthroscopic Procedures. Orthopedics. 2016;39(3):e474-8.
11. Bahl V, Goyal A, Jain V, Joshi D, Chaudhary D. Effect of haemarthrosis on the rehabilitation of anterior cruciate ligament reconstruction--single bundle versus double bundle. J Orthop Surg Res. 2013;19;8:5.
12. Alvarez J, Santiveri FJ, Ramos MI, Gallart L, Aguilera L, Puig-Verdie L. Clinical trial on the effect of tranexamic acid on bleeding and fibrinolysis in primary hip and knee replacement. Rev Esp Anestesiol Reanim. 2019;66(6):299-306.
13. Kirsch JM, Bedi A, Horner N, Wiater JM, Pauzenberger L, Koueiter DM, et al. Tranexamic acid in shoulder arthroplasty: A systematic review and meta-analysis. JBJS Rev. 2017;5(9):e3.
14. Karaaslan F, Karaoğlu S, Yurdakul E. Reducing Intra-articular Hemarthrosis After Arthroscopic Anterior Cruciate Ligament Reconstruction by the Administration of Intravenous Tranexamic Acid: A Prospective, Randomized Controlled Trial. Am J Sports Med. 2015;43(11):2720-6.
15. Liu YF, Hong CK, Hsu KL, Kuan FC, Chen Y, Yeh ML, Su WR. Intravenous Administration of Tranexamic Acid Significantly Improved Clarity of the Visual Field in Arthroscopic Shoulder Surgery. A Prospective, Double-Blind, and Randomized Controlled Trial. Arthroscopy. 2020;36(3):640-647.
16. Felli L, Revello S, Burastero G, Gatto P, Carletti A, Formica M, Alessio-Mazzola M. Single Intravenous Administration of Tranexamic Acid in Anterior Cruciate Ligament Reconstruction to Reduce Postoperative Hemarthrosis and Increase Functional Outcomes in the Early Phase of Postoperative Rehabilitation: A Randomized Controlled Trial. Arthroscopy. 2019;35(1):149-57.
17. Avery DM, Gibson BW, Carolan GF. Surgeon-rated visualization in shoulder arthroscopy: a randomized blinded controlled trial comparing irrigation fluid with and without epinephrine. Arthroscopy. 2015;31(1):12-8.
18. Coupens SD, Yates CK. The effect of tourniquet use and hemovac drainage on postoperative hemarthrosis. Arthroscopy. 1991;7(3):278-82.
19. Lysholm J, Gillquist J. Evaluation of knee ligament surgery results with special emphasis on use of a scoring scale. Am J Sports Med. 1982;10(3):150-4.
20. Bayram E, Yıldırım C, Ertürk AK, Yılmaz M, Atlıhan D. Comparison of the efficacy of irrigation with epinephrine or tranexamic acid on visual clarity during arthroscopic rotator cuff repair: A double-blind, randomized-controlled study. Jt Dis Relat Surg. 2021;32(1):115-21.
21. Ersin M, Demirel M, Büget Mİ, Edipoğlu İS, Atalar AC, Erşen A. The effect of intravenous tranexamic acid on visual clarity during arthroscopic rotator cuff repair: A randomized, double-blinded, placebo-controlled pilot study. Acta Orthop Traumatol Turc. 2020;54(6):572-6.
22. Kirkley A, Rampersaud R, Griffin S, Amendola A, Litchfield R, Fowler P. Tourniquet versus no tourniquet use in routine knee arthroscopy: a prospective, double-blind, randomized clinical trial. Arthroscopy. 2000;16(2):121-6.
23. Johnson DS, Stewart H, Hirst P, Harper NJ. Is tourniquet use necessary for knee arthroscopy? Arthroscopy. 2000;16(6):648-51.
24. Nakayama H, Yoshiya S. The effect of tourniquet use on operative performance and early postoperative results of anatomic double-bundle anterior cruciate ligament reconstruction. J Orthop Sci. 2013;18(4):586-91.
25. Júnior LH, Soares LF, Gonçalves MB, Gomes TP, Oliveira JR, Coelho MG, Santos RL, Andrade MA, Silva Gde L, Novais EN. Tourniquet Versus No Tourniquet Use In Knee Videoarthroscopy: A Multicentric, Prospective, Double-Blind, Randomized Clinical Trial. Rev Bras Ortop. 2015;12;45(5):415-7.
26. deAndrade JR, Grant C, Dixon AS. Joint distention and reflex muscle inhibition in the knee. J Bone Joint Surg Am. 1965;47:313-22.
27. Thorblad J, Ekstrand J, Hamberg P, Gillquist J. Muscle rehabilitation after arthroscopic meniscectomy with or without tourniquet control. A preliminary randomized study. Am J Sports Med. 1985;13(2):133-5.
28. DiStefano VJ, Kalman VR, O'Malley JS. Femoral nerve palsy after arthroscopic surgery with an infusion pump irrigation system. A report of three cases. Am J Orthop (Belle Mead NJ). 1996;25(2):145-8.
29. Fried JW, Bloom DA, Hurley ET, Baron SL, Popovic J, Campbell KA, et al. Tranexamic Acid Has No Effect on Postoperative Hemarthrosis or Pain Control After Anterior Cruciate Ligament Reconstruction Using Bone-Patellar Tendon-Bone Autograft: A Double-Blind, Randomized, Controlled Trial. Arthroscopy. 2021;37(6):1883-9.
30. Nugent M, May JH, Parker JD, Kieser DC, Douglas M, Pereira R, et al. Does Tranexamic Acid Reduce Knee Swelling and Improve Early Function Following Arthroscopic Meniscectomy? A Double-Blind Randomized Controlled Trial. Orthop J Sports Med. 2019;29;7(8):2325967119866122.

J Surg Med. 2023;7(5):334-338.
DOI: 10.28982/josam.7789

Research article

Journal of Surgery and Medicine
e-ISSN: 2602-2079
https://jsurgmed.com/

Comparison of the effects of neural therapy injection and extracorporeal shock wave therapy on pain and hand functions in the treatment of lateral epicondylitis

Ülkü Dönmez [1], Olgu Aygün [2]

[1] Buca Seyfi Demirsoy Education and Research Hospital, Department of Physical Therapy And Rehabilitation, Izmir, Turkey
[2] Bozyaka Education and Research Hospital, Department of Family Medicine, Izmir, Turkey

ORCID ID of the author(s)

ÜD: 0000-0002-0007-1517
OA: 0000-0002-9767-011X

Corresponding Author
Olgu Aygün
Buca Seyfi Demirsoy Education and Research Hospital, Department of Physical Therapy And Rehabilitation, Izmir, Turkey
E-mail: olgu4780@gmail.com

Ethics Committee Approval
The study was approved by the Buca Seyfi Demirsoy Training and Research Hospital non-interventional research ethics committee (date/protocol no: 28.09.2022/09-112). All procedures in this study involving human participants were performed in accordance with the 1964 Helsinki Declaration and its later amendments.

Conflict of Interest
No conflict of interest was declared by the authors.

Financial Disclosure
The authors declared that this study has received no financial support.

Published
2023 May 22

Abstract

Background/Aim: Lateral epicondylitis (LE), commonly known as “tennis elbow”, is a painful inflammatory condition affecting wrist extensor tendons. Various treatments, such as extracorporeal shockwave therapy (ESWT) and neural therapy injections, have been used to alleviate symptoms of LE. However, there is a limited number of comparative studies available. This study aims to compare the effectiveness of sequential neural therapy injections and ESWT in reducing pain and improving functionality in patients with LE.

Methods: A retrospective cohort study analyzed data from 128 LE patients. Among them, 30 patients underwent neural therapy, while 30 underwent ESWT, following the exclusion criteria. Pain levels were measured using the visual analog scale (VAS), and functionality was assessed using the Duruöz hand index (DHI) before and after treatment.

Results: Both neural therapy injections and ESWT led to substantial reductions in pain and improvements in functionality, with no notable differences observed between the two treatment methods. Additionally, no significant variations were found based on age, body mass index, gender, or the side of the elbow treated.

Conclusion: The findings suggest that both neural therapy injections and ESWT are equally effective in managing symptoms of LE. Treatment choice may depend on patient preference, cost, availability, or other factors. Further research is necessary to examine long-term outcomes, potential side effects, and factors predicting a better response to one treatment.

Keywords: lateral epicondylitis, pain, neural therapy, extracorporeal shock wave therapy

How to cite: Dönmez Ü, Aygün O. Comparison of the effects of neural therapy injection and extracorporeal shock wave therapy on pain and hand functions in the treatment of lateral epicondylitis. J Surg Med. 2023;7(5):334-338.

Introduction

Lateral epicondylitis (LE) is an inflammatory condition that affects the attachment site of the wrist extensor tendons. It is commonly referred to as tennis elbow due to the repetitive wrist-elbow-straining movements often seen in tennis players [1]. The primary symptom experienced by patients is pain in the lateral epicondyle, which can radiate to the humerus and forearm [2]. The main goals of treatment include pain reduction, inflammation resolution, and restoration of functionality [2,3].

Extracorporeal shockwave therapy (ESWT) is a commonly utilized physical therapy for treating LE, although the existing literature presents conflicting results [4-6]. ESWT induces inflammation and enhances blood flow in the targeted area, stimulating the body's self-repair mechanisms and promoting healing in chronic muscle-tendon disorders [5]. Furthermore, alternative injection methods such as local corticosteroids, platelet-rich plasma, and autologous blood injection have been employed as substitutes for conventional approaches in treating LE for a considerable period.

In contrast to these injections, neural therapy is also utilized to treat various musculoskeletal conditions. However, insufficient literature on studies involving neural therapy injections is lacking. Building upon this premise, our study aimed to compare the effects of sequential neural therapy injections and ESWT treatment on pain and functionality in patients diagnosed with LE.

Materials and methods

Our study is designed as a retrospective cohort study. We retrospectively evaluated the data of 128 patients with LE who sought treatment at the physical therapy outpatient clinic for elbow pain between January 2021 and January 2022. The data from those volunteers who met the inclusion criteria were analyzed.

Inclusion and Exclusion Criteria

The inclusion criteria were: patients who have experienced elbow pain within the last 3 months; patients who have received a diagnosis of lateral epicondylitis through physical examination and/or radiological imaging; and patients who have completed all tests assessing treatment efficacy. The exclusion criteria were: pregnancy or lactation; the presence of severe inflammatory diseases, muscle diseases such as myasthenia gravis, sepsis, or a diagnosis of cancer; all rheumatological diseases that may cause arthritis/arthralgia in the elbow; history of any recent injection into the painful elbow, elbow fracture, or the presence of metal implants (e.g., screws or nails) in the elbow; the presence of psychiatric diseases such as schizophrenia or mental retardation; patients who have undergone ESWT for symptomatic elbow treatment within the last 6 months; and patients with a history of decompensated heart failure, 2nd and 3rd degree AV block, bradycardia, or the use of anticoagulant agents.

In our study, we screened the data of patients who did not experience any changes in their medical treatments (such as oral analgesics or myorelaxants) and did not receive additional injections in their elbows throughout the study period. The study received approval from the Ethics Committee of Buca Seyfi Demirsoy Training and Research Hospital for non-interventional research (date/protocol no: 28.09.2022/09-112).

Intervention

We analyzed the data of 128 patients diagnosed with LE. Among these patients, it was observed that 86 received additional treatments in addition to medical treatment. Of the 86 selected patients, 34 underwent neural therapy injections, while the remaining 52 underwent ESWT treatments.

Patients who actively participated in each treatment protocol and attended the evaluation follow-ups were included in our study. Four of the 34 patients who received neural therapy injections were excluded from the study as they did not maintain their weekly follow-up appointments. To ensure comparability, we selected 30 patients from the 52 individuals who received ESWT treatment, matching them in terms of age and gender with the neural therapy group. In summary, we compared the data of 30 patients from both treatment groups.

The ESWT and neural therapy injection groups followed treatment protocols consisting of once-weekly sessions for three consecutive weeks.

The first group (n=30) comprised patients who received neural therapy injections in their painful elbows. The neural therapy injections were locally administered using the quaddle method, targeting the muscle tendon and ligament directly in the affected area. Five ampules of jetcaine were prepared by diluting them with 100 cc saline. Each injection contained 2 mL of lidocaine and was administered at a 10–20 mm depth using an insulin injector. For segmental effect, intracutaneous injections were applied around the tendon from a total of 6–8 points. Each injection session lasted approximately 5–8 minutes.

In the second group (n=30), ESWT was administered once a week for three consecutive weeks. The ESWT protocol involved using a frequency of 6 Hz, an intensity of 1.6 Barr, and delivering 2000 beats per session. Gel was applied around the painful area while the patient's elbow was flexed at 80–90°. Each ESWT session lasted approximately 15 min.

Evaluation criteria were established by a different doctor prior to the initiation of treatment and at its completion. The clinical and demographic data of the patients, including age, sex, physical examination findings, duration of symptoms, medication usage, presence of secondary diseases, and body mass index (BMI), were recorded and assessed before the treatment phase.

The Visual Analog Scale (VAS) was utilized to assess patients' pain levels before and after the administration of ESWT or neural therapy injections. Patients were asked to rate their pain on a scale of 0 to 10, with 0 indicating no pain and 10 representing unbearable pain before and after the treatment.

Our study also employed the Duruöz Hand Index (DHI) [7] as another assessment tool. The DHI evaluates hand-related activity limitations and is used to measure functional performance [7]. This test comprises 18 questions and is relatively easy to administer. Prior to treatment initiation, as well as after treatment, DHI data were recorded in both groups. The DHI assesses the utilization and functionality of the affected hand and elbow during daily activities such as kitchen tasks, clothing management, cleaning, workplace activities, and other activities of daily living. Each item is scored on a scale of 0 (no

difficulty) to 5 (impossible to do), reflecting the individual's ability. The maximum total score is 90, with higher scores indicating more severe activity limitations.

Statistical analysis

All statistical analyses were performed using SPSS 27.0. Additionally, all data are presented as the arithmetic mean with standard deviation (SD). Mann Whitney U and Wilcoxon tests were utilized to compare within and between groups. Furthermore, linear regression analysis was conducted to examine the independent variables influencing VAS and DHI values after treatment. A significance level of $P<0.05$ was considered statistically significant for all analyses.

Results

According to the inclusion criteria, we compared the data of 30 patients who received neural therapy injections with those of 30 patients who received ESWT in our study. The neural therapy group had a mean age of 49.4 years, while the ESWT group had a mean age of 49.9 years. Upon examination of the patients' age and BMI values, no significant difference was found between the two groups (Table 1).

Of the participants, 25% were males, and 75% were females. The right elbow accounted for 86.7% of the treatments, while the left accounted for 13.3%. No significant difference was observed between the two groups regarding the patients' gender and the treated elbow's direction (Table 1).

Table 1: Demographic data

	Neural therapy (n=30)	ESWT (n=30)	*P*-value
Age, year, Mean (SD)	49.4 (11.96)	49.9 (10.16)	0.862
BMI, kg/m^2, Mean (SD)	26.74 (2.37)	26.53 (1.66)	0.347
Gender, n (%)			
Female	21 (70)	24 (80)	0.551
Male	9 (30)	6 (20)	
Side, n (%)			
Right	26 (86.7)	26 (86.7)	1.000
Left	4 (13.3)	4 (13.3)	

SD: standard deviation

The two groups had no statistically significant differences in the pretreatment VAS scores (Table 2). However, both groups significantly improved pain scores after treatment ($P<0.001$). In the ESWT group, the median VAS score decreased from 7 before treatment to 4 after treatment. Similarly, in the neural therapy group, the VAS score decreased from 7 before treatment to 4 after treatment, which was also considered statistically significant (Table 2).

There was no statistically significant difference in the pretreatment median DHI values between the two groups ($P=0.399$). However, both groups exhibited a statistically significant improvement in DHI scores after treatment ($P<0.001$) (Table 2). In the ESWT group, the median DHI value decreased from 59 before treatment to 43.5 after treatment, with this reduction being statistically significant. Similarly, in the neural therapy group, the median DHI value decreased from 58.5 before treatment to 39 after treatment (Table 2), which is also statistically significant. When comparing the improvements in these scores between the groups, no superiority was observed between the two treatment methods.

Table 2: Comparison of VAS and DHI values within and between groups

	Group				Statistic test	*P*-value
	ESWT		Neural therapy			
	Mean (SD)	Median (Min–Max)	Mean (SD)	Median (Min–Max)		
VAS 0	6.8 (0.92)	7 (5–8)	6.83 (0.99)	7 (5–9)	U=446	0.951
VAS 3	3.93 (1.55)	4 (1–6)	4.67 (1.27)	4 (2–7)	U=353	0.140
Statistic test	Z=−4.48		Z=−4.401			
***P*-value**	<0.001		<0.001			
DHI 0	58.33 (9.08)	59 (37–75)	55.83 (10.02)	58.5 (37–73)	U=393	0.399
DHI 3	40.37 (12.33)	43.5(13–59)	40.83 (12.62)	39 (13–70)	U=396.5	0.429
Statistic test	Z=−4.705		Z=−4.374			
***P*-value**	<0.001		<0.001			

U: Mann Whitney U Test, Z: Wilcoxon Test, SD: standard deviation, Min: minimum, Max: maximum, VAS: Visual analog scale, DHI: Duruöz hand index

Discussion

LE is a disease that can be mostly treated using conservative methods [2-4]. Despite the various methods employed for LE treatment, there is no clear consensus on their efficacy. To the best of our knowledge, no study has demonstrated the impact of neural therapy injection, known to provide analgesia in several musculoskeletal diseases, on treating LE. Additionally, no literature study has been found comparing the effectiveness of ESWT and neural therapy injection in treating this disease. With this in mind, our study aimed to determine the efficacy of neural therapy injections and compare them with ESWT. We also believed that this study would contribute to the literature as the first to compare the effectiveness of these two treatment methods. Upon retrospectively reviewing the data of patients with LE who underwent these two treatment methods, we concluded that neural therapy is equally effective as ESWT, particularly in terms of alleviating elbow pain and improving functionality.

Neural therapy is a treatment approach that effectively alleviates chronic pain by injecting local anesthetics into various tissues, including scars, peripheral nerves, autonomic ganglia, trigger points, and glands. This therapeutic method aims to restore balance to the autonomic nervous system, which is responsible for triggering or perpetuating several chronic diseases [8, 9]. Different administration forms, such as segmental, intramuscular, and intravenous, are available [9]. The most commonly employed technique involves an intracutaneous injection directly into the affected area (known as the quaddle method). Procaine and lidocaine are the most frequently used medications for these injections. It is widely recognized that the local anesthetics utilized in neural therapy possess anti-inflammatory and neuroprotective properties that benefit the nervous system [9].

In our study, we assessed the data of patients who received intracutaneous injections of a solution containing lidocaine hydrochloride at 6–8 points surrounding the symptomatic elbow. As a result, we observed an improvement in pain and functionality scores in these patients after three injection sessions conducted over three consecutive weeks. Nevertheless, no definitive consensus exists regarding the optimal number and frequency of neural therapy sessions for treating musculoskeletal pain. We speculate that the sustained improvement in pain scores over the long term may be attributed to increased treatment sessions. Further investigations are necessary to evaluate the long-term effectiveness of neural therapy.

A single study in the literature investigated the injection of lidocaine diluted with saline into the elbows of patients with

LE [10]. This study involved 28 participants who were divided into three groups. The first group received a mixture of saline and lidocaine, the second group received corticosteroid and lidocaine, and the third group received autologous blood and lidocaine. The study reported minimal pain score reduction in each group following treatment, with no significant differences observed in shoulder-hand disability scores. It is important to note that this study involved a single-session injection.

In contrast, our study demonstrated positive outcomes regarding elbow pain and functionality following neural therapy injections administered once a week for three consecutive weeks. Based on these findings, we believe that the effectiveness of neural therapy increases with consecutive and repetitive treatment sessions, as the therapy enhances muscle blood supply through vasodilation resulting from segmental stimulation. Furthermore, our study utilized intracutaneous administration, while other injections were delivered into the tissue or joint. Consequently, we aimed to investigate the regulatory effect of bioelectrical activity on the cell wall rather than focusing solely on the anesthetic properties of the substances used.

While there is a lack of studies focusing on neural therapy for LE treatment, several studies have evaluated other types of injections [11-15]. These injection treatments are also recommended for patients who do not respond to alternative methods. A meta-analysis of 70 studies involving 1,381 patients compared eight injection methods used in LE treatment with a placebo [12]. The pooled results indicated autologous blood and platelet-rich plasma demonstrated statistically significant superiority over placebo. Botulinum toxin showed limited benefits for alleviating elbow pain but was associated with finger extension paresis [13]. Both hyaluronic acid and prolotherapy were more effective than placebo; however, no significant difference was found in the response to polidocanol and glycosaminoglycan. Some studies have reported significant improvements in pain scores in LE patients who received saline injections alone [16,17]. They suggested that these improvements could be attributed to a placebo effect or the modulation of osmolarity and sodium ions.

ESWT application is another therapeutic option widely utilized for musculoskeletal problems over the past 25–30 years [18]. This noninvasive therapy employs focused acoustic waves to target specific body parts for pain relief and to facilitate healing processes [19]. ESWT promotes neovascularization, reduces calcification, and directly stimulates tissue healing through hyperstimulation of the treated tissues [5,6]. However, the effectiveness of ESWT in treating LE remains controversial in the literature. For instance, a systematic review comparing the treatment of LE reported no significant advantage of ESWT over placebo, with only two pooled results favoring ESWT [6]. In another study involving 50 patients with LE, ESWT was as effective as therapeutic ultrasound in reducing elbow pain and improving functionality [20]. Furthermore, in a review encompassing 13 articles on LE treatment methods, 501 out of 1,035 patients underwent ESWT, while the remaining 534 underwent other treatment modalities [21]. The findings of this review suggested that ESWT is more effective and safer than other treatment methods, particularly in addressing pain, hand functions, and grip strength loss.

The conflicting results in previous studies have been attributed to variations in the dosage and devices used for ESWT, as standardized procedures for ESWT in musculoskeletal conditions are still lacking, and extensive research is needed to determine the optimal dosages and frequency of administration. In our study, we administered ESWT once a week for three consecutive weeks using the most commonly employed method in the literature, with a frequency of 6 Hz, intensity of 1.6 bar, and 2000 beats per session. Notably, our study demonstrated a statistically significant improvement in elbow pain and daily living activity scores among patients who received ESWT, which is consistent with findings reported in the literature.

These studies have reported minimal side effects associated with ESWT [6,18-20]. The most frequently reported side effects include temporary pain, skin redness, nausea, and swelling.

Furthermore, it was noted that these side effects typically had a short duration and resolved after the completion of treatment. In our study, no side effects were observed that impeded the course of treatment or necessitated dosage adjustments. Our patients successfully completed the three sessions without any issues within the dose and frequency parameters we utilized.

Limitations

While our study yielded important insights into the comparative effectiveness of neural therapy injections and ESWT in treating LE, it is essential to consider several limitations.

First, the study's retrospective nature inherently carries potential biases, including selection bias and information bias. Reliance on medical records introduces the possibility of inaccuracies or incomplete information.

Second, the sample size was relatively small, which may have limited our ability to detect smaller yet potentially significant differences between the two treatment methods. Further studies with larger sample sizes would be valuable in confirming our findings.

Third, our study lacked a control group. Without a control group receiving no or a placebo treatment, we cannot exclude the possibility that some observed improvements were due to natural recovery or placebo effects.

Fourth, our study solely assessed the short-term effects of the treatments. Longer-term follow-up is necessary to assess the durability of treatment effects and determine if one treatment yields superior long-term outcomes.

Lastly, our study did not consider potential side effects or complications associated with the treatments. Future research should encompass an evaluation of the safety profiles of the treatments in addition to their efficacy.

Despite these limitations, our study offers preliminary evidence suggesting that both neural therapy injections and ESWT can be effective treatments for LE. Further research is warranted to confirm and expand upon our findings.

Conclusion

Both neural therapy injections and ESWT effectively reduced pain and improved functionality among patients with LE. No significant differences were observed between the two treatment methods regarding effectiveness. Additionally,

treatment outcomes did not show significant variations based on age, BMI, gender, or the side of the elbow treated.

These findings indicate that both treatments offer viable options for managing LE symptoms, and patient preferences, cost, availability, and other individual factors can influence treatment selection. Further research is necessary to investigate these treatments' long-term outcomes and potential side effects. Additionally, identifying factors that may predict treatment response and help determine which patients would benefit more from one treatment over the other would be valuable.

References

1. Chumbley EM, O'Connor FG, Nirschl RP. Evaluation of overuse elbow injuries. Am Fam Phys. 2000;61:691-700.
2. Wilson JJ, Best TM. Common overuse tendon problems: a review and recommendations for treatment. Am Fam Phys. 2005;72:811-8.
3. Taylor SA, Hannafin JA. Evaluation and management of elbow tendinopathy. Sports Health. 2012;4:384-93.
4. Sims SEG, Miller K, Elfar JC, Hammert WC. Non-surgical treatment of lateral epicondylitis: a systematic review of randomized controlled trials. Hand N Y N. 2014;9:419-46.
5. Notarnicola A, Moretti B. The biological effects of extracorporeal shock wave therapy (eswt) on tendon tissue. Muscles Ligaments Tendons J. 2012;2:33-7.
6. Buchbinder R, Green SE, Youd JM, Assendelft WJJ, Barnsley L, Smidt N. Shock wave therapy for lateral elbow pain. Cochrane Database Syst Rev. 2005;2005:CD003524.
7. Duruöz MT, Poiraudeau S, Fermanian J, Menkes CJ, Amor B, Dougados M, Revel M. Development and validation of a rheumatoid hand functional disability scale that assesses functional handicap. J Rheumatol. 1996;23:1167-72.
8. Frank BL. Neural therapy. Phys Med Rehabil Clin N Am. 1999;10:573-82.
9. Hollmann MW, Durieux ME. Local anesthetics and the inflammatory response: a new therapeutic indication? Anesthesiology. 2000;93:858-75.
10. Wolf JM, Ozer K, Scott F, Gordon MJV, Williams AE. Comparison of autologous blood, corticosteroid, and saline injection in the treatment of lateral epicondylitis: a prospective, randomized, controlled multicenter study. J Hand Surg Am. 2011;36:1269-72.
11. Vukelic B, Abbey R, Knox J, Migdalski A. Which injections are effective for lateral epicondylitis? J Fam Pract. 2021;70:461-3.
12. Krogh TP, Bartels EM, Ellingsen T, Stengaard-Pedersen K, Buchbinder R, Fredberg U, et al. Comparative effectiveness of injection therapies in lateral epicondylitis: a systematic review and network meta-analysis of randomized controlled trials. Am J Sports Med. 2013;41:1435-46.
13. Rabago D, Best TM, Zgierska AE, Zeisig E, Ryan M, Crane D. A systematic review of four injection therapies for lateral epicondylosis: prolotherapy, polidocanol, whole blood and platelet-rich plasma. Br J Sports Med. 2009;43:471-81.
14. Simental-Mendía M, Vilchez-Cavazos F, Álvarez-Villalobos N, Blázquez-Saldaña J, Peña-Martínez V, Villarreal-Villarreal G, et al. Clinical efficacy of platelet-rich plasma in the treatment of lateral epicondylitis: a systematic review and meta-analysis of randomized placebo-controlled clinical trials. Clin Rheumatol. 2020;39:2255-65.
15. Shiple BJ. How effective are injection treatments for lateral epicondylitis? Clin J Sport Med. 2013;23:502-3.
16. Gao B, Dwivedi S, DeFroda S, Bokshan S, Ready LV, Cole BJ, et al. The therapeutic benefits of saline solution injection for lateral epicondylitis: a meta-analysis of randomized controlled trials comparing saline injections with nonsurgical injection therapies. Arthrosc - J Arthrosc Relat Surg. 2019;35:1847-59.
17. Acosta-Olivo CA, Millán-Alanís JM, Simental-Mendía LE, Álvarez-Villalobos N, Vilchez-Cavazos F, Peña-Martínez VM, et al. Effect of normal saline injections on lateral epicondylitis symptoms: a systematic review and meta-analysis of randomized clinical trials. Am J Sports Med. 2020;48:3094-102.
18. Yang TH, Huang YC, Lau YC, Wang LY. Efficacy of radial extracorporeal shock wave therapy on lateral epicondylosis, and changes in the common extensor tendon stiffness with pretherapy and posttherapy in real-time sonoelastography: a randomized controlled study. Am J Phys Med Rehabil. 2017;96:93-100.
19. Stasinopoulos D, Johnson MI. Effectiveness of extracorporeal shock wave therapy for tennis elbow (lateral epicondylitis). Br J Sports Med. 2005;39:132-6.
20. Yalvaç B, Mesci N, Geler Külcü D, Yurdakul OV. Comparison of ultrasound and extracorporeal shock wave therapy in lateral epicondylosis. Acta Orthop Traumatol Turc. 2018;52:357-62.
21. Yao G, Chen J, Duan Y, Chen X. Efficacy of extracorporeal shock wave therapy for lateral epicondylitis: a systematic review and meta-Analysis. BioMed Res Int. 2020;2020:2064781.

J Surg Med. 2023;7(5):339-342.
DOI: 10.28982/josam.7695

Research article

Journal of Surgery and Medicine
e-ISSN: 2602-2079
https://jsurgmed.com/

The effect of a breath-hold technique on conformal and intensity-modulated radiotherapy techniques at right-sided breast cancer radiotherapy including internal mammarian fields

Serap Yücel [1], Erhan Dişçi [2], Zeynep Güral [1], Sedenay Oskeroğlu [3], Hüseyin Kadıoğlu [4], Fulya Ağaoğlu [1]

[1] Department of Radiation Oncology, School of Medicine, Acıbadem University, Istanbul, Turkey
[2] Department of Radiation Oncology, Acıbadem Atakent Hospital, Istanbul, Turkey
[3] Department of Radiation Oncology, Acıbadem Atasehir Hospital, Istanbul, Turkey
[4] Department of General Surgery, Yeniyuzyil University, Istanbul, Turkey

ORCID ID of the author(s)

SY: 0000-0003-4948-8927
ED: 0000-0002-7857-5045
ZG: 0000-0003-3968-8255
SO: 0000-0001-7295-3722
HK: 0000-0003-1953-4400
FA: 0000-0002-4868-9543

Corresponding Author
Serap Yucel
Acibadem Atakent Hospital, Kucukcekmece, Istanbul, Turkey
E-mail: serapbaskaya@yahoo.com

Ethics Committee Approval
The study does not require any ethical permissions since it is a dosimetric study.

Conflict of Interest
No conflict of interest was declared by the authors.

Financial Disclosure
The authors declared that this study has received no financial support.

Published
2023 May 23

Abstract

Background/Aim: Significantly lower heart doses can be achieved by breath-hold technique at left-sided breast cancer radiotherapy (RT). We see high doses at organs at risk such as lung, heart, and contralateral breast during right-sided breast cancer RT planning especially in the presence of RT indication for mammaria interna (MI) lymph nodes. This study compared RT-planning methods that are conformal with intensity-modulated RT (IMRT) with breath holding and free breathing for right-sided breast cancer RT including full axillary and MI lymph node fields.

Methods: Computed tomography (CT) simulations were performed using free-breath (FB) and breath-hold (BH) methods in 10 patients with right-sided breast cancer. A total of 40 RT treatment plans were calculated. Right-sided breast, level 1-2-3 axillary regions, and MI regions served for the target-planning volume. Left-sided breast, heart, as well as right-sided and left lungs were contoured as critical organs according to the atlas of the "Radiation Therapy Oncology Group." We used a Varian Eclipse v.13 for treatment planning. Conformal “FieldinField” RT (FinFRT) and dynamic IMRT (dIMRT) planning were performed separately for each patient over breath-hold and free-breath images. For PTV, 50 Gy was prescribed in 25 fractions and optimized such that the planned target volume (PTV) remained between 95% and 110% of the dose. The mean and maximum doses of the heart, V5 and V20 of the lungs, as well as V95 doses for MI were recorded. Statistical analyses were performed with SPSS version 22, and a paired t-test was used for comparison.

Results: Four treatment plans (FB FinFRT, BH FinFRT, FB dIMRT, BH dIMRT) were made separately for 10 patients. For comparison, common FB FinFRT plans were accepted as the baseline plan. As expected, there were no significant differences in PTV coverage. The mean dose received by 95% of the MI volume was between 42.27 Gy and 42.4 Gy. For the maximum heart dose, the breath hold technique had no significant effect on plans. The lowest average maximum heart dose was seen in the BH FinFRT group. Mean heart doses are between 1.28 Gy – 4.85 Gy. There was no significance between BH FinFRT and FB FinFRT plan (P=0.504), and there was a significant difference for heart mean dose versus dIMRT plans (P=0.001). The mean V20 of the lungs ranged from 11.9 to 17.8. There was a significant decrease in V20 with BH or FB dIMRT plans (P=0.001). There was no difference between BH FinFRT (P=0.138). On the contrary, lung V5 values were significantly higher in dIMRT plans, and the lowest mean V5 value was seen in BH FinFRT plan.

Conclusion: With the BH method, lower doses (but not significantly lower doses) were obtained in critical organ doses. There was a significant decrease with FinFRT plans in terms of heart mean and maximum dose and lung V5 percentages. The dIMRT plans were significant only in lung V20 percentages. When planning RT, we recommend evaluating all treatment techniques individually for right-sided breast cancer patients to obtain lower doses in critical organs.

Keywords: breath-hold, radiotherapy, internal mammarian field, breast cancer

How to cite: Yücel S, Dişçi E, Güral Z, Oskeroğlu S, Kadıoğlu H, Ağaoğlu F. The effect of breath-hold technique on conformal and intensity modulated radiotherapy techniques at right-sided breast cancer radiotherapy including internal mammarian field. J Surg Med. 2023;7(5):339-342.

Introduction

Adjuvant radiotherapy (RT) efficacy has been evaluated in studies with high patient numbers and meta-analyses. There is strong evidence for RT indications. The Breast Cancer Trials Collaborative Group (EBCTCG) published reports of 10- and 20-year locoregional recurrence and breast cancer-related mortality rates. These showed a significant decrease in the recurrence and breast cancer-related mortality rates in patients who received breast-conserving treatment with RT [1]. RT is currently applied after surgery as a standard in breast-conserving treatments. Likewise, significant advantages were also observed with RT in patients with mastectomy and pathological node-positive patients. Nodal RT was mostly applied to the patients that had mastectomy and were node-positive. Recurrence and breast-related death rates were significantly lower with RT regardless of the number of lymph nodes involved or whether they received systemic treatment [2].

There have been many improvements in RT over time due to technological developments. Conventional RT can be used to understand classical conformal RT techniques. However, conformal planning is increasingly common due to rapid progress in planning systems that allow the use of virtual wedges and field-in field (FinF) calculations. Modern RT techniques can produce more homogeneous and conformal dose distributions in PTV using both dIMRT and breath-hold (BH) techniques. Better protection of critical organs can be achieved [3, 4]. However, modern RT techniques is thought to be associated with the risk of second cancer due to the low dose distribution at body and an increase in monitor unit (MU) values. Modern RT techniques are often preferred for patients who have significant benefit in dose distribution rather than being used for each patient [5].

Here, the impact of the BH technique on conformal RT and dIMRT techniques was examined in large-area breast cancer planning. The treatment planning of the patients was studied, and PTV coverage and critical organ doses were recorded.

Materials and methods

Ten patients were randomly selected among the patients who would receive radiotherapy treatment with the diagnosis of right-sided breast cancer. The exclusion criteria were having funnel chests, pathologically enlarged hearts, and any other anatomical variation. Computed tomography (CT) simulation images (SOMATOM Force, Siemens Healthiners) were obtained using free-breath (FB) and BH methods. A special breast board (Civco Medical Instruments Co. Inc. Coralville, Iowa, USA) on which patients placed their right arm overhead was used for immobilization.

A Varian real-time position management (RPM) system was used for the BH method. An RPM localizer box was placed on the skin between the chest and abdomen of the patients. Thus, we could follow the respiratory cycle of the patient on the monitor of the treatment device by following the box with cameras during treatment. During the BH treatments, the technicians directed the patient to take a deep breath for about 10-20 seconds and observe the respiratory movement of the patient from the monitor.

The atlas of the "Radiation Therapy Oncology Group" was used as a guide the contour of the patients. The PTV was determined to include the right-sided breast as well as level 1-2-3 axillary areas. The MI area was created as a separate contour in the PTV and defined as PTVmi. All PTV contours were cut 5 mm from the skin surface. The left breast, heart, as well as right and left lungs were contoured separately within the organ volumes at risk (OAR).

The eclipse planning program (version 13.6, Varian Medical Systems, Palo Alto, CA, USA) was used for treatment planning. Treatment plans were created for the Varian TrueBeam linear accelerator device. Conformal FieldinField RT (FinF RT) and dIMRT were planned separately for FB and BH contours for each patient. There were 40 plans (FB FinFRT, BH FinFRT, FB dIMRT, BH dIMRT) for 10 patients in total. Of these plans, those with a FB FinF RT technique (used broadly at clinics) was accepted as the basal plan. For PTV, 50 Gy was prescribed in 25 fractions and optimized such that the PTV remained between 95% and 110% of the dose.

Statistical analysis

Descriptive statistics used the mean (SD) and maximum doses of the heart. These were defined as OAR, V5, and V20 of the lungs; V95 doses for MI were used to present continuous data with normal distribution. Median values with minimum-maximum values were applied for continuous variables without a normal distribution. Numbers and percentages were used for categorical variables. Data analysis used Chi-Square, Kruskal-Wallis, and Mann-Whitney U tests with SPSS program version 16.0 (SPSS Inc.). A paired-t test was used for comparisons.

Results

No significant differences were seen in PTV dose coverage when all treatment plans were compared with the baseline plan (P=0.442). The average dose received by 95% of the MI volume was 42.27 Gy. It was 42.15 Gy in FinFRT plans and 42.4 Gy in dIMRT plans.

Analyses for OAR are detailed in Tables 1 and 2. Versus the maximum dose of the heart, there was no significant difference in the maximum dose of the heart in BH plans. The lowest mean dose was seen in the BH-FinFRT group. The mean heart dose averages were recorded between 1.28 Gy and 4.85 Gy across all plans. There was no significant difference between BH FinFRT and FB FinFRT plan (P=0.504). Significantly higher doses were observed for a heart mean dose versus dIMRT plans (P=0.001).

The mean V20 of the lungs ranged from 11.9 to 17.8. There was a significant decrease in V20 with BH or FB dIMRT plans (P=0.001). There was no difference between BH FinFRT (P=0.138). On the contrary, V5 of the lungs were observed significantly higher in dIMRT plans. The lowest mean V5 value was seen in the BH FinFRT plan (Table 3).

Table 1: Results of statistical analyses of OAR with RT techniques

	Free-Breath FinF RT	Breath-hold FinF RT		Free-Breath IMRT		Breath-hold IMRT	
	Mean	Mean	*P*-value	Mean	*P*-value	Mean	*P*-value
Mean heart dose (Gy)	1.37	1.28	0.504	4.85	0.001	4.17	0.001
Max heart dose (Gy)	19.42	14.67	0.287	21.25	0.716	24.40	0.320
Lungs V20 (%)	17.88	15.74	0.138	14.29	0.04	11.9	0.001
Lungs V5 (%)	29.66	27.45	0.06	43.67	0.001	42.43	0.001

Table 2: Values of OAR with RT techniques

Plans	FB FinF TFRT			BH FinF TFRT			FB dIMRT			BH dIMRT		
	Mean	Min	Max	Mean	Min	Max	Mean	Min	Max	Mean	Min	Max
Heart Mean (Gy)	1.37	0.78	2.68	1.28	0.94	1.68	4.85	2.43	8.56	4.17	3.15	5.18
Heart Maks (Gy)	19.4	4.7	46.7	14.6	7	31.7	21.2	15.7	40.1	24.4	8.35	28.75
Lung V20 (%)	17.8	11.38	27	15.7	8.8	31	14.29	12.3	18	11.9	9,7	15.5
Lung V5 (%)	29.6	21.3	37	27.45	18.8	41	43.67	34.6	53	42.43	37	46.8

Table 3: The significance between RT techniques

Organs	Treatment Plans											
	SN FinF TFRT			NT FinF TFRT			SN dIMRT			NT dIMRT		
	P-value			*P*-value			*P*-value			*P*-value		
	BH FinF RT	FB dIMRT	BH dIMRT	FB FinF RT	FB dIMRT	BH dIMRT	FB FinF RT	BH FinF RT	BH dIMRT	FB FinF RT	BH FinF RT	FB dIMRT
Heart Mean	0.504	0.001	0.001	0.504	0.001	0.001	0.001	0.001	0.229	0.001	0.001	0.229
Heart Max	0.287	0.716	0.320	0.287	0.026	0.05	0.716	0.26	0.267	0.320	0.05	0.267
Lung V20	0.138	0.04	0.001	0.138	0.512	0.032	0.04	0.512	0.032	0.001	0.032	0.032
Lung V5	0.68	0.001	0.001	0.068	0.001	0.001	0.001	0.001	0.560	0.001	0.001	0.560

Discussion

Late adverse effects have a significant impact quality of life and survival among breast cancer patients due to prolonged survival. Reports have demonstrated cardiac anomalies from myocardial perfusion data years after RT in left-sided breast cancer patients [6]. Nevertheless, early cardiac imaging of patients who received RT with BH technique showed no anomaly regarding perfusion or wall motion [7]. Another study showed a decrease of 3.6% in heart volume receiving 30 Gy in patients whose RT plan were executed with BH technique instead of FB for left-sided breast cancer [8]. A retrospective study reported that RT planning with BH technique for left-sided breast cancer resulted in a mean heart dose of 2.7 Gy instead of 5.2 Gy with the FB technique [9]. Here, RT planning of left-sided breast cancer patients use the BH technique as long as the RT devices are eligible to do so. On the other hand, the BH technique is not an essential requirement in right-sided breast cancer patients given that heart doses are expected to be significantly lower. Here, we analyzed the effect of the BH technique on heart dose in right-sided breast cancer patients who had a high-volume PTV and whose MI fields were irradiated with a dIMRT technique.

OAR doses were not significantly lower with the BH technique, but we found that the planning technique was equally important. The dIMRT technique is associated with a higher mean heart dose as well as increased volume of lung receiving a low dose. The FinFRT technique resulted in a higher mean heart dose than in patients whose irradiation volume comprised only right breast, but this technique for PTVs with all the fields included was significantly lower than in dIMRT techniques.

Current analyses show no significant difference between heart doses between the BH and FB techniques. The evidence that contradicts left-breast planning might result from inadequate exclusion of the heart from the target volume due to high PTV volumes despite using the BH technique. The mean and maximum heart dose as well as lung V5 were significantly lower in the FinFRT technique; only lung V20 was significantly lower with the dIMRT technique.

Several results have been reported in the literature regarding lung doses. Some studies show a significant decrease in lung doses with the BH technique, but there are also studies finding no significant difference [10-12]. dIMRT planning is more convenient in terms of dose homogeneity. These increase low-dose areas in lung and heart with a decrease in high-dose regions [13-16].

Limitations

The retrospective design and small sample size limit this study. The low number of subjects in the treatment plan might impact the significance of some results.

Conclusion

In conclusion, we report a dosimetric study that compares non-standard treatment methods in right-sided breast cancer. Our results might be improved by higher patient numbers in future work. The choice of RT techniques must be tailored with respect to patient-specific dose preferences regarding critical organ doses.

References

1. EBCTCG (Early Breast Cancer Trialists' Collaborative Group), McGale P, Taylor C, Correa C, Cutter D, Duane F, Ewertz M, et al. Effect of radiotherapy after mastectomy and axillary surgery on 10-year recurrence and 20-year breast cancer mortality: meta-analysis of individual patient data for 8135 women in 22 randomised trials. Lancet. 2014;383:2127-359.
2. Early Breast Cancer Trialists' Collaborative Group (EBCTCG), Darby S, McGale P, Correa C, Taylor C, Arriagada R, Clarke M, et al. Effect of radiotherapy after breast-conserving surgery on 10-year recurrence and 15-year breast cancer death: meta-analysis of individual patient data for 10,801 women in 17 randomised trials. Lancet. 2011;378:1707-16.
3. Dogan N, Cuttino L, Lloyd R, Bump EA, Arthur DW. Optimized dose coverage of regional lymph nodes in breast cancer: the role of intensity modulated radiotherapy. Int J Radiat Oncol Biol Phys. 2007;68(4):1238-50.
4. Kestin LL, Sharpe MB, Frazier RC, Vicini FA, Yan D, Matter RC, Martinez AA, Wong JW. Intensity modulation to improve dose uniformity with tangential breast radiotherapy: initial clinical experience. Int J Radiat Oncol Biol Phys. 2000;48(5):1559-68.
5. Hall EJ. Intensity-modulated radiation therapy, protons, and the risk of second cancers. Int J Radiat Oncol Biol Phys. 2006;65:1–7.
6. Sioka C, Exarchopoulos T, Tasiou I, et al. Myocardial perfusion imaging with 99 mTc -tetrofosmin SPECT in breast cancer patients that received postoperative radiotherapy: a case control study. Radiat Oncol. 2011;6:151.
7. Zagar TM, Kaidar-Person O, Tang X, Jones EE, Matney J, Das SK, et al. Utility of deep inspiration breath hold for left sided breast radiation therapy in preventing early cardiac perfusion defects: a prospective study. Int J Radiat Oncol Biol Phys. 2017;97(5):903-9.
8. Remouchamps VM, Letts N, Vicini FA, Sharpe MB, Kestin LL, Chen PY, et al. Initial clinical experience with moderate deep inspiration breath hold using an active breathing control device in the treatment of patients with left-sided breast cancer using external beam radiation therapy. Int J Radiat Oncol Biol Phys. 2003;56(3):704-15.
9. Nissen HD, Appelt AL. Improved heart, lung and target dose with deep inspiration breath hold in a large clinical series of breast cancer patients. Radiother Oncol. 2013;106(1):28-32.
10. Korreman SS, Pedersen AN, Nottrup TJ, Specht L, Nystrom H. Breathing adapted radiotherapy for breast cancer: comparison of free breathing gating with the breath-hold technique. Radiother Oncol. 2005;76:311-8.
11. Borst GR, Sonke JJ, den Hollander S, Betgen A, Remeijer P, van Giersbergen A, et al. Clinical results of image-guided deep inspiration breath hold breast irradiation. Int J Radiat Oncol Biol Phys. 2010;78:1345-51.

12. Hayden AJ, Rains M, Tiver K. Deep inspiration breath hold technique reduces heart dose from radiotherapy for left-sided breast cancer. J Med Imaging Radiat Oncol. 2012;56:464-72.
13. Pignol JP, Olivotto I, Rakovitch E, Gardner S, Sixel K, Beckham W, et al. A multicenter randomized trial of breast intensity modulated radiation therapy to reduce acute radiation dermatitis. J Clin Oncol. 2008;26: 2085–92.
14. Donovan E, Bleakley N, Denholm E, Evans P, Gothard L, Hanson J, et al; Breast Technology Group. Randomised trial of standard 2D radiotherapy (RT) versus intensity modulated radiotherapy (IMRT) in patients prescribed breast radiotherapy. Radiother Oncol. 2007;82:254–64.
15. Vicini FA, Sharpe M, Kestin L, Martinez A, Mitchell CK, Wallace MF, Matter R, Wong J. Optimizing breast cancer treatment efficacy with intensity-modulated radiotherapy. Int J Radiat Oncol Biol Phys. 2002;54:1336–44.
16. Keller LM, Sopka DM, Li T, Klayton T, Li J, Anderson PR, Bleicher RJ, Sigurdson ER, Freedman GM. Five-year results of whole breast intensity modulated radiation therapy for the treatment of early stage breast cancer: the Fox Chase Cancer Center experience. Int J Radiat Oncol Biol Phys. 2012;84:881–7.

J Surg Med. 2023;7(5):343-346.
DOI: 10.28982/josam.7794

Research article

Journal of Surgery and Medicine
e-ISSN: 2602-2079
https://jsurgmed.com/

The relationship between the PRE-DELIRIC score and the prognosis in COVID-19 ICU patients

Bilge Banu Taşdemir Mecit

Department of Anesthesiology and Reanimation, Afyonkarahisar University of Health Sciences, Faculty of Medicine, Afyonkarahisar, Turkey

ORCID ID of the author(s)

BBTM: 0000-0002-7994-7816

Corresponding Author
Bilge Banu Taşdemir Mecit
Department of Anesthesiology and Reanimation, Afyonkarahisar University of Health Sciences, Faculty of Medicine, Afyonkarahisar, Turkey
E-mail: bilgebanutasdemir@hotmail.com

Ethics Committee Approval
The study was approved by Afyonkarahisar University Medical Faculty Clinical Research Ethics Committee (Decree no: 510, date: 2021). All procedures in this study involving human participants were performed in accordance with the 1964 Helsinki Declaration and its later amendments.

Conflict of Interest
No conflict of interest was declared by the authors.

Financial Disclosure
The authors declared that this study has received no financial support.

Published
2023 May 27

Abstract

Background/Aim: The PRE-DELIRIC score is a test to detect delirium in the intensive care unit (ICU). Delirium has been studied as a factor associated with the clinical course of patients in COVID-19 intensive care. Our study aimed to investigate the relationship between the PRE-DELIRIC score and prognosis in patients followed in the COVID-19 ICU.

Methods: Patients hospitalized in the COVID-19 ICU between March 2020 and May 2021 were retrospectively analyzed, and 461 patients were included in the study. The PRE-DELIRIC scores of the patients were calculated using data obtained from the hospital information system. Patients with a PRE-DELIRIC score ≥50 were considered Group 1, and those with a score <50 were considered Group 2. The groups were compared in terms of gender, Glasgow Coma Scale (GCS), Acute Physiology and Chronic Health Evaluation (APACHE II) score, Sequential Organ Failure Evaluation Score (SOFA), length of hospital stay, and mortality rates.

Results: Of the 461 patients included in the study, 153 were female, and 308 were male. A high PRE-DELIRIC score was determined in 157 (34.1%) patients (Group 1), while 304 patients (65.9%) had lower scores (Group 2). The hospitalization duration was 9.6 (6.7) days, and the mortality rate was 87.2% in Group 1, compared to 8.2 (6.03) days and 38.1% in Group 2, respectively. A significant difference was observed in the length of hospital stay and mortality between the groups (P<0.001). The rate of patients who were intubated and followed up on an invasive mechanical ventilator (MV) was 81.5% in Group 1, whereas it was 16.4% in Group 2 (P<0.001).

Conclusion: Our study found that patients with a high PRE-DELIRIC score indicating delirium had higher mortality rates and longer hospital and MV stays. Delirium is one of the factors affecting mortality in COVID-19 disease. We believe that the PRE-DELIRIC score, as one of these factors, can serve as an important prognostic test in COVID-19 ICU patients.

Keywords: delirium, critical care, COVID-19, mortality, PRE-DELIRIC score

Introduction

Delirium is defined as the impairment of attention, awareness, and consciousness that develops within hours or days due to a critical illness [1]. Despite affecting over 20% of hospitalized patients, delirium is frequently overlooked [2,3].

Critically ill patients receiving treatment in the intensive care unit (ICU) are exposed to an unfavorable environment characterized by uncontrolled lighting and noise. Additionally, pain can cause agitation, sleep disruption, and delirium in these patients. Delirium is linked to detrimental clinical outcomes, including prolonged ICU stays, increased mechanical ventilation duration, and higher mortality rates [4,5]. Consequently, early identification and management of delirium are crucial. Patients who are promptly diagnosed with delirium and receive prompt treatment exhibit similar prognoses to those who do not develop delirium [6].

A study conducted in an ICU demonstrated that individuals who experienced delirium during hospitalization had an elevated risk of developing cognitive impairment or psychiatric issues after discharge [7]. This condition, known as post-intensive care syndrome, adversely affects patients' quality of life [8]. To mitigate this situation, early mobilization, minimizing sedation, and providing emotional and psychiatric support are crucial [9].

SARS-CoV-2 infection can potentially invade the central nervous system, leading to delirium and neurological symptoms, thereby increasing the risk of delirium in patients. Factors such as sedation, immobilization, social isolation, mechanical ventilation, and organ failure significantly worsen the prognosis [10]. Furthermore, patients who experience delirium in the ICU may continue to experience neuropsychological disorders even after discharge [11].

The PRE-DELIRIC score, introduced in 2012, serves as a predictive test for delirium in ICU patients [12]. Our study aimed to examine the prognostic impact of the PRE-DELIRIC score, specifically in COVID-19 ICU patients, where it is utilized as a delirium prediction tool.

Materials and methods

This study was retrospectively conducted in the COVID-19 ICU between March 2020 and May 2021. Approval for the study was obtained from the Clinical Research Ethics Committee of the Afyon Health Sciences University Medical Faculty, in accordance with the Ministry of Health (Decree no: 510, date: 2021). Patients under the age of 18, pregnant or lactating individuals, those diagnosed with brain death, individuals with a history of dementia or chronic alcoholism, and those already diagnosed with delirium before ICU admission were excluded from the study. Figure 1 shows the flow chart that includes patients in the study. The following data were recorded for all patients: age, gender, duration of hospitalization, Glasgow Coma Scale (GCS) score, Sequential Organ Failure Evaluation (SOFA) score, and Acute Physiology and Chronic Health Evaluation (APACHE II) score on the first day of ICU admission, pre-delirium score, and prognosis.

Figure 1: Flow chart shows the patient selection process

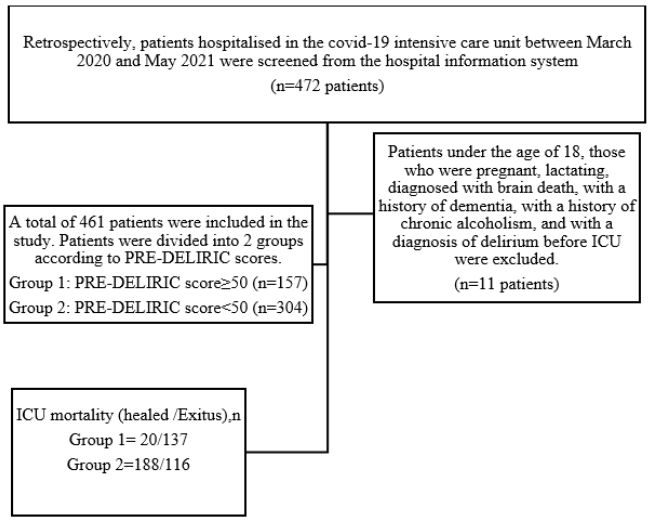

The study enrolled patients with severe pneumonia associated with COVID-19, confirmed by a positive RT-PCR test for SARS-CoV-2. Additionally, patients with a negative RT-PCR test who were classified as suspected COVID-19 cases according to the diagnosis, treatment, and follow-up guidelines of the Ministry of Health of the Republic of Turkey were also included.

The PRE-DELIRIC scoring system evaluates various factors, including age, APACHE II score, blood urea level, morphine usage, sedation, metabolic acidosis, coma status, infection, planned/emergency ICU admission, and reason for hospitalization. A score is obtained based on these criteria, as shown in Table 1. The PRE-DELIRIC score has been validated, and it has been reported that a score of ≥50 is associated with a high incidence of delirium [12]. For this study, we adopted the same cut-off value. Patients with a PRE-DELIRIC score of ≥50 were classified as the high delirium risk group (Group 1), while those with a score of <50 were classified as the low delirium risk group (Group 2). The study compared gender, GCS score, Sequential Organ Failure Assessment (SOFA) score, duration of hospital stay, and mortality rates between the two groups.

Table 1: PRE-DELIRIC scoring system [12]

Parameters
+ 0.04 x age
+ 0.06 x APACHE II score
+ 0 no coma or 0.55 drug-associated coma or 2.70 different comas or 2.84 coma combinations
+ 0 for surgical patients or 0.31 for medical patients 1.13 for trauma patients or 1.38 for neurology/neurosurgery patients
+ 1.05 for infection
+ 0.29 for metabolic acidosis
+ 0 no morphine use or 0.41 0.01-7.1 mg/24 h for morphine or 0.13 7.2-18.6 mg/24 h for morphine or 0.51>8.6 mg/24 h for morphine use
+ 1.39 for use of sedatives
+ 0.03 x urea concentration (mmol/L)
+ 0.40 for urgent admission

APACHE II: Acute Physiology and Chronic Health Assessment

Statistical analysis

Statistical analysis was performed using IBM SPSS Statistics version 20. The data were presented as percentages, median with interquartile range (IQR), and mean, standard deviation (SD) values. The normal distribution of variables was assessed through visual examination (histogram) and analytical methods (Kolmogorov-Smirnov test). Continuous variables were compared using either Student's t-test or the Mann-Whitney U test, while categorical variables were compared using the chi-

square test. Statistical significance was defined as *P*-values less than 0.05.

Results

Four-hundred-sixty-one patients who were followed up in the COVID-19 ICU between March 2020 and May 2021 were included in the study. Among them, 157 patients (31.2%) were in Group 1, while 304 patients (60.8%) were in Group 2. There was no statistically significant difference between the groups regarding gender (*P*=0.817). The median age of Group 1 was significantly higher than that of Group 2 (*P*=0.011). The hospitalization duration was 9.6 (6.7) days in Group 1 and 8.2 (6.03) days in Group 2. The duration of hospital stay in the ICU was significantly higher in Group 1 than in Group 2 (*P*<0.001). When examining intensive care mortality, the mortality rate was 87.2% in Group 1 and 38.1% in Group 2 (*P*<0.001). In Group 1, 81.5% of the patients were intubated and followed up on an invasive mechanical ventilator (MV), whereas, in Group 2, this rate was 16.4% (*P*<0.001) (Table 2).

Table 2: Demographic data, intensive care mortality and distribution of intensive care unit length of stay according to PRE-DELIRIC scores of the patients

	Group 1 (n=157)	Group 2 (n=304)	*P*-value
Gender (Female/Male), n	51/106	102/202	0.817*
Age (Year), median;IQR	70;14	67;15	0.011#
ICU mortality (healed /Exitus),n	20/137	188/116	<0.001*
ICU length of stay (days), median;IQR	9;9	7;7	<0.001#
İnvasive MV,yes/no, n	128/29	50/204	<0.001*

Group 1: PRE-DELIRIC score ≥50, Group 2: PRE-DELIRIC score <50, ICU: Intensive care, MV: mechanical ventilation, * Chi-Square, #Mann-Whitney U, Values are given as number, median; IQR (interquartile range)

The distribution of comorbidities was analyzed in relation to the groups, and it was observed that the incidence of hypertension (HT) in Group 1 was higher than in Group 2 (*P*=0.004) (Table 3).

Table 3: Distribution of additional diseases of patients according to groups

	Group 1 (n=157)	Group 2 (n=304)	*P*-value*
Hypertension, yes/no, n	88/69	128/176	0.004
DM, yes/no, n	59/98	89/215	0.070
CAD, yes/no, n	46/111	67/237	0.086
Lung disease, yes/no, n	30/127	69/235	0.374
CRF, yes/no, n	10/147	28/276	0.293
Liver disease, yes/no, n	5/152	5/299	0.282
Malignancy, yes/no, n	16/141	41/263	0.308

Group 1: PRE-DELIRIC score ≥50, Group 2: PRE-DELIRIC score <50, DM: Diabetes Mellitus, CAD: Coronary Artery Disease, CRF: Chronic renal failure, *Chi-Square

The SOFA and APACHE II scores were higher in Group 1 compared to Group 2 (*P*<0.001) (Table 4). The median GCS was 12 in Group 1 and 14 in Group 2, with a statistically significant difference between them (*P*<0.001) (Table 4). Analyzing all the patients who survived and died, it was observed that the PRE-DELIRIC score was lower in the patients who survived (*P*<0.001).

Table 4. Distribution of patients' GCS, SOFA and APACHE II scores according to groups

	Group 1 (n=157)	Group 2 (n=304)	*P*-value#
GKS	12;4	14;3	<0.001
SOFA	4;2	3;2	<0.001
APACHE II	22;7	20;6	<0.001

Group 1: PRE-DELIRIC score ≥50, Group 2: PRE-DELIRIC score <50, GCS: Glasgow Coma Scale, SOFA: Sequential Organ Failure Evaluation Score, APACHE II: Acute Physiology and Chronic Health Evaluation, # Mann-Whitney U, Values are given as number, median; IQR (Interquartile range).

Discussion

Our study found that the PRE-DELIRIC score of patients monitored in the ICU was significantly associated with mortality, duration of ICU stay, and the need for mechanical ventilation (MV).

The PRE-DELIRIC score was initially developed in 2012 by van der Boogaard et al. [12]. This scoring system incorporates various factors, including age, APACHE II score, blood urea level, morphine usage, sedation, metabolic acidosis, coma status, infection, planned/emergency ICU admission, and reason for hospitalization to calculate a score. The researchers found that this assessment tool is valuable for the early prediction of delirium, particularly when the PRE-DELIRIC score exceeds 50. In a subsequent study conducted by van der Boogaard et al. [13] in 2014, they further examined the PRE-DELIRIC score using a sample of 1,824 patients from ICUs in different countries. The findings indicated that the score remained effective despite variations between countries and patient groups.

Linkaitė et al. [14] conducted a study in the ICU. Their findings demonstrated that the PRE-DELIRIC score exhibited reliable predictive capability for the occurrence of delirium within 24 h of ICU admission.

Likewise, a comprehensive review of 33 studies revealed a strong association between delirium and several factors, including age, history of dementia, hypertension (HT), pre-intensive care trauma or emergency surgery, high APACHE II score, mechanical ventilation, metabolic acidosis, and coma [15]. Importantly, these very parameters are incorporated into the PRE-DELIRIC scoring system.

A study conducted in South Korea explored the risk factors associated with the occurrence of delirium. The analysis revealed several significant correlations, including age, mechanical ventilation, APACHE II score, presence of comorbidities, patient restraint applications, and the education level of the patients [16]. These factors were found to be closely linked to the likelihood of developing delirium.

Delirium affects approximately one-third of patients admitted to the ICU. According to a recent meta-analysis, the prevalence of delirium among ICU patients was found to be 31% [17]. Studies have shown that delirium occurs in 60% to 80% of mechanically ventilated patients and in 20% to 50% of non-ventilated patients [18]. In the context of COVID-19, the incidence of delirium in ICU patients ranges from 65% to 80% [19]. It is worth noting that the risk of delirium may be amplified by the restrictions imposed due to COVID-19. The reduced number of nurses in the ICU and the increased workload can limit access to patient rooms, resulting in decreased screening for delirium. Additionally, the greater need for sedation and the occasional use of muscle relaxants due to the frequent application of the prone position may contribute to the occurrence of delirium.

A point prevalence survey conducted in COVID-19 ICUs revealed a low level of implementation of the ABCDEF bundle, which includes regular delirium assessment, in COVID-19 patients [20]. The ABCDEF package is an integral part of multidisciplinary care in the ICU and comprises the assessment of pain (A), spontaneous breathing trials (B), choice of sedation (C), delirium assessment (D), early mobilization (E), and family participation (F). However, several factors hindered the utilization of bundles, including changes in the ICU team

structure due to COVID-19, insufficient availability of personal protective equipment, physical constraints, heightened sedation requirements, and limited respirator supplies [21].

A meta-analysis revealed that delirium in elderly patients is associated with poor outcomes, irrespective of major confounding factors such as age, gender, comorbidities, disease severity, and baseline dementia [22]. Furthermore, Peterson et al. [23] found a significant increase in the incidence of delirium among intensive care patients aged 65 and above. In our study, patients in group 1, who had higher PRE-DELIRIC scores, also exhibited a higher average age. However, it is important to note that our study had limitations, as we did not specifically investigate the relationship between PRE-DELIRIC scores and mortality in patients over 65 years of age.

While our study did not find a relationship between PRE-DELIRIC scores and gender, a study by Ragheb reported that 70% of patients with delirium were women [19]. It is worth noting that in certain studies, being male has been identified as a risk factor for delirium [24, 25].

Delirium is a frequent occurrence in mechanically ventilated adults and has been linked to extended durations of mechanical ventilation and hospital stays [26]. In our study, we observed that the number of patients who required invasive mechanical ventilation (MV) and the duration of their stay in the ICU were higher in Group 1, consisting of individuals with a PRE-DELIRIC score of ≥50.

In a study examining psychiatry consultations in a hospital during the COVID-19 pandemic, it was determined that 50.68% of intensive care patients were diagnosed with delirium. Additionally, delirium was identified as a strong predictor of mortality in the same study [27]. Similarly, in the study conducted by İnal et al. [28] in the ICU, patients with high PRE-DELIRIC scores exhibited higher mortality rates. Consistent with these findings, we also observed a high mortality rate among our COVID-19 ICU patients with elevated PRE-DELIRIC scores.

Previous studies have shown an increased incidence of delirium in patients with comorbid conditions [25]. While our study did not establish a relationship with other comorbidities, we did find that patients with hypertension (HT) had significantly higher PRE-DELIRIC scores.

Limitation

Our study has several limitations. First, delirium screening was not conducted for the patients included in the study. Additionally, the PRE-DELIRIC score was calculated retrospectively, and its impact on prognosis was investigated. It is important to note that numerous factors can influence mortality in COVID-19 cases, and our study did not account for certain variables such as ferritin levels, CRP level, and Pao2/Fio2 ratio in the relationship between PRE-DELIRIC score and mortality. This omission represents another limitation of our study. Future prospective studies could be conducted to address these limitations, encompassing these additional factors, for a more comprehensive analysis.

Conclusion

Identifying parameters that can predict the clinical trajectory of COVID-19 patients is crucial for guiding appropriate treatment decisions and optimizing the utilization of limited resources. Early recognition and management of delirium play a pivotal role in the prognosis of ICU patients. We believe that the PRE-DELIRIC score holds the potential as a valuable prognostic tool for COVID-19 patients receiving intensive care.

References

1. American Psychiatric Association. Diagnostic and Statistical Manual of Mental Disorders. 5th ed. Washington, DC: APA Press; 2013.
2. Bellelli G, Morandi A, Di Santo SG, Mazzone A, Cherubini A, Mossello E, et al; Italian Study Group on Delirium (ISGoD). "Delirium Day": a nationwide point prevalence study of delirium in older hospitalized patients using an easy standardized diagnostic tool. BMC Med. 2016;14:106.
3. Inouye SK. Delirium in older persons. N Engl J Med. 2006;354:1157-65.
4. Seo Y, Lee HJ, Ha EJ, Ha TS. 2021 KSCCM clinical practice guidelines for pain, agitation, delirium, immobility, and sleep disturbance in the intensive care unit. Acute Crit Care. 2022;37(1):1-25.
5. Luz M, Brandão Barreto B, de Castro REV, Salluh J, Dal-Pizzol F, Araujo C, et al. Practices in sedation, analgesia, mobilization, delirium, and sleep deprivation in adult intensive care units (SAMDS-ICU):an international survey before and during the COVID-19 pandemic. Ann Intensive Care. 2022;4;12(1):9.
6. Dubois MJ, Bergeron N, Dumont M, Dial S, Skrobik Y. Delirium in an intensive care unit: a study of risk factors. Intensive Care Med. 2001;27:1297-304.
7. Ko RE, Kang D, Park H, Cho J, Suh GY, Chung CR. Association between the presence of delirium during intensive care unit admission and cognitive impairment or psychiatric problems: the Korean ICU National Data Study. J Intensive Care. 2022;10(1):7.
8. Hashem MD, Nallagangula A, Nalamalapu S, Nunna K, Nausran U, Robinson KA, et al. Patient outcomes after critical illness: a systematic review of qualitative studies following hospital discharge. Crit Care. 2016;20(1):345.
9. Karnatovskaia LV, Johnson MM, Benzo RP, Gajic O. The spectrum of psy chocognitive morbidity in the critically ill: a review of the literature and call for improvement. J Crit Care. 2015;30(1):130-7.
10. Helms J, Kremer S, Merdji H, Schenck M, Severac F, Clere-Jehl R, et al. Delirium and encephalopathy in severe COVID-19:a cohort analysis of ICU patients. Crit Care. 2020;24(1):491.
11. Ragheb J, McKinney A, Zierau M, Brooks J, Hill-Caruthers M, Iskander M, et al. Delirium and neuropsychological outcomes in critically Ill patients with COVID-19:a cohort study. BMJ Open. 2021;11(9):e050045.
12. van den Boogaard M, Pickkers P, Slooter AJ, Kuiper MA, Spronk PE, van der Voort PH, et al. Development and validation of PRE-DELIRIC (PREdiction of DELIRium in ICu patients) delirium prediction model for intensive care patients: observational multicentre study. BMJ. 2012;344:1-11.
13. van den Boogaard M, Schoonhoven L, Maseda E, Plowright C, Jones C, Luetz A, et al. Recalibration of the delirium prediction model for ICU patients (PRE-DELIRIC): a multinational observational study. Intensive Care Med. 2014;40:361-9.
14. Linkaitė G, Riauka M, Bunevičiūtė I, Vosylius S. Evaluation of PRE-DELIRIC (PREdiction of DELIRium in ICu patients) delirium prediction model for the patients in the intensive care unit. Acta Med Litu. 2018;25(1):14-22.
15. Zaal IJ, Devlin JW, Peelen LM, Slooter AJ. A systematic review of risk factors for delirium in the ICU. Crit Care Med. 2015;43(1):40-7.
16. Kim NY, Ryu SA, Kim YH. Factors Related to Delirium of Intensive Care Unit Patients in Korea: A Systematic Review. Iran J Public Health. 2021;50(8):1526-35.
17. Krewulak KD, Stelfox HT, Leigh JP, Ely EW, Fiest KM. Incidence and prevalence of delirium subtypes in an adult ICU: a systematic review and meta-analysis. Crit Care Med. 2018;46(12):2029-35.
18. Palakshappa JA, Hough CL. How We Prevent and Treat Delirium in the ICU. Chest. 2021;1 60(4):1326-34.
19. Ragheb J, McKinney A, Zierau M, Brooks J, Hill-Caruthers M, Iskander M, et al. Delirium and neuropsychological outcomes in critically Ill patients with COVID-19: a cohort study. BMJ Open. 2021;11(9):e050045.
20. Liu K, Nakamura K, Katsukawa H, Elhadi M, Nydahl P, Ely EW, et al. ABCDEF Bundle and Supportive ICU Practices for Patients With Coronavirus Disease 2019 Infection: An International Point Prevalence Study. Crit Care Explor. 2021;3(3):e0353.
21. Devlin JW, O'Neal HR Jr, Thomas C, Barnes Daly MA, Stollings JL, Janz DR, et al. Strategies to Optimize ICU Liberation (A to F) Bundle Performance in Critically Ill Adults With Coronavirus Disease 2019. Crit Care Explor. 2020;2(6):e0139.
22. Witlox J, Eurelings LS, de Jonghe JF, Kalisvaart KJ, Eikelenboom P, van Gool WA. Delirium in elderly patients and the risk of post discharge mortality, institutionalization, and dementia: a meta-analysis. JAMA. 2010;304(4):443-51.
23. Peterson JF, Pun BT, Dittus RS, Thomason JW, Jackson JC, Shintani AK, et al. Delirium and its motoric subtypes: a study of 614 critically ill patients. J Am Geriatr Soc. 2006;54:479-84.
24. Kyziridis TC. Post-operative delirium after hip fracture treatment: a review of the current literature. GMS Psycho-Social Medicine. 2006;3:1-12.
25. Nomark D. Predicting the onset of delirium in the postoperative patient. Age Ageing. 2009;38:368-73.
26. Mehta S, Cook D, Devlin JW, Skrobik Y, Meade M, Fergusson D, et al. SLEAP Investigators; Canadian Critical Care Trials Group. Prevalence, risk factors, and outcomes of delirium in mechanically ventilated adults. Crit Care Med. 2015;43(3):557-66.
27. Bulut NS, Yorguner N. Analysis of the psychiatric consultations requested for hospitalized COVID-19 patients: One year results from a major pandemic hospital. J Surg Med. 2022;6(3):322-30.
28. İnal MT, Memiş D, İnal V, Uyar AŞ, Tek ŞÇ, Çiftçi T, et al. Yoğun Bakım Hastalarında Pre-Deliryum Skorunun Değerlendirilmesi. J Turk Soc Intensive Care. 2018;16:26-9.

J Surg Med. 2023;7(5):347-354.
DOI: 10.28982/josam.7669

Review

Journal of Surgery and Medicine
e-ISSN: 2602-2079
https://jsurgmed.com/

Graded motor imagery in orthopedic and neurological rehabilitation: A systematic review of clinical studies

Busra Candiri [1], Burcu Talu [1], Gul Oznur Karabicak [2]

[1] Inonu University, Faculty of Health Sciences, Physiotherapy and Rehabilitation Department, Malatya, Turkey
[2] Adnan Menderes University, Faculty of Health Sciences, Department of Physiotherapy and Rehabilitation, Aydin, Turkey

ORCID ID of the author(s)
BC: 0000-0001-7413-6371
BT: 0000-0002-5623-8291
GOK: 0000-0003-3248-0638

Corresponding Author
Busra Candiri
Inonu University Faculty of Health Sciences, Physiotherapy and Rehabilitation Department, Campus 44280, Malatya, Turkey
E-mail: candiri_17@hotmail.com

Ethics Committee Approval
This article is not a study with human participants. There are no experiments on animals. This article does not contain any studies on human participants or animals performed by the author. There is no identifying information of participants.

Conflict of Interest
No conflict of interest was declared by the authors.

Financial Disclosure
The authors declared that this study has received no financial support.

Published
2023 May 1

Abstract

Background/Aim: Graded motor imagery is an increasingly popular motion representation technique. However, treatment protocols for graded motor imagery vary depending on various diseases. This study aims to summarize the cases in which graded motor imagery therapy is used, study protocols, and outcome measures in studies.

Methods: The literature search was done with Web of Science, Pubmed, Scopus, and PEDro databases. The last search was carried out on September 13, 2022. A series-specific bias risk assessment tool was used with randomized, non-randomized, and case reports. All clinical studies that performed graded motor imagery, available in full text, describing their methods and findings, were included. The gender of the participants was not significant. The intervention was graded motor imagery. Outcome measures were mainly pain severity, other pain-related measures (e.g., pressure pain threshold, pain catastrophe), range of motion, strength, reaction time, kinesiophobia, neurophysiological measures, depression, function, or quality of life measures.

Results: Complex regional pain syndrome, distal radius fracture, phantom limb pain, stroke, cancer, pathological pain (phantom pain after amputation, pain after brachial plexus avulsion), elbow stiffness, frozen shoulder, chronic shoulder pain, and osteoarthritis conditions were included. The intervention duration in the studies varies from 2 to 8 weeks. A common outcome measure could not be determined among studies. The pain was assessed in 15 studies, although different rating scales were used. Graded motor imagery resulted in a reduction in pain in 14 of the 15 studies.

Conclusions: Due to the heterogeneity of the studies, a general conclusion regarding the effect of the disease-specific intervention was not possible. Based on pain outcome, graded motor imagery effectively decreased pain severity in various painful conditions.

Keywords: graded motor imagery, pain, chronic pain, motor imagery, rehabilitation

How to cite: Candiri B, Talu B, Karabicak GO. Graded motor imagery in orthopedic and neurological rehabilitation: A systematic review of clinical studies. J Surg Med. 2023;7(5):347-354.

Introduction

Graded motor imagery (GMI) is a movement representation technique used to achieve cortical reorganization through neuroplasticity, gradually activating cortical level activation and reducing cortical disinhibition [1,2]. GMI, which is used for definitions of "brain exercises" and "training the brain", basically consists of three stages [3,4]. These stages are implicit motor imagery (lateralization), explicit motor imagery, and mirror therapy [1]. The first of these stages, lateralization, activates the premotor cortex without activating the primary motor areas. The second stage causes the activation of motor areas similar to the realization of normal movement. The mirror therapy phase also provides input for normal movement [5]. The sequential implementation of these three phases is important [6]. The first known research on GMI started in 2004 with complex regional pain syndrome [7]. Looking at the literature, it is seen that it is used in various neurological and orthopedic conditions. Distal radius fracture [2], complex regional pain syndrome (CRPS) [3,6-13], pathological pain [4], post-amputation phantom limb pain [14], chronic shoulder pain [15], cancer [16], knee osteoarthritis [17], frozen shoulder [18], stroke [19,20], and elbow stiffness [21] are the conditions in which graded motor imagery has been used in all its stages in the literature. While the usage area of GMI is expanding, another issue is the different application protocols in the literature. Again, in the first known study, all three stages of GMI were applied at every waking hour of the day [7]. When the following literature was examined, different application forms were seen. For example, Lagueux et al. [8] suggested applying it three times a day because of their study's low feasibility of each waking hour.

The advantages of GMI are that it is suitable for home use, requires minimal equipment, and is low risk [20]. While the application areas of GMI are increasing, only two systematic reviews about GMI have been found. A systematic review focused on the effect of GMI on chronic pain and examined studies using any of the three stages of GMI [22]. Another systematic review investigated GMI or mirror therapy's effectiveness in patients with CRPS type 1 [23]. Only randomized controlled trials were selected in these reviews. There were three studies in total in which the three stages of GMI were used sequentially. Although the mechanism of GMI has not been fully elucidated, it has been applied to facilitate sensory and motor cortex reorganization and gradually activate cortical networks without causing a protective pain reaction [2,15]. For these, it is necessary to apply the stages of GMI sequentially [22]. Examining the studies in which the three stages of GMI are applied sequentially will be useful for future research. It is also necessary to examine GMI in situations other than CRPS and chronic pain conditions. We believe that a detailed literature review would be beneficial due to heterogeneous studies in different fields. Therefore, this review aims to examine in detail the different situations, application protocols, and outcome measures in studies in which all stages of GMI are applied sequentially.

Materials and methods

This systematic review has been prepared according to the rules of Preferred Reporting Items for Systematic Reviews and Meta-analysis (PRISMA) [24].

1. Search strategy

The search was performed using Web of Science, Pubmed, Scopus, and PEDro databases. "Graded motor imagery" was used as a keyword, and no time or language filters were selected. The last search was carried out on September 13, 2022. Reference sections of included studies were also reviewed. Duplicates were removed using the Endnote 9 software program (Figure 1).

2. Eligibility criteria

In this review, accordance was made by considering the PICOS (population, intervention, control, outcomes, and study design) criteria [25].

2.1. Population

Studies, including the GMI program, were reviewed. Clinical trials using the three phases of the GMI program (implicit motor imagery, explicit motor imagery, and mirror therapy) sequentially, available in full text, and in which the article was particularly clear in terms of methods and findings, were included. The gender of the participants was not significant.

2.2. Intervention and control

The intervention was graded motor imagery. Only the three phases of the GMI (implicit motor imagery, explicit motor imagery, and mirror therapy) had to be applied sequentially. All studies with or without any comparison group were included.

2.3. Outcomes

Since the purpose of the review was to summarize the literature, no limitations were made. Outcome measures were mainly pain severity, other pain-related measures (e.g., pressure pain threshold, pain catastrophe), range of motion, strength, reaction time, kinesiophobia, neurophysiological measures, depression, function, or quality of life measures.

2.4. Study design

Randomized controlled trials, non-randomized studies, prospective studies, case reports, and case series were selected. The Jovell & Navarro-Rubio classification was used to assess the methodological quality of the included studies [26].

3. Selection criteria and data extraction

The first author reviewed the titles and abstracts of all studies to identify potentially relevant studies, and removed duplicated articles based on search results. The full texts of all potentially relevant studies were reviewed. Afterward, the articles were examined with other authors according to the inclusion and exclusion criteria, and the final articles were determined with a joint decision. The data described in the article's findings were extracted by a standardized data extraction form, which ensures that the most relevant information is obtained [27].

4. Risk of bias assessment

The risk of bias (ROB) for the non-randomized studies included was assessed using the Risk Of Bias In Non-randomized Studies of Interventions (ROBINS-I) tool [28]. Higgins et al.'s [29] risk of bias criteria (RoB 2) was used for the bias assessment of randomized controlled trials. Case reports and

case series were evaluated with a tool based on selection, ascertainment, causality, and reporting [30].

Results

The flow chart is shown in Figure 1. Eighteen studies were included in this review. The main characteristics of the included articles (author information, publication year, demographic information of the participants, pathological condition, number of study groups, and type of blinding) are given in Table 1.

Figure 1: Flow chart of participant selection according to PRISMA.

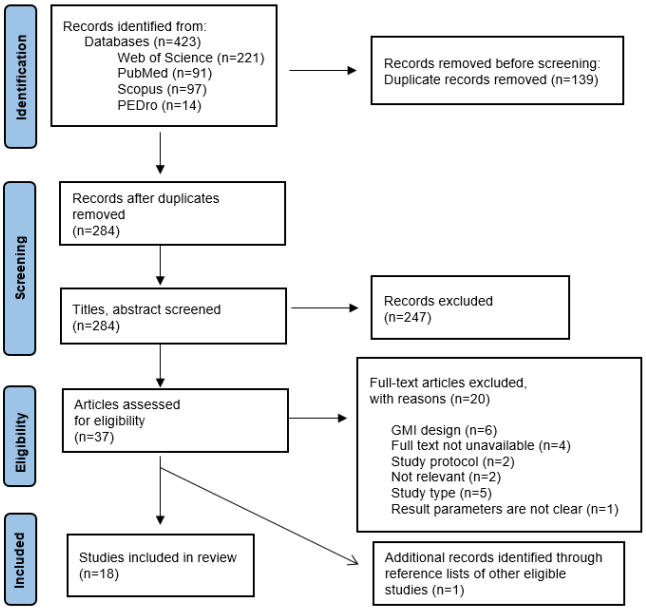

Study selection

As a result of the literature search made from databases, 423 articles were found. Of these, 139 copies were extracted, and 284 studies were reviewed. As a result, 37 articles were included in the review. Twenty studies were excluded because they did not meet the eligibility criteria. These studies included discrepancies or deficiencies in the order of the stages of GMI [18,31-35], lack of full-text access [36-39], protocol of the study [40,41], not fully implementing the GMI [42,43], study type (1 letter to the editor, 2 abstract conference papers, 2 reviews) [5,44-47] and were excluded due to unclear outcome parameters [13]. As a result, 17 eligible studies were reviewed, and after reviewing the reference sections of these studies, one more study [6] was added, and a total of 18 articles were included in this systematic review (Figure 1).

Study characteristics

These 18 studies included CRPS [3,6-12], distal radius fracture [2], phantom limb pain [14], stroke [19,20], cancer [16], pathological pain (phantom pain after amputation, post-brachial plexus avulsion, and CRPS) [4], chronic shoulder pain [15], osteoarthritis [17], frozen shoulder [48], and elbow stiffness [21] (Figure 2). Studies case report and patient series (n=4), randomized controlled (n=10) (two waiting list crossover), randomized (n=1), randomized parallel design (n=1), and a single-arm prospective (n=1) consisting of a non-randomized controlled trial (n=1). The sample of the studies included a total of 513 participants. The demographic information of the participants is given in Table 1. The methodological quality levels of the included studies based on the Jovell and Navarro-Rubio [26] classification are given in Table 2.

Figure 2: Distribution of diseases included in our systematic review. The x-axis is the number of studies included.

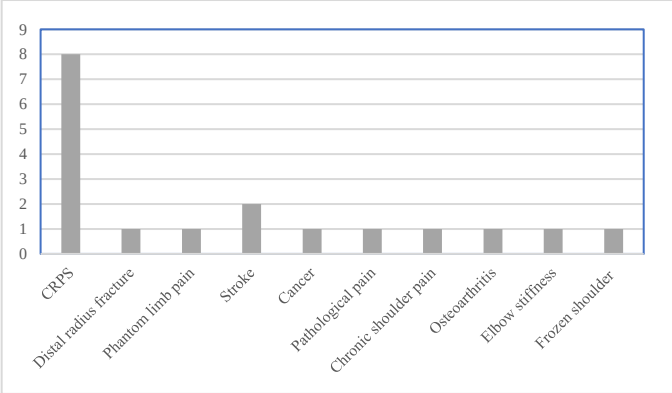

Risk of bias assessment

The ROB evaluation of randomized studies is summarized in Table 3. Of twelve randomized controlled studies, eight had “high” ROB, and the remaining four had “some concerns”. The ROB of non-randomized studies is shown in Table 4. Of the two included studies, a severe ROB was identified in one and a moderate ROB in the other. The evaluation of the case report and series are shown in Table 5.

Interventions

GMI was administered alone or in combination with any treatment. Since our aim in this review is also to reveal the different uses of GMI, all studies are included, even if they are used in addition to different treatments. First, when randomized studies were examined, GMI was applied together with traditional rehabilitation in four studies [2,17,20,48]. Three studies included GMI alone in the intervention group [4,7,14]. In one study, while GMI was applied sequentially to the intervention group, the order of the GMI was changed in the control groups [6]. In one study, 6 weeks of home exercise were applied after a 6-week GMI program [21]. Two of the studies were combined with the waiting protocol [9,10]. In another study, GMI with transcranial magnetic stimulation (tDCS) was compared with the group that received GMI with sham tDCS [11]. A non-randomized study used GMI with motor rehabilitation [19]. GMI alone was also included in a single-arm prospective study [15]. Considering case reports and patient series, one study used pain neuroscience education before GMI and graded functional exposure after GMI [3]. In another study, GMI was associated with neural mobilization [16]. It was used alone in two studies [8,12].

Graded Motor Imagery

In all studies, the three stages of GMI, implicit motor imagery (lateralization), explicit motor imagery, and mirror therapy, were applied sequentially. Only one study had a modified GMI program. In this program, mirror therapy was first applied with mobilization of the unaffected hand, followed by mobilization of both hands [8].

Table 1: Characteristics of patients in studies.

	Author and year	Participants			Contents	Study Group	Blind
		N (I/C)	Age	Gender (F/M)			
1	Dilek et al. 2017	17/19	I: 52.59±9.8; C: 47.16±10.5	I: 12/5 C:12/7	Distal radius fracture	2	Assessor
2	Limakatso et al. 2019	11/10	Median: I:63 (53-65) C: 62 (59-67)	I: 3/8 C: 2/8	Phantom limb pain	2	Assessor
3	Moseley et al. 2004	7/6	I:35±15; C:38±14	I:5/2 C:4/2	Chronic CRPS1	2	Assessor
4	Moseley et al. 2006	25/25	Unspecified	NC	Phantom limb pain after amputation, brachial plexus avulsion, CRPS1	2	Assessor
5	Gurudut et al. 2020	5/5	I:45.80±8.44 C:55.80±6.83	Unspecified	Knee osteoarthritis	2	Unspecified
6	Moseley, 2005	7/6/7	G1:36±8 G2:27±7 G3:39±8	G1:5/2 G2:4/2 G3:5/2	CRPS1	3	Researcher
7	Ji et al. 2021	17/20	I: 53.29±17.09 C: 61.75±11.59	I: 8/9 C: 7/13	Chronic stroke	2	Unspecified
8	Birinci et al. 2022	25/25	I: 42.1±11.2 C: 41.7±10.5	I: 8/17 C: 10/15	Elbow stiffness	2	Assessor, patients
9	Gurudut et al. 2022	10/10	I: 57±7.24 C: 58±7.25	I: 7/3 C: 7/3	Frozen shoulder	2	Assessor
10	Strauss et al. 2021	21/21	I: 54.71±14.13 C: 52.19±14.76	I:17/4 C:17/4	CRPS	2	Unspecified
11	Lagueux et al. 2017	11/11	I: 41 ± 9 C: 53 ±10	I: 8/3 C: 6/5	CRPS	2	Patients
12	Strauss et al. 2021	20/20	I: 54.7±14.3 C: 52.2±14.7	I:17/3 C:16/4	CRPS	2	Assessor
13	Polli et al. 2017	14/14	I: 56.6±12.4 C: 58.75 ±13.3	I: 4/10 C: 3/11	Stroke	2	Assessors
14	Araya-Quintanilla et al. 2020	107/-	65.7±4.8	68/39	Chronic Shoulder Pain Syndrome	No	No
15	Shepherd et al. 2018	1/-	57	Female	CRPS1	No	Unspecified
16	Lagueux et al. 2012	7/-	45±9.36	6/1	CRPS1-acute phase	No	Unspecified
17	García et al. 2015	7	5-18	Unspecified	Cancer	No	Unspecified
18	Walz et al. 2013	1/1	37/37	F/F	CRPS	2	Unspecified

I: Intervention, C: Control, F: Female, M: Male, CRPS: Complex regional pain syndrome, NC: Not clear.

Table 2: Intervention, comparison, outcomes, and design of the studies.

	Intervention		Control	Outcomes		Study Design	
	Exercise Type	Exercise Content/ Duration/ Frequency/ Time		Outcome	Results	D	Q
1	GMI and traditional rehabilitation	Traditional rehabilitation and lateralization, motor imagery and mirror therapy 8 wk/ twice on the wk/ 60 min L: 3 wk/3 times every waking hour (about 10 min) MI: 3 wk/3 times every waking hour (about 15 min) MT: 2 wk/10 times each waking hour.	Traditional rehabilitation including ROM and strengthening exercises 8 wk/ twice on the wk/60 min	VAS, active ROM, grip strength, DASH, MHQ	The GMI group showed greater improvement in pain intensity, wrist ROM and forearm ROM, and functional status (DASH, MHQ).	RCT	III
2	GMI, routine physiotherapy	Left/right judgements, imagined movements, mirror therapy 6 wk/ 2 supervised exercises (30 min) in the first week of each phase L: 2 wk MI: 2 wk MT: 2 wk Each phase 10 min each waking hour (12 sessions per day)	Routine physiotherapy (NC) 6 wk/NC	Brief Pain Inventory (Pain severity scale and pain interference scale), VAS of the EuroQol EQ-5D-5L	Significant improvements have been demonstrated in the interaction of pain and pain with function.	RCT	III
3	GMI, physical therapy	Recognition of hand laterality, imagined hand movements and mirror therapy 6 wk/ Unspecified L: 2 wk/three times each waking hour (<10 min) MI: 2 wk/ three times each waking hour (<15 min) MT: 2 wk/(Repeat 20 movements 10 times each waking hour)	Physical therapy 12 wk/ 2- 3 times per week.	Neuropathic pain scale, finger circumference, response time	In the GMI group, a reduction in pain, edema and response time was demonstrated.	RCT	III
4	GMI, standard rehabilitation	Limb laterality recognition, movement imagery, mirror movements 6 wk/ NC L: 2 wk/NC MI: 2 wk/NC MT: 2 wk/NC	Standard physiotherapy 6 wk/NC	Patient-specific task-related numerical rating scale, VAS	Improvements in pain and function were maintained at 6 months.	RCT	III
5	Progressive muscle relaxation, GMI, traditional rehabilitation	Left/right discrimination, explicit therapy, mirror therapy, traditional rehabilitation 2 wk/5 sessions per wk/ 20 min L and MI: First week MT: Second week	Jacobson's relaxation technique, traditional rehabilitation 2 wk/5 sessions per wk/ 20min	WOMAC, Knee flexion ROM	Knee flexion range of motion and WOMAC scores were significantly better in the GMI group than in the PMR group.	RCT	III
6	GMI	G1: Respectıvely (L, MI, MT) L: 2 wk/3 times every waking hour (~10 min) MI: 2 wk/ Twice every waking hour (~10 min) MT: 2 wk/Repeat each picture 5 times at each wake-up time (~10 min)	G2: Respectıvely (MI, L, MI) G3: Respectıvely (L, MT, L) L: 2 wk/3 times every waking hour (~10 min) MI: 2 wk/ Twice every waking hour (~10 min) MT: 2 wk/Repeat each picture 5 times at each wake-up time (~10 min)	Neuropathic pain scale, 11-point numerical rating scale (activity difficulties)	Sequential administration of GMI (G1) produced further reductions in pain and disability.	RCT	III
7	GMI, conventional therapy	Implicit motor imagery, explicit motor imagery, and mirror therapy, conventional therapy 8 wk/30 min a day L: NC MI: NC MT: NC	Conventional therapy (Task-oriented active/passive range of motion training) 8 wk/30 min a day	MFT, Fugl-Meyer Assessment, Modified Barthel Index	The MFT arm motion score was significantly better in the GMI group than in the controls.	RCT	III
8	GMI, structured exercise program	Left-right discrimination, motor imagery, and mirror therapy Home exercises (6 weeks after GMI) 6 wk/ twice a wk (GMI) L: 2 wk (1-2 wk) MI: 2 wk (2-3 wk) MT: 4 wk (3,-6 wk)	Structured exercise program Home exercise (6 weeks after exercise program) 6 wk/ twice a wk	DASH, ROM, VAS, Tampa Scale, muscle strength, left-right , discrimination, Global Rating of Change scale.	Function, elbow AROM, pain, fear of movement-related pain, and muscle strength were significantly different in the GMI group compared to the control group.	RCT	III
9	GMI, conventional physiotherapy	Laterality recognition, movement visualization, mirror therapy, conventional physiotherapy 3 wk/ three times a wk L: 1 wk/NC MI: 1 wk MT: 1 wk	Conventional physiotherapy 3 wk/ three times a wk	ROM, fear avoidance belief questionnaire, VAS, SPADI.	Pain, functional disability, fear of movement, and abduction ROM, in the GMI group, was significantly better than in the control group	RCT	III

GMI: Graded motor imagery, L: Lateralization, MI: Motor imagery, MT: Mirror therapy, VAS: Visual Analog Scale, ROM: Range of motion, DASH: Disabilities of the Arm, Shoulder and Hand, MHQ: Michigan Hand Outcomes Questionnaire, MFT: Manual Function Test, tDCS: Transcranial Magnetic Stimulation, fMRI: Functional Magnetic Resonance Imaging, FMA: Fugl-Meyer Assessment, PCS: Pain catastrophizing scale, WMFT: Wolf Motor Function Test, RCT: Randomized Controlled Trials, WOMAC: Western Ontario and McMaster Universities Osteoarthritis Index, SPADI: Shoulder Pain And Disability Index, G1: Group 1, G2: Group 2, G3: Group 3, NC: Not Clear, min: minute, wk: week, D: design, Q: quality.

Table 2: Continues.

	Intervention		Control	Outcomes		Study Design	
	Exercise Type	**Exercise Content/ Duration/ Frequency/ Time**		**Outcome**	**Results**	**D**	**Q**
10	GMI	Left/right judgments, imagined movements, mirror therapy 6 wk GMI followed by 6 wk wait L: 2 wk/10 min every waking hour MI: 2 wk/10 min every waking hour MT: 2 wk/10 min every waking hour	6 wk wait followed by 6 wk GMI	CRPS severity score (CSS), QuickDASH, VAS, cutaneous sensory threshold, spatiotactile resolution, Roeder Manipulative Aptitude Test, cortical excitability	Without waiting, GMI resulted in a minor effect on movement pain, reduction in CSS, increased use of the affected hand, and an improvement in motor function and spatial tactile performance .	Randomized controlled crossover study	III
11	GMI, Transcranial Direct Current Stimulation	GMI: Limb laterality recognition, imagined movements, mirror therapy L: 2 wk/6 times a wk/ 3 times per day/10 min MI: 2 wk/6 times a wk/ 3 times per day/10 min MT: 2 wk/6 times a wk/ 3 times per day/10 min tDCS: Constant current with a intensity of 2 mA (30 seconds ramp up, 30 seconds ramp down), (20 min) 1-2 wk: 5 days a wk 3-6 wk: 1 time per wk	GMI+ shamtDCS	Brief pain inventory shortform, SF-12, Tampa Scale, Pain catastrophizing scale, State-Trait Anxiety Inventory, Beck Depression Inventory	GMI + tDCS did not cause a significant change in pain compared to the sham group. There were significant group differences in kinesiophobia, catastrophizing pain, and anxiety.	Randomized parallel design	III
12	GMI	Mental rotation, movement imagery, mirror movements 6 wk GMI followed by 6 wk wait L: 2 wk/ 10 min every waking hour MI: 2 wk/ 10 min every waking hour MT: 2 wk/10 min every waking hour	6 wk wait followed by 6 wk GMI	VAS, response Time, fMRI Representation	GMI treatment alone, but not waiting, showed an effect on motion pain and hand reasoning task performance.	Randomized wait-list crossover design	III
13	GMI, motor rehabilitation	Implicit Motor Imagery, Explicit Motor Imagery and Mirror Therapy and motor rehabilitation (GMI 1 hour and motor rehabilitation 1 hour) 4 wk/5 days a wk L: 6-8 session/ 1 hour MI: 6-8 session/ 1 hour MT: 6-8 session/ 1 hour	C: Motor rehabilitation 4 wks/5 days a wk/ 2 hours	WMFT, FMA for Upper Limb, Tardieu Rating Scale, VAS, Functional Independence Measure, Satisfaction questionnaire	In FMA and WMFT, improvements have been shown in motor function, as well as in the pain section of FMA.	Non-randomized controlled trial	IV
14	GMI	Laterality training, imagined movements, and mirror therapy 6 wk/ 3 times a wk L: NC/1 hour a day MI: NC/3 times per day MT: NC/30 min	No	VAS, Tampa Scale, PCS, active ROM	A decrease in VAS, Tampa Scale and PCS and an increase in active ROM were shown.	Single-Arm Prospective Study	VI
15	Pain neuroscience education, Graded motor imagery, Graded functional exposure	Visit 1-7: Pain neuroscience education (pain metaphors were used to explain allodynia and central sensitivity) and GMI (laterality, explicit motor imagery and mirror therapy) Visit 8-20: Gradual weight bearing in walking, therapeutic exercise, manual therapy Visit 21-26: Motor performance exercises to improve strength and proprioception 9 month/ 26 visit L: NC MI: NC MT: NC	No	Foot and Ankle Ability Measure-Activities of Daily Living, Tampa Scale, Pain Catastrophizing Scale, patient's goals, Physical examination	Beneficial results have been demonstrated in functional and fear of movement outcomes.	Case Report	IX
16	Modified graded motor imagery (home exercise)	Phase 1: Hand laterality Phase 2: Imagined hand movements Phase 3: Mirror therapy with mobilization of the nonaffected hand Phase 4: Mirror therapy with mobilization of both hands Each phase 2 wk/6 days a wk/3 times a day/ 10 min	No	Short form of the McGill Pain Questionnaire, DASH, grip force, PGIC	No functionally (DASH) significant changes were observed, with significant changes in pain, grip strength, and PGIC.	Patient series	VIII
17	GMI, neural mobilization	Motor imagery: 5 days/wk for 1 week. Laterality recognition: 5 days/wk for 1 wk. Mirror therapy: 5 days/wk for 2 wk. Neural mobilization -Slump test in lateral decubitus (2 _ 20 at 0.5 Hz) – 2 days/wk for 4 weeks. Upper Limb Tension Test 1 – both arms (2 _ 20 at 0.5 Hz) – 2 days/wk for 4 wk.	No	VAS, pain thresholds, LANSS, catastrophizing survey	Improvement in pain threshold and pain perception was demonstrated.	Patient Series	VIII
18	GMI	GMI: Mental rotation, movement imagery, mirror movements 6 weeks L: 2 wk/ 5-10 min every waking hour MI: 2 wk/ 5-10 min every waking hour MT: 2 wk/5-10 min every waking hour	No intervention	Cerebral activation, VAS	There was a reduction in pain, changes in discriminative pain processing areas in the cortex, but no change in emotional pain processing areas.	Case report	IX

GMI: Graded motor imagery, L: Lateralization, MI: Motor imagery, MT: Mirror therapy, VAS: Visual Analog Scale, ROM: Range of motion, DASH: Disabilities of the Arm, Shoulder and Hand, MHQ: Michigan Hand Outcomes Questionnaire, MFT: Manual Function Test, tDCS: Transcranial Magnetic Stimulation, fMRI: Functional Magnetic Resonance Imaging, FMA: Fugl-Meyer Assessment, PCS: Pain catastrophizing scale, WMFT: Wolf Motor Function Test, RCT: Randomized Controlled Trials, WOMAC: Western Ontario and McMaster Universities Osteoarthritis Index, SPADI: Shoulder Pain And Disability Index, G1: Group 1, G2: Group 2, G3: Group 3, NC: Not Clear, min: minute, wk: week, D: design, Q: quality

Table 3: Risk of bias assessment for randomized controlled trials.

	Dilek et al. 2017	**Limakatso et al. 2019**	**Moseley et al. 2004**	**Moseley et al. 2006**	**Gurudut et al. 2020**	**Moseley 2005**	**Ji et al. 2021**	**Birinci et al. 2022**	**Gurudut et al. 2022**	**Strauss et al. 2021**	**Lagueux et al. 2017**	**Strauss et al. 2021**
Risk of bias arising from the randomization process	Low	Low	Low	Low	Some concerns	Low	Some concerns	Low	Some concerns	Some concerns	Low	Some concerns
Risk of bias due to deviations from intended interventions	Some concerns	Some concerns	Some concerns	Some concerns	Some concerns	Some concerns	High	Some concerns	Some concerns	Some concerns	Some concerns	Some concerns
Risk of bias due to missing outcome data	High	Low	Low	Low	Low	Low	Low	Low	Low	High	Low	Low
Risk of bias in measurement of the outcome	Low	Low	High	Low	High	High	High	Low	Low	High	High	Low
Risk of bias in selection of the reported result	Some concerns	Some concerns	Some concerns	Some concerns	Some concerns	Some concerns	Some concerns	High	Some concerns	Some concerns	Some concerns	Some concerns
Overall risk of bias	High	Some concerns	High	Some concerns	High	High	High	High	Some concerns	High	High	Some concerns

Table 4: Risk of bias assessment for non-randomized studies.

	Bias due to confounding	Bias in selection of participants into the study	Bias in classification of interventions	Bias due to deviations from intended interventions	Bias due to missing data	Bias in measurement of outcomes	Bias in selection of the reported result(s)	Overall bias
Polli et al. 2017	Moderate	Low	Moderate	Low	Low	Low	Moderate	Moderate
Araya-Quintanilla et al. 2020	Moderate	Low	Moderate	Serious	Low	Low	Moderate	Serious

Table 5: Risk of bias assessment for case reports and case series.

Domain	Leading explanatory question	Study			
		Shepherd et al. 2018	Lagueux et al. 2012	García et al. 2015	Walz et al. 2013
Selection	1. Do patients represent the whole investigator (center) experience?	No	Yes	Yes	No
Ascertainment	2. Was the exposure adequately ascertained?	Yes	Yes	No	Yes
	3. Was the outcome adequately ascertained?	No	Yes	Yes	Yes
Causality	4. Were alternative causes explaining the observation ruled out?	NA	NA	NA	NA
	5. Was there a challenge/rechallenge phenomenon?	NA	NA	NA	NA
	6. Was there a dose response effect?	NA	NA	NA	NA
	7. Was follow-up long enough for outcomes to occur?	Yes	No	No	Yes
Reporting	8. Was there sufficient detail to replicate the research?	No	Yes	No	Yes
Overall score		2/8	4/8	2/8	4/8

There are some differences regarding the duration and frequency of application of the total and each stage of GMI. Total administration ranged from 2 to 8 weeks. Detailed information on the implementation of all phases of the GMI is shown in Table 2.

Outcomes

Pain was the outcome measure in 15 of the studies. Visual analog scale (VAS) [2,4,9,10,12,15,16,19,21,48] was used the most in pain assessment. In other studies, brief pain inventory (BPI) [11,14], the McGill Pain Questionnaire (MPQ) [8], the neuropathic pain scale (NPS) [6,7], and LANSS [16] were used. Other parameters related to pain were pain threshold [16] and the pain catastrophizing scale [3,11,15,16]. Other tools used include: range of motion (ROM) [2,15,17,21,48] and strength [2,8,21] were other outcome measures. In the evaluation of kinesiophobia and functional status, the Tampa Scale [3,11,15,21], Fear Avoidance Belief Questionnaire [48], Disabilities of the Arm, Shoulder and Hand (DASH) [2,8,21], Quick DASH [9], Michigan Hand Outcomes Questionnaire (MHQ) [2], WOMAC [17] and Functional Independence Measure (FIM) [19], Shoulder Pain and Disability Index [48], Foot and Ankle Ability Measure-Activities of Daily Living (FAAM-ADL) [3]. In addition, VAS of the EuroQol EQ-5D-5L [14], Modified Barthel Index [20], SF-12 [11], and Numerical Rating Scale (NRS) [4,6] were used for quality of life and activities of daily living. Reaction time [7,9] was also included as an outcome measure. Anxiety and depression were evaluated with the State-Trait Anxiety Inventory and Beck Depression Inventory [11]. In the sensory evaluation, skin sensory threshold (von Frey hair filaments) and spatial tactile resolution [9] were present. Evaluations of motor function were performed with the help of the Manual Function Test [20], Fugl-Meyer Assessment (FMA) [19,20], Wolf Motor Function Test (WMFT) [19], Roeder Manipulative Aptitude Test [9]. Only one study used the Tardeu Scale [19] for spasticity assessment. Three studies evaluated changes in the cortex [9,10,12]. Apart from these, right-left discrimination [21], finger circumference measurement [7], patient's global impression of change scale [8], Global Rating of Change [21], CRPS severity score [9], patient goals [3], Satisfaction questionnaire [19] were available. The outcomes of the studies are detailed in Table 2.

Discussion

This systematic review included 18 articles applying the stages of the GMI in order and a total of 513 participants. The results of this systematic review, which examined different types of research in the literature, showed that GMI was used in many neurological and orthopedic conditions. In studies, application durations varied between 2 and 8 weeks and treatment protocols with different frequencies. In addition, the GMI reduced pain in 14 of the 15 studies whose outcome was pain.

While the studies on GMI are increasing, it is seen that there are different protocols in the studies. Moseley's [7] study has been used as a guide in many studies. Moseley et al. [1] have made significant contributions to the development of GMI. Moseley [7] applied each stage of the GMI for 2 weeks in the study. In 55.5% (n=10) of the studies included in this systematic review, the GMI application period was 6 weeks. In eight of these studies (including Moseley's study), each stage of the GMI was applied for 2 weeks [4,6,7,9-12,14]. Apart from this, the duration of application in the included studies ranged from 2 to 8 weeks.

Another difference in the studies on GMI is how many times a day they are applied. In Moseley's study [7], lateralization (<10 min) and motor imagery (<15 min) phases were applied three times per waking hour, and mirror therapy was applied as ten repetitions of 20 movements at each waking hour. In other words, each component was applied at every waking hour. In seven of the studies included in this review, each phase was performed at each waking hour [2,6,7,9,10,12,14]. Although beneficial effects of administration at each waking hour have been demonstrated, its feasibility is low [49]. Therefore, there are different forms of application. Lageux et al. [8] applied each step three times per day for 10 min. The result

of this study was significant improvements in pain, grip strength, and overall patient change. A study protocol planned for patients with distal radius fractures in 2018 was based on the work of Lageux et al. [49]. In another study included in this review, GMI was administered three times per day [11]. In other included studies, there are applications such as 20 min [17], 30 min [20], and 1 h [19] per day. In one study, the laterality phase was applied in short sessions for 1 h per day, the motor imagery phase was applied three times per day, and the mirror therapy was applied for 30 min per day [15]. In five studies, the mode of administration is unclear [3,4,16,21,48].

This systematic review has applied GMI in different conditions and for various purposes. It is known that GMI has effects on pain and movement [3]. It has been stated that mechanisms such as the development of cortical activation and reorganization are the basis of recovery in patients with CRPS1, phantom limb pain, and stroke. Therefore, it is thought that graded motor imagery will provide beneficial effects in these situations [50]. In a study, the effects of GMI and routine physiotherapy applied to patients with phantom limb pain after upper or lower extremity amputation were compared, and it was shown that GMI was more effective than routine physiotherapy [14]. In his study, Moseley [7] showed reductions in pain, edema, and reaction time, in which he compared the effects of routine medical treatment and GMI in individuals with chronic CRPS.

In another study, Moseley investigated the effect of changing the order of the 3 stages of GMI in patients with CRPS. As a result of this study, a significant difference was observed when three stages were applied consecutively (laterality, motor imagery and mirror therapy, respectively). This study has led to significant results. The sequential application of the three phases is more effective as it activates the premotor and, subsequently, the motor networks, resulting in a sequential exposure [6]. Strauss et al. [9] investigated the effects of 6 weeks of GMI therapy and 6 weeks of the waiting protocol in individuals with upper extremity chronic stage CRPS. GMI applied without waiting has been shown to cause improvements in functional parameters with a slight reduction in movement pain. In another study with a waiting protocol, 6 weeks of GMI treatment without waiting was shown to improve motion pain and hand laterality task performance [10]. In another study, it was thought that applying GMI and tDCS would increase the therapeutic effects. It did not appear to provide additional benefits when administered together [11].

In this systematic review, examining studies of lower methodological quality on GMI in CRPS also provides important contributions. We think that using different methods in these studies is important in examining the literature on GMI. For the patient with psychosocial problems, pain neuroscience training was added beforehand to make the GMI more solid and to provide an environment in which the patient would feel more confident. Improvements in functional and fear-related outcomes have been demonstrated [3]. In the case series of patients with upper extremity CRPS, the GMI was modified and applied. The motor imagery phase was applied by imagining the unaffected extremity while watching its reflection in the mirror. In addition, the third stage, mirror therapy, was applied in two different ways.

First, the mirror therapy was applied with the movement of the unaffected hand, and then, the fourth stage was added to be performed with the movement of both hands. There was a significant reduction in pain intensity and significant increases in grip strength but no significant changes in the functional capacity of the extremity. The results of this research are important in that mirror therapy is included in the motor imagery phase and that the mirror therapy phase is divided into two and applied in a total of four phases [8]. The case report by Walz et al. [12] evaluated the effects of GMI in a patient with CRPS by functional magnetic resonance imaging (fMRI) and compared the time effects with a healthy control participant. A reduction in pain has been demonstrated after GMI intervention. In addition, fMRI showed significant changes in discriminative pain processing areas during movement execution but not in affective pain processing areas. After the mental rotation phase, a change was observed in the processing area of the posterior parietal cortex. A comparison of results in this study with a healthy control group indicates that the effects are due to treatment. Dilek et al. [2] included GMI in the early phase of rehabilitation after distal radius fracture in their study. There were significant improvements in pain intensity, ROM, and upper extremity functional status in the group that included GMI in conventional rehabilitation. In addition, GMI has been tried in cases of osteoarthritis, elbow stiffness, shoulder pathologies, and cancer-related neuropathic pain [15-17,21,48]. In addition to traditional rehabilitation, GMI and progressive muscle relaxation exercises were applied in patients with osteoarthritis. It was reported that the GMI group was significantly better than the PMR group in terms of knee flexion range of motion and WOMAC scores [17]. In elbow stiffness, the GMI group caused significant improvements in function, ROM, pain, fear of movement-related pain, and muscle strength compared to the control group [21]. Significant improvements in the affective components of pain and range of motion have been demonstrated after GMI intervention in individuals with chronic shoulder pain due to tendinopathy or partial rotator cuff tear [15]. In frozen shoulder patients, the GMI was also better than conventional therapy alone in pain, functional disability, fear of movement, and ROM outcomes [48]. Casanova-García et al. [16] applied GMI as a non-invasive option for neuropathic pain in a group of children with cancer. Improvements were seen in pain perception and threshold, although the sample size was small.

GMI was applied in two studies after stroke, a neurological condition [19,20]. CRPS is also used to regulate GMI cortical disinhibition. Cortical disinhibition is a condition that causes motor problems in stroke. Therefore, GMI targeting cortical disinhibition was applied to improve motor function in stroke patients. GMI improved pain and function compared to normal rehabilitation [19]. As a result of another study investigating the effects of a home-based GMI program on upper extremity function after stroke, it was reported that applying for the GMI program with traditional rehabilitation would be beneficial [20].

This review has some limitations. First, the results were difficult to interpret due to the heterogeneous studies. GMI was

used alone or in addition to another treatment. This leads to contradictory results about whether the results can be attributed to GMI. In addition, the included studies used very different outcome measures, making it difficult to interpret the results.

Despite some limitations, this systematic review is important in that it summarizes the methods of the articles expanding in the field of GMI by examining and evaluating the risk of bias. In addition, although it is not known which of the stages of the GMI is effective, it is known that the order of the stages is necessary for cortical organization [2]. In this systematic review, it is important to understand GMI that the articles that are not applied sequentially are excluded.

Conclusion

Although some articles in this review have small sample sizes, the application protocols of GMI in neurological and orthopedic disorders have been examined in detail. Although heterogeneous, it has been observed that a 6-week application is common. Primarily effect of GMI on pain outcomes has been investigated in the literature. GMI is a safe and effective therapeutic tool that can be incorporated into a rehabilitation program to treat painful conditions. However, this literature summary suggests that more work is needed to uncover the role of GMI.

References

1. Moseley GL, Butler DS, Beames TB, Giles TJ. The graded motor imagery handbook: Noigroup publications; 2012.
2. Dilek B, Ayhan C, Yagci G, Yakut Y. Effectiveness of the graded motor imagery to improve hand function in patients with distal radius fracture: A randomized controlled trial. J Hand Ther. 2018;31(1):2-9.
3. Shepherd M, Louw A, Podolak J. The clinical application of pain neuroscience, graded motor imagery, and graded activity with complex regional pain syndrome-A case report. Physiother Theory Pract. 2020;36(9):1043-55.
4. Moseley GL. Graded motor imagery for pathologic pain: a randomized controlled trial. Neurology. 2006;67(12):2129-34.
5. Limakatso K, Corten L, Parker R. The effects of graded motor imagery and its components on phantom limb pain and disability in upper and lower limb amputees: A systematic review protocol. Systematic Reviews. 2016;5(1):145.
6. Moseley GL. Is successful rehabilitation of complex regional pain syndrome due to sustained attention to the affected limb? A randomised clinical trial. Pain. 2005;114(1-2):54-61.
7. Moseley GL. Graded motor imagery is effective for long-standing complex regional pain syndrome: a randomised controlled trial. Pain. 2004;108(1-2):192-8.
8. Lagueux E, Charest J, Lefrancois-Caron E, Mauger ME, Mercier E, Savard K, et al. Modified graded motor imagery for complex regional pain syndrome type 1 of the upper extremity in the acute phase: a patient series. Int J Rehabil Res. 2012;35(2):138-45.
9. Strauss S, Barby S, Härtner J, Pfannmöller JP, Neumann N, Moseley GL, et al. Graded motor imagery modifies movement pain, cortical excitability and sensorimotor function in complex regional pain syndrome. Brain Commun. 2021;3(4):1-14.
10. Strauss S, Barby S, Härtner J, Neumann N, Moseley GL, Lotze M. Modifications in fMRI Representation of Mental Rotation Following a 6 Week Graded Motor Imagery Training in Chronic CRPS Patients. J Pain. 2021;22(6):680-91.
11. Lagueux E, Bernier M, Bourgault P, Whittingstall K, Mercier C, Leonard G, et al. The Effectiveness of Transcranial Direct Current Stimulation as an Add-on Modality to Graded Motor Imagery for Treatment of Complex Regional Pain Syndrome: A Randomized Proof of Concept Study. Clin J Pain. 2018;34(2):145-54.
12. Walz AD, Usichenko T, Moseley GL, Lotze M. Graded motor imagery and the impact on pain processing in a case of CRPS. Clin J Pain. 2013;29(3):276-9.
13. Priganc VW, Stralka SW. Graded motor imagery. J Hand Ther. 2011;24(2):164-8.
14. Limakatso K, Madden VJ, Manie S, Parker R. The effectiveness of graded motor imagery for reducing phantom limb pain in amputees: a randomised controlled trial. Physiotherapy. 2020;109:65-74.
15. Araya-Quintanilla F, Gutierrez-Espinoza H, Jesus Munoz-Yanez M, Rubio-Oyarzun D, Cavero-Redondo I, Martinez-Vizcaino V, et al. The Short-term Effect of Graded Motor Imagery on the Affective Components of Pain in Subjects with Chronic Shoulder Pain Syndrome: Open-Label Single-Arm Prospective Study. Pain Med. 2020;21(10):2496-501.
16. Casanova-Garcia C, Lara SL, Ruiz MP, Dominguez DR, Sosa ES. Non-pharmacological treatment for neuropathic pain in children with cancer. Med Hypotheses. 2015;85(6):791-7.
17. Gurudut P, Jaiswal R. Comparative Effect of Graded Motor Imagery and Progressive Muscle Relaxation on Mobility and Function in Patients with Knee Osteoarthritis: A Pilot Study. Altern Ther Health Med. 2022;28(3):42-7.
18. Sawyer EE, McDevitt AW, Louw A, Puentedura EJ, Mintken PE. Use of Pain Neuroscience Education, Tactile Discrimination, and Graded Motor Imagery in an Individual With Frozen Shoulder. J Orthop Sports Phys Ther. 2018;48(3):174-84.
19. Polli A, Moseley GL, Gioia E, Beames T, Baba A, Agostini M, et al. Graded motor imagery for patients with stroke: a non-randomized controlled trial of a new approach. Eur J Phys Rehabil Med. 2017;53(1):14-23.
20. Ji EK, Wang HH, Jung SJ, Lee KB, Kim JS, Jo L, et al. Graded motor imagery training as a home exercise program for upper limb motor function in patients with chronic stroke: A randomized controlled trial. Medicine. 2021;100(3):1-5.
21. Birinci T, Kaya Mutlu E, Altun S. The efficacy of graded motor imagery in post-traumatic stiffness of elbow: a randomized controlled trial. J Shoulder Elbow Surg. 2022;31(10):2147-56.
22. Bowering KJ, O'Connell NE, Tabor A, Catley MJ, Leake HB, Moseley GL, et al. The effects of graded motor imagery and its components on chronic pain: a systematic review and meta-analysis. J Pain. 2013;14(1):3-13.
23. Méndez-Rebolledo G, Gatica-Rojas V, Torres-Cueco R, Albornoz-Verdugo M, Guzmán-Muñoz E. Update on the effects of graded motor imagery and mirror therapy on complex regional pain syndrome type 1: A systematic review. J Back Musculoskelet Rehabil. 2017;30(3):441-9.
24. Liberati A, Altman DG, Tetzlaff J, Mulrow C, Gøtzsche PC, Ioannidis JP, et al. The PRISMA statement for reporting systematic reviews and meta-analyses of studies that evaluate health care interventions: explanation and elaboration. Ann Intern Med. 2009;151(4):65-94.
25. Methley AM, Campbell S, Chew-Graham C, McNally R, Cheraghi-Sohi S. PICO, PICOS and SPIDER: a comparison study of specificity and sensitivity in three search tools for qualitative systematic reviews. BMC Health Serv Res. 2014 November 21;14:579.
26. Jovell AJ, Navarro-Rubio MD. [Evaluation of scientific evidence]. Medicina clinica. 1995;105(19):740-3.
27. Higgins JP, Thomas J, Chandler J, Cumpston M, Li T, Page MJ, et al. Cochrane handbook for systematic reviews of interventions: John Wiley & Sons; 2019.
28. Jüni P, Loke Y, Pigott T, Ramsay C, Regidor D, Rothstein H, et al. Risk of bias in non-randomized studies of interventions (ROBINS-I): detailed guidance. Br Med J. 2016.
29. Higgins J. Cochrane handbook for systematic reviews of interventions. Version 5.1. 0 [updated March 2011]. The Cochrane Collaboration. 2011.
30. Murad MH, Sultan S, Haffar S, Bazerbachi F. Methodological quality and synthesis of case series and case reports. BMJ Evid Based Med. 2018;23(2):60-3.
31. Dudhani S, Anwar KAM, Jain PK. Can Brain Cure Pain and Fear? Effect of Graded Motor Imagery on Post Operative Lumbar Degenerative Diseases-Randomized Control Trial. Website: www ijpot com. 2020;14(1):244.
32. Johnson S, Hall J, Barnett S, Draper M, Derbyshire G, Haynes L, et al. Using graded motor imagery for complex regional pain syndrome in clinical practice: failure to improve pain. Eur J Pain. 2012;16(4):550-61.
33. Louw A, Schmidt SG, Louw C, Puentedura EJ. Moving without moving: immediate management following lumbar spine surgery using a graded motor imagery approach: a case report. Physiother Theory Pract. 2015;31(7):509-17.
34. Quintal I, Poire-Hamel L, Bourbonnais D, Dyer JO. Management of long-term complex regional pain syndrome with allodynia: A case report. J Hand Ther. 2018;31(2):255-64.
35. Anderson B, Meyster V. Treatment of a Patient With Central Pain Sensitization Using Graded Motor Imagery Principles: A Case Report. J Chiropr Med. 2018;17(4):264-7.
36. Gu P, Ye L, Li S. Regional homogeneity in patients with cerebral infarction and upper extremity hemiparesis before and after graded motor imagery training: a resting-state fMRI study. Chinese Journal of Rehabilitation Medicine. 2020;35(6):662-9.
37. Hall J, Mattheus C, McCabe CS. Graded Motor Imagery Programmes in Complex Regional Pain Syndrome: One Size Doesn't Fit All? Rheumatology. 2009;48:13-I4.
38. Lacuey-Barrachina E, Cuello-Ferrando A, Buil-Mur MI. Effectiveness of graduated motor imaging in complex regional pain syndrome-I. Cuestiones de Fisioterapia. 2020;49(1):55-64.
39. Ramella M, Borgnis F, Giacobbi G, Castagna A, Baglio F, Cortesi M, et al. Modified Graded Motor Imagery for Musicians' Focal Dystonia: A Case Series. Med Probl Perform Art. 2021;36(1):10-7.
40. Lluch-Girbés E, Dueñas L, Mena-del Horno S, Luque-Suarez A, Navarro-Ledesma S, Louw A. A central nervous system-focused treatment approach for people with frozen shoulder: protocol for a randomized clinical trial. Trials. 2019;20(1):498.
41. Rierola-Fochs S, Varela-Vasquez LA, Merchan-Baeza JA, Minobes-Molina E. Development and Validation of a Graded Motor Imagery Intervention for Phantom Limb Pain in Patients with Amputations (GraMI Protocol): A Delphi Study. Int J Environ Res Public Health. 2021;18(22):12240.
42. Spera P, Poniewierski P, Kostiukow A, Samborski W. The impact of physical activity on the functional state of a small patient with cancer. Pol Merkur Lekarski. 2020;48(283):39-41.
43. Wand BM, O'Connell NE, Di Pietro F, Bulsara M. Managing Chronic Nonspecific Low Back Pain With a Sensorimotor Retraining Approach: Exploratory Multiple-Baseline Study of 3 Participants. Phys Ther. 2011;91(4):535-46.
44. Kumar SP, Kumar A, Shenoy K, D'Souza M, Kumar VK. Guided/Graded Motor Imagery for Cancer Pain: Exploring the Mind-Brain Inter-relationship. Indian J Palliat Care. 2013;19(2):125-6.
45. Lagueux E, Bourgault P, Tousignant-Laflamme Y. Effectiveness of transcranial Direct Current Stimulation (tDCS) and Graded Motor Imagery (GMI) on neuropathic pain of complex regional pain syndrome type I. Clin J Pain. 2015;16(4):S94-S.
46. Morales-Osorio MA, Mejía Mejía J. Graded motor imagery in the phantom limb syndrome with pain. Revista de la Sociedad Espanola del Dolor. 2012;19(4):209-16.
47. Birinci T, Mutlu EK, Altun S. Graded Motor Imagery in Posttraumatic Stiffness of the Elbow: A Pilot Study. Ann Rheum Dis. 2020;79:909-10.
48. Gurudut P, Godse AN. Effectiveness of graded motor imagery in subjects with frozen shoulder: a pilot randomized controlled trial. Korean J Pain. 2022;35(2):152-9.
49. McGee C, Skye J, Van Heest A. Graded motor imagery for women at risk for developing type I CRPS following closed treatment of distal radius fractures: a randomized comparative effectiveness trial protocol. BMC Musculoskelet Disord. 2018;19(1):202.
50. Acerra NE, Souvlis T, Moseley GL. Stroke, complex regional pain syndrome and phantom limb pain: can commonalities direct future management? J Rehabil Med. 2007;39(2):109-14.

J Surg Med. 2023;7(5):355-357.
DOI: 10.28982/josam.1122921

Case report

Journal of Surgery and Medicine
e-ISSN: 2602-2079
https://jsurgmed.com/

Primary pancreatic lymphoma and metastatic lymphoma cases diagnosed with ultrasonography guided tru-cut needle biopsy: Two case reports

Işıl Bağcı, Nazlı Sena Şeker

Department of Pathology, Osmangazi University Medicine Faculty, Eskişehir, Turkey

ORCID ID of the author(s)

IB: 0000-0001-5211-5430
NSŞ: 0000-0003-4588-7250

Abstract

Secondary pancreatic involvement can be seen up to 30% of advance staged non-Hodgkin's lymphoma cases, but primary pancreatic lymphomas constitute only 1% of extranodal lymphomas. Furthermore, 0.2% of the pancreatic space-occupying lesions are primary pancreatic lymphomas, which usually present as a mass in the head of the pancreas with nonspecific symptoms. Therefore, primary pancreatic lymphomas should be considered as differential diagnosis of pancreatic solid lesions. Herein, we report two cases with different clinical presentation and different course of disease resulting in the diagnosis of primary and metastatic pancreatic lymphoma.

Keywords: primary pancreatic lymphoma, pancreas, metastatic disease, diffuse large B-cell lymphoma, mantle cell lymphoma

Introduction

Hodgkin's and non-Hodgkin's lymphomas (NHL) are the two main types of lymphomas. Hodgkin's lymphomas rarely invade extranodal sites, but 30-40% of NHL's invade extranodal organs [1-5]. The gastrointestinal tract is the most common extranodal site and accounts for 15-20% of all NHL cases [2]. Secondary pancreatic involvement occurs up to 30% of cases especially in widespread nodal or extranodal disease [3,4]. Also, primary pancreatic lymphomas (PPL) accounts for approximately 1% of extranodal lymphomas and 0.2% of the pancreatic tumors [4,6].

In 1961, Dawson et al. [7] proposed criteria for the diagnosis of PPL: A pancreatic mass specified in surgery with the involvement of lymph nodes confined to the pancreas without any peripheral lymphadenopathy, involvement of mediastinal lymph node, or involvement of liver or spleen; normal peripheral white blood cell counting. In 1994, Behrns et al. [3] revised these criteria [8,9]: no palpable superficial lymphadenopathy; no enlargement of mediastinal lymph nodes on chest; normal leukocyte counting; the pancreatic mass predominates with grossly involved lymph nodes confined to the peripancreatic region at celiotomy; no hepatic or splenic involvement.

More recently, the World Health Organization (WHO) has provided the following diagnostic definition: PPL is an extranodal lymphoma of the pancreas with primary pancreatic clinical presentation and the bulk of the disease localized to this site even though contiguous lymph-node involvement and distant spread is seen [4,6]. Herein we report two cases with different clinical outcomes and resulting diagnosis.

Corresponding Author
Işıl Bağcı
Department of Pathology, Osmangazi University Faculty of Medicine, 26040, Odunpazarı, Eskişehir, Turkey
E-mail: bagcisil@gmail.com

Informed Consent
The authors stated that the written consent was obtained from the patients presented with images in the study.

Conflict of Interest
No conflict of interest was declared by the authors.

Financial Disclosure
The authors declared that this study has received no financial support.

Published
2023 April 29

How to cite: Bağcı I, Şeker NS. Primary pancreatic lymphoma and metastatic lymphoma cases diagnosed with ultrasonography guided tru-cut needle biopsy; Two case reports. J Surg Med. 2023;7(5):355-357.

Case presentation

Case 1

A 90-year-old male patient applied to the emergency department with the complaint of epigastric pain. Liver function tests (AST, ALT, and bilirubin) were high. Abdominal CT showed a 7-cm-diameter mass in the head of the pancreas. An USG guided tru-cut biopsy was performed on the pancreatic mass of the case followed up in the general surgery service. Histological evaluation revealed diffuse infiltration of medium-large sized neoplastic cells with lymphoid nature. Neoplastic cells were diffusely positive for CD20. Most of the cells were positive with Bcl-2 and MUM1, 20% of the cells were positive for Bcl-6, and few cells were positive for c-myc immunohistochemically. CyclinD1, CD5, CD21, CD23, CD43, and pan-cytokeratin immunohistochemical stains were negative. CD10 was nonspecific pale positive. There were CD3, CD5, CD43 positive T lymphocytes in between. The Ki-67 proliferation index was 80-90% (Figure 1). For the differential diagnosis of double/triple hit high grade B-cell lymphoma, Bcl-2, Bcl-6 and myc rearrangements were examined by fluorescent in situ hybridization method, and a Bcl-6 rearrangement was determined. The definitive diagnosis of the case was determined as diffuse large B-cell lymphoma and activated B-cell type. The case was evaluated as primary pancreatic lymphoma with clinical and radiological findings. Chemotherapy treatment was started for the patient by the hematology service. Antibiotic therapy was started due to fever, pleural effusion, and consolidated areas in the lung. The patient was taken to the intensive care unit due to his hypoxic state and died approximately 1 month after the diagnosis in the follow-ups.

Case 2

A 79-year-old male patient with a history of hypertension, diabetes, and Parkinson's disease was admitted to the hospital due to wheezing. Upon detection of a mass in the pancreas, an USG-guided biopsy was performed with the preliminary diagnosis of primary pancreatic tumor. On histological evaluation there were diffuse atypical small-medium sized lymphocytic infiltration. Tumor cells were diffusely positive with CD5, CD20, Bcl-2, and cyclinD1 immunohistochemical stains (Figure 2). Few cells were positive for CD23. CD21, CD10, Bcl-6, LEF1, pan-cytokeratin, and synaptophysin were negative. There were CD3-positive T lymphocytes in between. The Ki-67 proliferation index was 10-20%. The findings were consistent with mantle cell lymphoma. Imaging methods were used for staging after diagnosis. In the thorax CT, lymph nodes were detected in the mediastinum and around the lesser curvature of the stomach. PET CT showed lymph nodes with high glucose uptake detected in the cervical region, right hilar region, and distal end of the esophagus. In addition, high glucose uptake (SUV max 7.63) was detected in the 3.5 x 2.5 cm mass in the body-tail part of the pancreas. The case was clinically evaluated as stage 4 mantle cell lymphoma. The mass in the pancreas was evaluated as secondary involvement of lymphoma. Control PET CT was recommended after three cycles of chemotherapy, and the patient was followed up without complications.

Figure 1: A. Diffuse lymphoid neoplastic infiltration. (H&E staining-x400) B. Diffuse CD20 positivity on neoplastic cells. (CD20 staining-x100) C. High Ki-67 proliferation index of the tumor. (Ki-67 staining-x100)

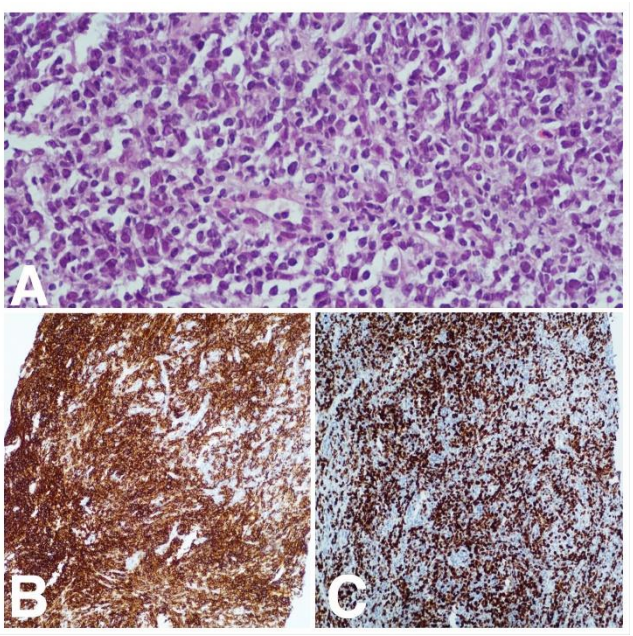

Figure 2: Diffuse lymphoid neoplastic infiltration. (H&E staining-x400) B. Diffuse cyclinD1 positivity on neoplastic cells. (cyclinD1 staining-x200) C. Diffuse CD5 positivity on neoplastic cells. (CD5 staining-x200)

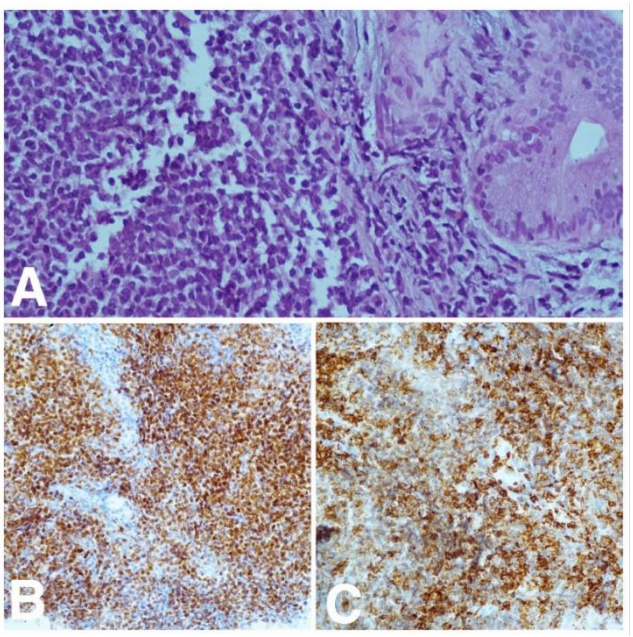

Discussion

Based on latest Global Cancer Incidence, Mortality, and Prevalence (GLOBOCAN) 2020 data, pancreatic tumors are the 12th most common tumors worldwide [10]. Of these, 85% of the pancreatic tumors are pancreatic ductal adenocarcinomas (PDAC), and 0.2% of tumors are PPLs [4,6]. Most cases of PPL are NHL's with diffuse large B cell lymphoma seen in 53.6% of the cases [7,8,12,13]. However, marginal zone lymphoma, follicular lymphoma, Burkitt's lymphoma, Hodgkin's lymphoma, small lymphocytic lymphoma, and T-cell non-Hodgkin lymphoma may also be detected [4,14]. As mentioned before, secondary pancreatic involvement of lymphomas occurs in up to 30% of cases [4] with the dominant subtype as diffuse large B cell lymphoma [15]. The tumors are mostly located in the pancreatic head, but the body and tail are also rarely involved [11]. Patients with PPL are usually seen around the 6th or 7th decade of life, and there is a slight male predominance. The main clinical

manifestations are abdominal pain, abdominal mass, weight loss, jaundice, nausea, vomiting, diarrhea. Some patients may also show up with pancreatitis, anorexia, early satiety, and bowel obstruction. Unfortunately, these are non-typical symptoms and symptoms of NHL such as fever, chills, and night sweats are rare [12]. With these nonspecific clinical manifestations, PPL should be considered as differential diagnosis of pancreatic space-occupying lesions. The differential diagnoses should be included for neuroendocrine tumors, gastrointestinal stromal tumors, PDAC, acinar cell carcinomas, PPL, inflammatory processes, and metastatic diseases [7,11].

Conclusion

Seeing that the clinical and radiological findings are not pathognomonic for PPL, the possibility of lymphoid neoplasia in pancreatic masses should be kept in mind even though PDAC's are more common. PPLs have a better outcome and different treatment options; thus, to prevent a delay or a mistake in diagnosis, a morphological and/or immunohistochemical examination should be made before any surgical treatment. A final diagnosis can be obtained with the help of minimal invasive diagnostic sampling methods such as guided tru-cut biopsies and fine needle aspirates. A correct diagnosis of PPL can prevent unnecessary surgeries, and patients can be provided with the right treatment.

References

1. Hayat M, Syed TA, Disbrow M, Tran NT, Asad ZU, Tierney WM. Recurrent pancreatitis secondary to diffuse large B cell lymphoma. J Gastrointest Cancer. 2019 Dec;50(4):1009-13. doi: 10.1007/s12029-018-0175-3.
2. Haji AG, Sharma S, Majeed KA, Vijaykumar DK, Pavithran K, Dinesh M. Primary pancreatic lymphoma: report of three cases with review of literature. Indian J Med Paediatr Oncol. 2009 Jan;30(1):20-3. doi: 10.4103/0971-5851.56331.
3. Behrns KE, Sarr MG, Strickler JG. Pancreatic lymphoma: is it a surgical disease? Pancreas. 1994 Sep;9(5):662-7.
4. Facchinelli D, Sina S, Boninsegna E, Borin A, Tisi MC, Piazza F, et al. Primary pancreatic lymphoma: clinical presentation, diagnosis, treatment, and outcome. Eur J Haematol. 2020 Oct;105(4):468-75. doi: 10.1111/ejh.13468.
5. Dunphy L, Abbas SH, Al Shoek I, Al-Salti W. Primary pancreatic lymphoma: a rare clinical entity. BMJ Case Rep. 2020 Jan 5;13(1):e231292. doi: 10.1136/bcr-2019-231292.
6. Bosman FT, Carnerio F, Aruban RH, These ND, editors. WHO Classification of Tumours of the Digestive System. 4th ed. In: Lymphoma of the pancreas. Lyon, France: IARC publishing; 2010. 332 p.
7. Rad N, Khafaf A, Mohammad Alizadeh AH. Primary pancreatic lymphoma: what we need to know. J Gastrointest Oncol. 2017 Aug;8(4):749-57. doi: 10.21037/jgo.2017.06.03.
8. Baysal B, Kayar Y, Ince AT, Arici S, Türkmen I, Şentürk H. Primary pancreatic lymphoma: a rare cause of pancreatic mass. Oncol Lett. 2015 Sep;10(3):1701-3. doi: 10.3892/ol.2015.3412.
9. Ravi S, Stephen SN, Gochhait D, Potakkat B, Niranjani R, Siddaraju N. Primary pancreatic diffuse large B-cell lymphoma diagnosed by endoscopic ultrasound guided FNAC: a rare entity. Diagn Cytopathol. 2020 Jan;48(1):57-60. doi: 10.1002/dc.24307.
10. Sung H, Ferlay J, Siegel RL, Laversanne M, Soerjomataram I, Jemal A, et al. Global cancer statistics 2020: GLOBOCAN estimates of incidence and mortality worldwide for 36 cancers in 185 Countries. CA Cancer J Clin. 2021;71(3):209-49.
11. Fukuba N, Moriyama I, Ishihara S, Sonoyama H, Yamashita N, Tada Y, et al. Primary pancreatic malignant lymphoma diagnosed from endoscopic ultrasound-guided fine-needle aspiration findings. Intern Med. 2016;55(1):31-5. doi: 10.2169/internalmedicine.55.5749.
12. Qiu T, Li W, Geng H, Shi S. Clinicopathological characteristics of primary pancreatic lymphoma: report of two cases. Int J Clin Exp Pathol. 2017 Nov 1;10(11):10941-6.
13. Yu L, Chen Y, Xing L. Primary pancreatic lymphoma: two case reports and a literature review. Onco Targets Ther. 2017 Mar 20;10:1687-94. doi: 10.2147/OTT.S121521.
14. Hans CP, Weisenburger DD, Greiner TC, Gascoyne RD, Delabie J, Ott G, et al. Confirmation of the molecular classification of diffuse large B-cell lymphoma by immunohistochemistry using a tissue microarray. Blood. 2004 Jan 1;103(1):275-82. doi: 10.1182/blood-2003-05-1545.
15. Sadaf S, Loya A, Akhtar N, Yusuf MA. Role of endoscopic ultrasound-guided-fine needle aspiration biopsy in the diagnosis of lymphoma of the pancreas: a clinicopathological study of nine cases. Cytopathology. 2017 Dec;28(6):536-41. doi: 10.1111/cyt.12442.

J Surg Med. 2023;7(5):358-360.
DOI: 10.28982/josam.1104984

Journal of Surgery and Medicine
e-ISSN: 2602-2079
https://jsurgmed.com/

Truncus arteriosus with meandering pulmonary arteries

Emre Oteyaka [1], Okan Eren Kuguoglu [1], Gizem Sari [2], Mehmet Turan Basunlu [2], Yilmaz Yozgat [2], Murat Ugurlucan [3], Halil Turkoglu [1]

[1] Istanbul Medipol University Faculty of Medicine, Department of Cardiovascular Surgery, Istanbul, Turkey
[2] Istanbul Medipol University Faculty of Medicine, Department of Pediatric Cardiology, Istanbul, Turkey
[3] Biruni University Faculty of Medicine, Department of Cardiovascular Surgery, Istanbul, Turkey

ORCID ID of the author(s)

EO: 0000-0001-5889-2257
OK: 0000-0001-7575-5297
GS: 0000-0001-6602-5946
MB: 0000-0001-9191-952X
YY: 0000-0001-5164-8534
MU: 0000-0001-6643-9364
HT: 0000-0003-4856-0974

Corresponding Author
Emre Oteyaka
Istanbul Medipol University, Faculty of Medicine, Department of Cardiovascular Surgery, TEM Avrupa Otoyolu, Goztepe Cikisi, No:1, 34214 Bagcilar, Istanbul, Turkey
E-mail: eoteyaka@gmail.com

Informed Consent
The authors stated that the written consent was obtained from the parents of the patient presented with images in the study.

Conflict of Interest
No conflict of interest was declared by the authors.

Financial Disclosure
The authors declared that this study has received no financial support.

Published
2023 May 24

Abstract

Truncus arteriosus is a rare, cyanotic, and congenital heart defect occurring due to failure in the differentiation of the aorta and the pulmonary artery during fetal development. The disease is categorized into four sub-categories in the Van Praagh and Collett & Edwards classification systems according to the origin of the pulmonary arteries. Surgical correction of the pulmonary arteries and repair of the ventricular septal defect is the preferred treatment strategy of choice; this intervention is required early in life. Here, we report a four-month-old baby with truncus arteriosus consisting of atypical pulmonary anatomy undefined by either the Van Praagh or the Collett & Edwards classification systems who underwent successful corrective surgery.

Keywords: truncus arteriosus, pulmonary artery, classification, surgical treatment

Introduction

Truncus arteriosus (TA) is a rare congenital cardiac defect encompassing 1.4%-2.8% of congenital heart diseases [1]. TA consists of a common arterial trunk superior to the ventricular septal defect. The solitary truncal artery is the only systemic, pulmonary, and coronary circulation supplier, and the aorta of such patients is wider than normal . The aortic valve and arch anomalies are common in patients with TA [2]. Nevertheless, the cardiac defects most related to TA include tricuspid valve dysplasia or dysfunction, ventricular septal defects (VSD), aortic arch abnormalities, and coronary artery malformations [3].

Patients with TA frequently have a clinical presentation of dyspnea, recurrent lung infections, and growth retardation. Symptoms may range from dyspnea to co-incidental findings on radiographs. Imaging methods include echocardiography, angiography, computed tomography, or magnetic resonance for screening and diagnosis. After diagnosing TA, the pathology is classified according to Collett & Edwards or the Van Praagh classification systems. These classification methods are based on the anatomical structure of the left pulmonary artery, right pulmonary artery, and aorta. The surgical treatment strategy is also planned according to the type of TA. Our article focuses on the diagnosis and surgical management of a 4-month-old male patient with findings of an atypical TA with meandering pulmonary arteries.

How to cite: Oteyaka E, Kuguoglu OE, Sari G, Basunlu MT, Yozgat Y, Ugurlucan M, Turkoglu H. Truncus arteriosus with meandering pulmonary arteries. J Surg Med. 2023;7(5):358-360.

Case presentation

Here, a 4-month-old male patient without an antenatal or postnatal diagnosis was referred to our institution with increasing dyspnea, easy fatigability, poor feeding, and growth retardation. His parents reported recurrent pulmonary infections and bouts of cough . The patient weighed 3800 g (birth weight: 3250 g) and was 60 cm tall. The body surface area was calculated as 1.24 m^2. On physical examination, pulmonary rales were present, the heart was hyperdynamic with a 2-3/6 systolic murmur at the mesocardiac focus, and the patient had slight hepatomegaly. The patient's blood pressure was 81/43 mmHg. Electrocardiography showed tachycardia (180 beats/min), normal sinus rhythm with regular intervals, and a normal QRS axis. The cardiothoracic index increased with significant bilateral hilar opacities on plain chest X-ray (Figure 1). Following physical examination, there was a high suspicion of congenital cardiac anomaly, which directed us to perform echocardiography. Echocardiography showed truncus arteriosus with a peri-membranous outlet VSD, right-sided aortic arch, a patent foramen ovale with a right to left shunt, and pulmonary hypertension. The aortic valve was tricuspid and exhibited trivial regurgitation. Both pulmonary arteries were present; however, neither their origin nor course could be identified. Therefore, the classification of pathology could not be determined. Anti-congestive therapy with digoxin, captopril, and furosemide was immediately initiated. Diagnostic cardiac catheterization suggested TA. Although there were two well-developed pulmonary arteries, their origins could not be identified (Figure 2). The patient was scheduled for corrective surgery.

After describing the pathology, the patient's parents were informed about the risks and benefits of treatment alternatives. Consent for the procedure and use of the materials for academic purposes was acquired. Following a median sternotomy, the pericardium was excised and harvested. An anatomical examination exhibited a truncal pulmonary artery originating on the anterior aspect of the ascending aorta with a short course dividing into the right and left branches. The right pulmonary branch coursed left and followed a path inferior to the ascending aorta before reaching the right lung. The left branching pulmonary artery curled to the left inferior to the right pulmonary artery before going to the left lung (Figure 3). Pulmonary arteries were prepared and looped. Extracorporeal circulation was initiated following aortic and bicaval cannulation. Cardiac arrest was achieved at 32°C with an antegrade hypothermic Del Nido cardioplegia infusion. The truncal pulmonary arteries were snared and resected from the ascending aorta, and the ascending aorta was repaired with an autologous glutaraldehyde-treated pericardial patch. A right ventricular infundibular incision was made, and the ventricular septal defect was patched with an autologous glutaraldehyde-treated pericardial patch.

The right ventricular outflow tract was reconstructed with a 12 mm bovine jugular vein graft (Contegra, Medtronic PLC, 710 Medtronic Parkway Minneapolis, MN 55432–5604 USA). The graft was anastomosed to the right ventricle and the branching pulmonary arteries after anatomically correcting the meandering pulmonary arteries. The patient was weaned off cardiopulmonary bypass with a moderate dose of inotropic support (0.75 mcg/kg/min milrinone, 0.1 mcg/kg/min adrenaline, and 0.1 mcg/kg/min noradrenaline), and the operation was finalized. The total cross-clamp and cardiopulmonary bypass periods were 95 min and 108 min, respectively. The patient was hospitalized at the intensive care unit and extubated 16 h after the operation. The patient was transferred to the ward on the fourth day following the procedure. After spending nine days in good condition, the patient was discharged from the hospital and was followed actively. The patient showed normal myocardial function with considerable weight gain and growth.

Figure 1: The cardiothoracic index increased with significant bilateral hilar opacities on plain chest X-ray.

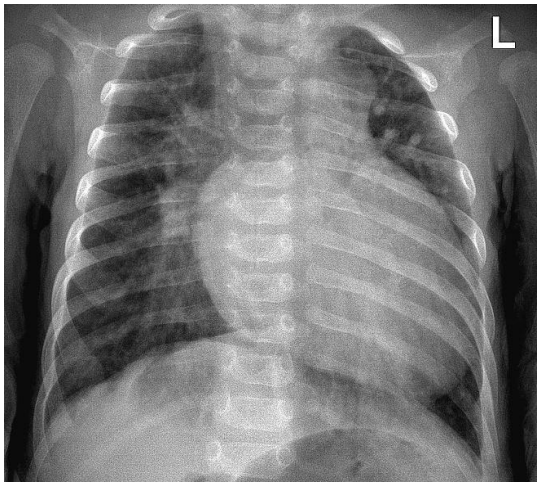

Figure 2: Diagnostic cardiac catheterization indicated two well-developed pulmonary arteries; their origins could not be identified.

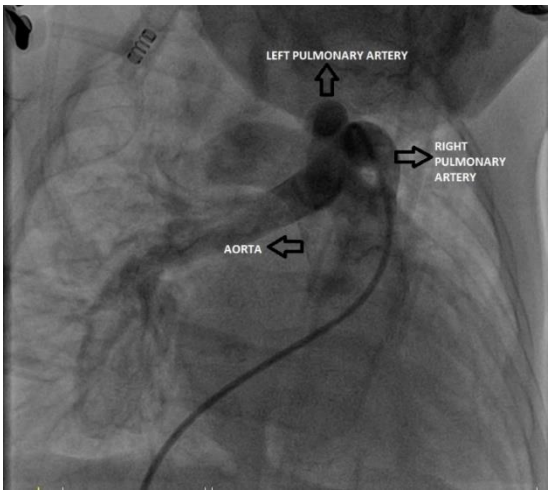

Figure 3: Perioperative view of the main pulmonary artery originating from the anterior surface of the ascending aorta with a concise course that then divides into right and left branches.

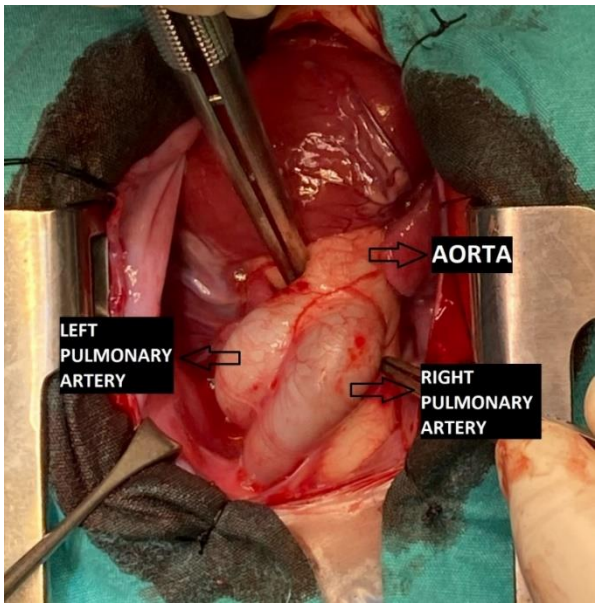

Discussion

Truncus arteriosus is a congenital cyanotic heart defect in the pediatric population. It arises from a single truncal valve extending as a single truncal vessel before separating into the aorta and pulmonary arteries. Truncus arteriosus constitutes 4% of critical cases among congenital heart defects. When screening for TA, several anatomical structures are evaluated. These structures include the anatomical orientation and the functionality of the tricuspid valve, the origin of the pulmonary arteries, anomalies of the aortic arch, and the location of the ventricular septal defect [4]. The original and more popular classification of TA was devised by Collett & Edwards in 1949 and divides this anomaly into four types [5]:

- Type I: the truncal pulmonary artery, which splits into right and left pulmonary arteries after emerging from the truncal root (commonly seen in 80% of patients).
- Type II: left and right pulmonary arteries arising separately from the posterior part of the truncus.
- Type III: pulmonary arteries arising from the lateral aspect of the truncus with separate origins.
- Type IV: neither pulmonary arterial branch emerges from the common trunk (pseudo truncus). The pulmonary arteries arise from the descending aorta.

In 1965, Van Praagh modified the classification system to include four primary types [6].

- Type A1: identical to type I proposed by Collett & Edwards.
- Type A2: a separation in the origin of branching pulmonary arteries from the left and right lateral portions of the common trunk.
- Type A3: the branching pulmonary artery (commonly the right) originates from the pulmonary trunk. The branching of the opposite lung is supplied either by collaterals or a pulmonary artery arising from the aortic arch.
- Type A4: interrupted aortic arch coexists with the truncus.

The Van Praagh classification has recently been preferred [8] instead of Collett & Edwards's [7] perhaps because of the inclusion of pulmonary architecture since patients with an underdeveloped aortic arch (interrupted or hypoplastic) with a broad patent ductus arteriosus attached to the descending aorta (15% of the patients with truncus arteriosus) are recognized within the Van Praagh classification [8].

Our patient had a TA consisting of left- and right-branching pulmonary arteries with a conjoined origin separated after emerging from the anterior aspect of the truncal root proximally. This finding is not present in the Collett & Edwards classification or the Van Praagh classification, thus defining the abovementioned architecture as an atypical truncus arteriosus. The atypical formation with such an architecture can be attributed to the embryological development of the heart. The conotruncal septum separates the truncal root into a developed main pulmonary artery and an ascending aorta when the fifth week of gestation concludes. Defects that occur during the formation of the conotruncal septum result in a wide variety of conotruncal abnormalities including TA with a single truncal valve [9].

Neural crest cells and derangements in neural tube development have also been indicated as contributing factors in the development of TA and other conotruncal malformations [10,11]. Apart from developmental abnormalities, environmental and genetic factors also contribute to conotruncal malformations including truncus arteriosus. These risk factors include gestational cigarette smoking [12], advancing maternal age [13], and DiGeorge Syndrome (deletion of 22q11.2) [14]. A genetic screening test with a detailed investigation of the risk factors that the patient or the parents have been exposed to can be performed to further understand the underlying factors that play a role in the formation of atypical cases of truncus arteriosus.

Conclusions

While familial predisposition and risk factors have a significant role in the etiology, the abnormal meandering course and curling of the branching pulmonary arteries could be attributed to a long-standing elevated pulmonary arterial pressure. The architecture of the pulmonary vasculature did not affect the corrective procedure. However, the left and right pulmonary arteries required anatomical alignment because of their unusual presentation in our case. Investigations into similar truncus arteriosus cases can help further explain the underlying etiology of meandering pulmonary arteries.

References

1. McGoon DC, Rastelli GC, Ongley PA. An operation for the correction of truncus arteriosus. JAMA. 1968 Jul 8;205(2):69-73. PMID: 4872743.
2. Ugurlucan M, Sayin OA, Surmen B, Sungur Z, Tireli E, Dayioglu E. Rastelli and Norwood combination for the treatment of type I truncus arteriosus and hypoplastic aortic arch: a case report. Heart Surg Forum. 2007;10(1):E6-8. doi: 10.1532/HSF98.20061141. PMID: 17162406.
3. Sojak V, Lugo J, Koolbergen D, Hazekamp M. Surgery for truncus arteriosus. Multimed Man Cardiothorac Surg. 2012 Jan 1;2012:mms011. doi: 10.1093/mmcts/mms011. PMID: 24414715.
4. Potter A, Pearce K, Hilmy N. The benefits of echocardiography in primary care. Br J Gen Pract. 2019 Jul;69(684):358-359. doi: 10.3399/bjgp19X704513. PMID: 31249096; PMCID: PMC6592347.
5. COLLETT RW, EDWARDS JE. Persistent truncus arteriosus; a classification according to anatomic types. Surg Clin North Am. 1949 Aug;29(4):1245-70. doi: 10.1016/s0039-6109(16)32803-1. PMID: 18141293.
6. Van Praagh R, Van Praagh S. The anatomy of common aorticopulmonary trunk (truncus arteriosus communis) and its embryologic implications: A study of 57 necropsy cases. Am J Cardiol. 1965 Sep;16(3):406-25. doi: 10.1016/0002-9149(65)90732-0. PMID: 5828135.
7. Collett RW, Edwards JE. Persistent truncus arteriosus: a classification according to anatomic types. Surg Clin North Am. 1949 Aug;29(4):1245-70. doi: 10.1016/s0039-6109(16)32803-1. PMID: 18141293.
8. Martínez-Quintana E, Portela-Torrón F. Truncus arteriosus and truncal valve regurgitation. Transl Pediatr. 2019 Dec;8(5):360-362. doi: 10.21037/tp.2019.02.01. PMID: 31993347; PMCID: PMC6970119.
9. Pexieder T. Prenatal development of the endocardium: a review. Scan Electron Microsc. 1981;(Pt 2):223-53. PMID: 7034166.
10. Scholl AM, Kirby ML. Signals controlling neural crest contributions to the heart. Wiley Interdiscip Rev Syst Biol Med. 2009 Sep-Oct;1(2):220-7. doi: 10.1002/wsbm.8. PMID: 20490374; PMCID: PMC2873602.
11. Kirby ML, Gale TF, Stewart DE. Neural crest cells contribute to normal aorticopulmonary septation. Science. 1983 Jun 3;220(4601):1059-61. doi: 10.1126/science.6844926. PMID: 6844926.
12. Alverson CJ, Strickland MJ, Gilboa SM, Correa A. Maternal smoking and congenital heart defects in the Baltimore-Washington Infant Study. Pediatrics. 2011 Mar;127(3):e647-53. doi: 10.1542/peds.2010-1399. Epub 2011 Feb 28. PMID: 21357347.
13. Long J, Ramadhani T, Mitchell LE. Epidemiology of nonsyndromic conotruncal heart defects in Texas, 1999-2004. Birth Defects Res A Clin Mol Teratol. 2010 Nov;88(11):971-9. doi: 10.1002/bdra.20724. Epub 2010 Sep 28. PMID: 20878913.
14. Momma K. Cardiovascular anomalies associated with chromosome 22q11.2 deletion syndrome. Am J Cardiol. 2010 Jun 1;105(11):1617-24. doi: 10.1016/j.amjcard.2010.01.333. PMID: 20494672.

J Surg Med. 2023;7(5):361-363.
DOI: 10.28982/josam.7349

Journal of Surgery and Medicine
e-ISSN: 2602-2079
https://jsurgmed.com/

A rare case of bleeding into the Sylvian arachnoid cyst: A case report

Ilyas Tadayyon Einaddin Karakoc [1], Feyzi Birol Sarica [2]

[1] Department of Neurosurgery, Giresun University Education and Research Hospital, Giresun, Turkey
[2] Department of Neurosurgery, Giresun University Faculty of Medicine, Giresun University Education and Research Hospital, Giresun, Turkey

ORCID ID of the author(s)

ITEK: 0000-0002-6155-4897
FBS: 0000-0001-9985-0184

Abstract

Arachnoid cysts are primarily developmental in origin and constitute rare, benign lesions. Sylvian arachnoid cysts may infrequently present with subdural and/or intracystic hemorrhage. Hemorrhage is typically of venous origin and occurs due to stretching and tearing of bridging veins, depending on minor traumas. The annual risk of bleeding associated with Sylvian arachnoid cysts, with no additional complaints other than headache and an asymptomatic course, has been reported to be 0.04%. Symptoms can range from headache to coma, depending on the mass effect after hemorrhage. If there is no clinical evidence linking the arachnoid cyst, it is sufficient to perform surgery only for the hematoma without resecting it. In this case report, we present a rare instance of hemorrhage due to a Sylvian arachnoid cyst that developed after trauma and was observed in a patient who came to our clinic with a headache. In our patient, the cyst-dependent left parietal subdural hemorrhage was evacuated through a burr-hole craniotomy, and a closed-system drainage with a Hemovac drain was applied for 48 hours. During post-operative follow-up, complete resorption of subdural and intracystic hemorrhages was observed. A case-based surgical approach is necessary for bleeding due to arachnoid cysts in the Sylvian region.

Keywords: arachnoid cyst, hemorrhage into the cyst, intracranial cystic lesions, subdural hemorrhage

Introduction

Arachnoid cysts result from defects in the fusion of two layers of the arachnoid membrane during the early fetal period, which leads to a cyst's formation with cerebrospinal fluid accumulation between the two arachnoid membranes [1,2]. Arachnoid cysts account for 1% of nontraumatic space-occupying lesions in the skull [3,4]. Most arachnoid cysts in children are congenital [5,6], while in adults, they can be primary, congenital, or develop secondary to trauma, tumor, or infection [5]. The most common location is the middle cranial fossa (4/6), followed by the posterior cranial fossa (1/6), and the suprasellar, frontal, cerebral convexity, interhemispheric fissure, and quadrigeminal cistern (1/6) [2,7]. Arachnoid cysts are more common in children than adults [8], and Sylvian arachnoid cysts account for 40-50% of all intracranial cases [3]. In this case report, we emphasize the importance of a case-based surgical approach in hemorrhages associated with arachnoid cysts in the Sylvian region.

Corresponding Author
Ilyas Tadayyon Einaddin Karakoc
Giresun University Education and Research Hospital, Department of Neurosurgery, Teyyaredüzü Mahallesi, Atatürk Bulvarı, No:323, 28100, Giresun, Turkey
E-mail: ilyaskarakoc58@gmail.com

Informed Consent
The authors stated that the written consent was obtained from the legal guardians of patient presented with images in the study.

Conflict of Interest
No conflict of interest was declared by the authors.

Financial Disclosure
The authors declared that this study has received no financial support.

Published
2023 May 23

How to cite: Karakoc ITE, Sarica FB. A rare case of bleeding into the Sylvian arachnoid cyst: A case report. J Surg Med. 2023;7(5):361-363.

Case presentation

A 16-year-old male patient who had sustained a head injury with a slipped foot 20 days prior was admitted to our hospital with a complaint of severe headache that did not respond to analgesic treatments. The neurological examination was performed and evaluated as normal, and no pathology was detected in the fundus examination. Upon reviewing the patient's records in the radiology department of our hospital prior to the trauma, a well-contoured, thin-walled arachnoid cyst without mass effect was found in the Sylvian localization on Brain Magnetic Resonance Imaging (MRI). The arachnoid cyst was hypointense in the T1 axial sequence (Figure 1A), hyperintense in the T2-axial sequence (Figure 1B), and isointense with cerebrospinal fluid (CSF) in the FLAIR sequence (Figure 1C).

Figure 1: Brain magnetic resonance imaging of the patient (pre-traumatic period). 1A: An arachnoid cyst in the Sylvian localization, with smooth contours, thin walls and no mass effect, hypointense in the T1-axial sequence, 1B: hyperintense in the T2-axial sequence, 1C: isointense with the CSF in the FLAIR sequence.

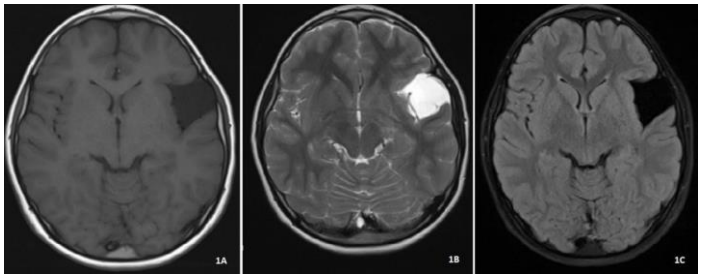

After the head injury, a brain computed tomography (CT) scan was performed during the patient's admission to our hospital. A hyperdense hematoma was found within the arachnoid cyst in the left temporal region, and a subdural hemorrhage was detected in the left fronto-temporo-parietal region. The subdural hemorrhage was measured as 9 mm at its widest part in the extra-axial area and appeared slightly hyperdense. In addition, approximately 6 mm of subfalcine herniation was detected to the right in the midline structures of the brain (Figure 2A, 2B, 2C). Given the patient's clinical picture of persistent headache and resistance to analgesic therapy, it was decided to perform surgical treatment.

Figure 2: Brain computerized tomography of the patient (post-traumatic period). 2A: Hyperdense hematoma areas in the arachnoid cyst and the left temporal extra-axial region. 2B: A subfalcine herniation of approximately 6 mm to the right in the midline structures of the brain. 2C: A Subdural hemorrhage in the left fronto-temporo-parietal region measuring 9 mm at its widest point.

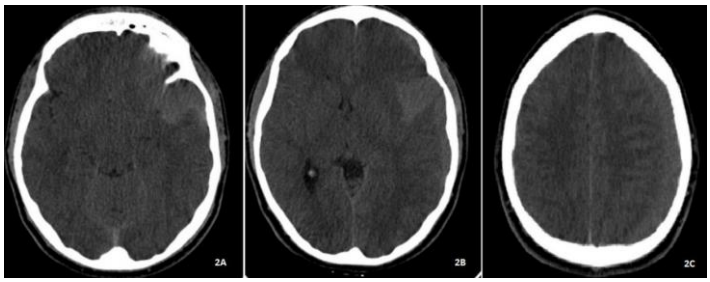

The subdural hematoma adjacent to the cyst was evacuated by performing a burr-hole craniotomy in the left parietal region, and closed-system drainage was applied for 48 hours. Following this treatment, the patient's headache resolved dramatically. In the post-operative period, a follow-up brain CT scan was performed, which showed that the subdural hematoma area had completely disappeared, and the hemorrhage in the left Sylvian arachnoid cyst had also disappeared (Figure 3). No additional neurodeficiencies were detected in the post-operative period, and the patient was discharged.

In this case report, we obtained a "written consent document" from the father of the child patient to use the patient's radiological images.

Figure 3: Brain computerized tomography (CT) of the patient (post-operative period). The disappearance of bleeding areas in the subdural space and within the arachnoid cyst and hypodensity in the arachnoid cyst.

Discussion

Arachnoid cysts are cystic cavities filled with CSF-like fluid within the arachnoid membranes. They are mostly formed due to developmental defects during the fetal period and are rare benign lesions containing collagen and cells. They may occur due to congenital, traumatic or inflammatory causes [9].

In a retrospective analysis of 208 cases of intracranial cysts performed by Rengachary and Watanabe from 1831 to 1980, Sylvian fissure-localized arachnoid cysts were reported most frequently, with a localization rate of 49%. This was followed by cerebellopontine angle (11%), supracollicular (10%), vermian and suprasellar (9%), interhemispheric (5%), convexity (4%), and clival (3%) localizations [5,10,11].

Middle cranial fossa cysts most commonly present with headaches, epileptic seizures, and contralateral muscle weakness. In addition, macrocrania, mental retardation, and behavioral disorders are among the symptoms of most pediatric patients [12,13].

It was reported in the literature that Sylvian arachnoid cysts were rarely (2.4%) associated with subdural and/or intracystic hemorrhage and hygroma clinics. The hemorrhages are almost always of venous origin and develop with the stretching and rupture of the bridging veins depending on minor traumas. Depending on the mass effect after the hemorrhage, various symptoms, from headaches to coma, may be observed in a previously asymptomatic patient [5,10].

Gassali et al. [5] proposed a classification system based on the appearances of Sylvian fissure-localized arachnoid cysts. Type-I Sylvian arachnoid cysts are small lenticular cysts located in the Sylvian fissure, the anterior pole of the middle fossa, and posterior to the sphenoid wing. This group has no mass effect and no midline shift. Type-II Sylvian arachnoid cysts are rectangular and involve the middle and proximal portions of the fissure outside the insular cortex. There is minimal midline shift in the Type-II group.

Type-III Sylvian arachnoid cysts are large, lenticular-shaped lesions and typically exhibit midline shifts. Macrocrania, or asymmetric bone enlargement in the middle cranial fossa, is commonly observed in this group. Cases of hemorrhage in or

adjacent to middle fossa cysts have been reported in the literature [5].

Arachnoid cysts are usually diagnosed through prenatal ultrasonography, cranial ultrasonography, brain CT, and brain MRI [14]. Brain MRI is the preferred diagnostic method as it provides information in three planes, eliminates bone artifacts, and provides detailed information about the exact localization and extensions of the cyst [15]. Diffusion MRI is useful for distinguishing epidermoid tumors, often confused with arachnoid cysts. The constructive interference in the steady state (CISS) MRI sequence is another important radiological examination for differential diagnosis of arachnoid cysts and determining surgical options. Brain CT can identify many arachnoid cysts and is used to differentiate them from cystic tumors that mimic arachnoid cysts and other cystic lesions by administering intravenous contrast material [5,6].

Treating arachnoid cysts is controversial, and many methods have been recommended [16]. Spontaneous regression has also been reported rarely in these cases [7,17].

Asymptomatic arachnoid cysts that do not show progressive growth or cause ventriculomegaly may be observed clinically and radiologically. As is generally recommended, if an arachnoid cyst is incidentally detected or is followed conservatively, the patient should be monitored at regular intervals (every 6 months for the first 2 years) with cranial CT and/or MRI. If the patient's clinical and radiological stability is in question at the end of this period, follow-up should be conducted annually. However, the literature has no definite consensus on this subject [18].

Absolute surgical treatment indications for arachnoid cysts include the observation of compression findings on neural tissues with mass effect, the development of symptoms of increased intracranial pressure syndrome, resistant epilepsy compatible with electroencephalogram (EEG) findings, and progressive hydrocephalus [8,12].

It has been reported that head trauma in arachnoid cysts increases the incidence of subdural hygroma or hematoma, potentially causing asymptomatic cases to become symptomatic in this way [19].

There is still no consensus on the preferred surgical method in the literature for treating arachnoid cysts, and treatment protocols vary depending on the case. Arachnoid cyst cases not complicated by hemorrhage may be sufficient in pure arachnoid cyst mouthing with subarachnoid distance. Commonly used surgical techniques include endoscopic cyst fenestration and cystoperitoneal shunt insertion. Both methods have been reported to yield positive results in the literature. Another technique involves internal shunt application to the subdural space, yielding positive results. Total resection of the cyst is often not possible during surgery. Although there are not enough reported cases in the literature, it has been reported that acetazolamide and corticosteroid treatment can be effective in cases treated conservatively [20].

In arachnoid cysts complicated by subdural hematoma or hygroma, in addition to mouthing the cyst with the subarachnoid space, evacuation of the hematoma or hygroma is recommended as part of the treatment [10,11,21].

Different treatment approaches have been reported for cases where Sylvian-localized arachnoid cysts are complicated by subdural hemorrhage [10,11,21]. The main question in these cases is whether the cyst should be treated in addition to draining the hematoma. According to a retrospective study by Parsch et al. [22], the risk of developing subdural hemorrhage or hygroma is five times higher in Sylvian arachnoid cyst cases compared to the normal population (2.43% vs. 0.46%). However, as in our case, it has been reported in the literature that the annual risk of hemorrhage is 0.04% in Sylvian-localized arachnoid cysts that do not have additional complaints other than a headache or show an asymptomatic course. Additionally, it has been reported that surgical treatment for hematoma evacuation alone is sufficient in these asymptomatic cases, as in our patient [11,23].

Conclusion

Traumatic subdural hematomas that develop as a complication of arachnoid cysts are rare. If there is no clinical evidence to suggest an association with the arachnoid cyst, it is usually sufficient to operate only on the hematoma without resecting it. In conclusion, a case-based surgical approach is required for bleeding due to arachnoid cysts in the Sylvian region.

References

1. Aydogmus E, Hicdonmez T. Spontaneous Intracystic Haemorrhage of an Arachnoid Cyst Associated with a Subacute Subdural Haematoma: A Case Report and Literature Review. Turk Neurosurg. 2019;29(6):940-4. doi: 10.5137/1019-5149.JTN.20885-17.2
2. Bakım B, Karamustafalıoğlu KO, Özalp G, Tankaya O, Kahraman N, Yavuz BG, et al. Arachnoid cyst and bipolar disorder: a case report. Journal of Mood Disorders. 2012;2(2):70-3.
3. Li L, Begbie F, Grimmond N, Kontorinis G. Arachnoid cysts on magnetic resonance imaging: just an incidental finding? J Laryngol Otol. 2020;134(5):424–30. doi: 10.1017/S0022215120000808
4. Adin ME, Yıldız MS, Deniz MA, Behzadi AH, Mata-Mbeda D. Arachnoid cysts with spontaneous intracystic hemorrhage and associated subdural hematoma: Report of management and follow-up of 2 cases. Radiol Case Rep. 2017 Dec;2(6):516–21. doi: 10.1016/j.radcr.2017.12.006
5. Galassi E, Tognetti F, Gaist G, Fagioli L, Frank F, Frank G. CT scan and metrizamide CT cisternography in arachnoid cysts of the middle cranial fossa: classification and pathophysiological aspects. Surg Neurol. 1982 May;17(5):363-9. doi: 10.1016/0090-3019(82)90315-9
6. Ciricillo SF, Cogen PH, Harsh GR, Edwards MS. İntracranial arachnoid cysts in children. A comparison of the effects of fenestration and shunting. J Neurosurg. 1991 Feb;74(2):230-5. doi: 10.3171/jns.1991.74.2.0230
7. Harding BN, Copp AJ. Malformations. In: Graham DI, Lantos PL, eds. Greenfield's Neuropathology. Oxford University Press, 7th ed.; 2002. pp. 451-52.
8. Al-Holou WN, Yew AY, Boomsaad ZE, Garton HJ, Muraszko KM, Maher CO. Prevalence and natural history of arachnoid cysts in children. J Neurosurg Pediatr. 2010 Jun;5(6):578-85. doi: 10.3171/2010.2.PEDS09464
9. Menkes JH. Arachnoidal Cysts. In: Sarnat HB, Menkes HJ, eds. Child Neurology. Philadelphia: Lippincott Williams and Wilkins, 6th ed.; 2000. pp.377-78.
10. Balestrino A, Piatelli G, Consales A, Cama A, Rossi A, Pacetti M, et al. Spontaneous rupture of middle fossa arachnoid cysts: surgical series from a single center pediatric hospital and literature review. Child's Nerv Syst. 2020 Nov;36(11):2789-99. doi: 10.1007/s00381-020-04560-3
11. Liu Bei, Wang C, Qu Y. Treatment of Arachnoid Cyst With Spontaneous Hemorrhage With Atorvastatin. Front Pharmacol. 2019 Nov;10:1343. doi: 10.3389/fphar.2019.01343
12. Erman T, Göçer Aİ, Tuna M, Ergin M, Zorludemir S, Çetinalp E. Intracranial arachnoid cysts: clinical features and management of 35 cases and review of the literature. Neurosurgery Quarterly. 2004 June;14(2):84-9. doi: 10.1097/01.wnq.0000126102.32911.43
13. Wester K. Peculiarities of intracranial arachnoid cysts: Location, sidedness and sex distribution in 126 consecutive patients. Neurosurgery. 1999 Oct;45(4):775-9. doi: 10.1097/00006123-199910000-00008
14. Gelabert-Gonzalez M, Santin-Amo JM, Aran-Echabe E, Garcia-Allut A. Imaging diagnosis of arachnoid cysts. Neurocirugia. 2015 Nov-Dec;26(6);284-91. doi: 10.1016/j.neucir.2015.02.009
15. Aydın S, Dogan S, Abas F. Konjenital araknoid kistler. Uludağ Üniversitesi Tıp Fakültesi Dergisi. 2002;28(1):37-41.
16. Samii M, Carvalho GA, Schuhmann MU, Matthies C. Arachnoid cysts of the posterior fossa. Surg Neurol. 1999 Apr;51(4):376-82. doi: 10.1016/s0090-3019(98)00095-0.
17. Bilginer B, Onal MB, Oguz KK, Akalan N. Arachnoid cyst associated with subdural hematoma: report of three cases and review of the literature. Childs Nerv Syst. 2009 Jan;25(1):119-24. doi: 10.1007/s00381-008-0728-z
18. Beltramello A, Mazza C. Spontaneous disappearance of a large middle fossa arachnoid cyst. Surg Neurol. 1985 Aug;24(2):181-3. doi: 10.1016/0090-3019(85)90182-x
19. Wester K. Gender distrubution and sidedness of middle fossa arachnoid cysts: a review of cases diagnosed with computed imaging. Neurosurgery. 1999 Nov;31(5):940-4. doi: 10.1227/00006123-199211000-00018
20. Greenfield JP, Souweidane MM. Endoscopic management of intracranial cysts. Neurosurg Focus. 2005 Dec;19(6):E7. doi: 10.3171/foc.2005.19.6.8
21. Fuentes S, Palombi O, Pouit B, Bernard C, Desgeorges M. Arachnoid cysts of the middle fossa and associated subdural hematoma. Three case reports and review of the literature. Neurochirurgie. 2000 Sep;46(4):376-82.
22. Parsch CS, Krauss J, Hofmann E, Meixensberger J, Roosen K. Arachnoid cysts associated with subdural hematomas and hygromas: analysis of 16 cases, long-term follow-up, and review of the literature. Neurosurgery. 1997;40(3):483-90. doi: 10.1097/00006123-199703000-00010
23. Ibarra R, Kesava PP. Role of MR imaging in the diagnosis of complicated arachnoid cyst. Pediatr Radiol. 2000 May;30(5):329-31. doi: 10.1007/s002470050751.